INVESTIGATION OF RARE EARTHS EXTRACTION POTENTIAL FROM
VARIOUS SOLID FOSSIL FUEL WASTES

A THESIS SUBMITTED TO
THE GRADUATE SCHOOL OF NATURAL AND APPLIED SCIENCES
OF
MIDDLE EAST TECHNICAL UNIVERSITY

BY

KARDEN BÜYÜKTANIR AKTAR

IN PARTIAL FULFILLMENT OF THE REQUIREMENTS
FOR
THE DEGREE OF DOCTOR OF PHILOSOPHY
IN
MINING ENGINEERING

JUNE 2024

Approval of the thesis:

INVESTIGATION OF RARE EARTHS EXTRACTION POTENTIAL FROM VARIOUS SOLID FOSSIL FUEL WASTES

submitted by **KARDEN BÜYÜKTANIR AKTAR** in partial fulfillment of the requirements for the degree of **Doctor of Philosophy** in **Mining Engineering, Middle East Technical University** by,

Prof. Dr. N. Emre Altun
Dean, **Graduate School of Natural and Applied Sciences**   _____

Prof. Dr. N. Emre Altun
Head of the Department, **Mining Engineering**   _____

Prof. Dr. N. Emre Altun
Supervisor, **Mining Engineering, METU**   _____

Examining Committee Members:

Prof. Dr. İlkay Bengü Can
Mining Engineering, Hacettepe University   _____

Prof. Dr. N. Emre Altun
Mining Engineering, METU   _____

Assoc. Prof. Dr. Mustafa Erkayaoğlu
Mining Engineering, METU   _____

Assoc. Prof. Dr. Çağlar Sınayuç
Petroleum and Natural Gas Eng., METU   _____

Assoc. Prof. Dr. Ergin Gülcan
Mining Engineering, Hacettepe University   _____

Date: 26.06.2024

I hereby declare that all information in this document has been obtained and presented in accordance with academic rules and ethical conduct. I also declare that, as required by these rules and conduct, I have fully cited and referenced all material and results that are not original to this work.

Name Last name : Karden Büyüktanır Aktar

Signature :

ABSTRACT

INVESTIGATION OF RARE EARTHS EXTRACTION POTENTIAL FROM VARIOUS SOLID FOSSIL FUEL WASTES

Büyüktanır Aktar, Karden
Doctor of Philosophy, Mining Engineering
Supervisor : Prof. Dr. N. Emre Altun

June 2024, 142 pages

Solid fossil fuels and -wastes are the important sources of rare earth elements. Rare Earth Elements have strategic importance because they find numerous applications in various sectors of the global economy. Furthermore, solid fossil fuels are resources primarily used for electric power generation and the residues should be utilized. This study aimed at examining extraction methods of rare earth elements (Scandium, Yttrium and Lanthanides) in solid fossil fuels, such as lignite, hard coal, asphaltite by products, mainly fly ash.

Within the scope of the study, chemical characterization was first carried out. Total rare earth element contents of lignite, hard coal, and asphaltite fly ash samples were determined (365 ppm, 428 ppm and 439 ppm, respectively). The major impurities of the samples were found to be Ca, Al, Si, and Fe.

Then, hydrometallurgical leaching experiments were conducted. Fly ash samples were treated with two inorganic, and one organic acid leach containing sulfuric acid, hydrochloric acid and citric acid. The best leaching conditions were determined as 24 hours of leaching at 90°C at 30% acid concentration for all the direct leaching experiments. As a result of the statistical analysis, the effects of the parameters were

examined and the post-leaching state of the materials was examined with XRD and SEM analysis.

Later, since it was seen that sequential leaching would increase the leaching efficiency, inorganic sequential leaching was performed. The first hydrometallurgical leaching was done using sulfuric acid. The leach sediment was subjected to a second leaching process involving hydrochloric acid. The total rare earth element productivity of sequential leaching of fly ashes was determined as 86.05% for lignite fly ash, 96.93% for asphaltite fly ash, and 73.45% for hard coal fly ash, respectively.

As the last stage, neutralization - selective precipitation experiments were carried out on the pregnant leach solution whose efficiency was increased by sequential leaching. The pH values of the obtained pregnant leach solutions were first increased to 4.5 and then to 8.5 using 10 M NaOH solution. Precipitation processes were carried out in two stages in order to purify it from impurities. In the first stage, Al and Fe^{+3} impurities were precipitated, and in the second stage, pH was increased to 8.5 and rare earth elements were precipitated. Fly ash materials responded positively to hydrometallurgical leaching and neutralization - selective precipitation processes, and sediments containing high grade total rare earth elements (2830 ppm (lignite fly ash), 2765 ppm (asphaltite fly ash) and 2232 ppm (hard coal fly ash)) were obtained.

Keywords: Leaching, Hydrometallurgy, Precipitation, Rare Earth Elements, Fly Ash

ÖZ

ÇEŞİTLİ KATI FOSSIL YAKITLARININ YAN ÜRÜNLERİNDEN NADİR TOPRAK ELEMENTLERİ EKSTRAKSİYONU POTANSİYELİNİN İNCELENMESİ

Büyüktanır Aktar, Karden
Doktora, Maden Mühendisliği
Tez Yöneticisi: Prof. Dr. N. Emre Altun

Haziran 2024, 142 sayfa

Katı fosil yakıtlar ve yan ürünleri nadir toprak elementleri içeren önemli kaynaklardır. Nadir toprak elementleri stratejik bir öneme sahiptir çünkü küresel ekonominin çeşitli sektörlerinde sayısız uygulamada kullanılmaktadırlar. Ayrıca, katı fosil yakıtlar elektrik üretiminde kullanılan birincil kaynaklardır ve yanma sonucu ortaya çıkan yan ürünler değerlendirilmelidir. Bu çalışmanın amacı, katı fosil yakıtlardan, linyit, taşkömürü ve asfaltit uçucu küllerinden nadir toprak elementlerinin (Sc, Y ve lanthanit grubu) ekstraksiyon yöntemlerinin incelenmesidir. Çalışmanın odak noktası, bu malzemelerden nadir toprak metal ekstraksiyonu olanaklarını belirlemektir.

Çalışma kapsamında ilk olarak kimyasal karakterizasyon yapılmıştır. Linyit, taşkömürü ve asfaltit uçucu kül örneklerinin toplam nadir toprak elementleri içerikleri belirlenmiştir (sırasıyla 365 ppm, 428 ppm ve 439 ppm). Örneklerin majör safsızlıkları Ca, Al, Si ve Fe olarak bulunmuştur.

Daha sonra hidrometalurjik liç deneylerine başlanmıştır. Uçucu kül örnekleri, sülfürik asit, hidroklorik asit ve sitrik asit içeren iki inorganik ve bir organik asit liçi

ile işleme tabi tutulmuştur. En iyi liç koşulları, tüm liç deneylerinde %30 asit konsantrasyonunda 90°C'de 24 saat süren liç işlemi olarak belirlenmiştir. Yapılan istatistiksel analiz sonucu parametrelerin etkileri incelenmiş, XRD ve SEM analizleri ile malzemlerin liç sonrası durumu incelenmiştir.

Daha sonrasında sıralı liç yapmanın liç verimini artıracağı görüldüğü için inorganik sıralı liç yapılmıştır. İlk hidrometalurjik liç sülfürik asit kullanılarak yapılmıştır. Liç çökeleği hidroklorik asit içeren ikinci bir liç işlemine tabi tutulmuştur. Uçucu küllerin sıralı liçinin toplam nadir toprak elementleri verimliliği sırasıyla linyit uçucu külü için %86,05, asfaltit uçucu külü için %96,93 ve taş kömürü uçucu külü için %73,45 olarak belirlenmiştir.

Son aşama olarak sıralı liç yapılarak verimlilik artırılmış yüklü solisyona nötralizasyon - seçici çökeltme deneyleri yapılmıştır. Elde edilen yüklü liç çözeltileri, 10 M NaOH çözeltisi kullanılarak pH değerleri önce 4,5'e, ardından 8,5'e yükseltilmiştir. Çöktürme işlemleri, safsızlıklardan arındırma amacıyla iki aşamalı olarak gerçekleştirilmiştir. İlk aşamada Al ve Fe^{+3} safsızlıkları çöktürülmüş, ikinci aşamada pH 8,5'e çıkarılıp nadir toprak elementlerinin çökmesi sağlanmıştır. Uçucu kül malzemeleri, hidrometalurjik liç ve nötralizasyon - seçici çöktürme işlemlerine olumlu yanıt vermiş ve yüksek tenörlü nadir toprak elementleri içeren çökelekler (2830 ppm (linyit uçucu külü), 2765 ppm (asfaltit uçucu külü) and 2232 ppm (taş kömürü uçucu külü))elde edilmiştir.

Anahtar Kelimeler: Liç, Hidrometalürji, Çöktürme, Nadir Toprak Elementleri, Uçucu Kül

To My Loving Family

ACKNOWLEDGMENTS

First and foremost, I would like to sincerely thank my supervisor, Prof. Dr. N. Emre Altun, for all of his help, encouragement, and advice during the course of my thesis work.

Second, I would like to thank Pro. Dr. İlkay Bengü Can and Assoc. Prof. Dr. Mustafa Erkayaoğlu for guiding me in my thesis monitoring committee. Also, I would like to thank Assoc. Prof. Dr. Ergin Gülcan and Assoc. Prof. Dr. Çağlar Sınayuç for their contribution to my doctoral thesis.

Thirdly, I want to express my gratitude to Yiğit Altınsel and Sena Sarılar for their help with my thesis.

Lastly, I want to sincerely thank my mother Gül, my father Özer Kemal, my brother Egemen and my husband Mehmet Aktar. My thesis would never be completed without their support.

TABLE OF CONTENTS

LIST OF TABLES

LIST OF FIGURES

FIGURES

LIST OF ABBREVIATIONS

ABBREVIATIONS	DESCRIPTION
ppm	Parts Per Million
ROM	Run-of-Mine
d_{50}	50 % passing particle size, μm
d_{80}	80 % passing particle size, μm
SEM	Scanning Electron Microscopy
T	Temperature, °C
XRD	X-Ray Diffraction
FT-IR Spectroscopy	Fourier Transform Infrared Spectroscopy
ICP-MS	Inductively Coupled Plasma-Mass Spectroscopy
ICP-OES	Inductively Coupled Plasma-Optical Emission Spectroscopy
EDS	Energy-dispersive X-ray Spectroscopy
RRE	Rare Earth Elements
RRO	Rare Earth Oxides
PLS	Pregnant Leach Solution
˚C	Celsius
cm	centimeter
mm	millimeter
μm	micron meter
g	gram
L	Liter
%	Percent
g/ton	gram/ton
h	hour
rev/min	revolution per minute
l/h	liters/hour

CHAPTER 1

INTRODUCTION

The 17 chemical elements known as rare earth elements (REEs) are grouped together on the periodic table and include yttrium, scandium, and the 15 lanthanides. Due to their comparable geochemical characteristics and tendency to occur in the same deposits as lanthanides, scandium and yttrium are included (Lin, et al., 2017). Because of their wide range of uses in the manufacturing of electronics, oil refining, medicine, and clean energy, rare earth (RE) metals are strategically significant. According to Lin et al. (2017), they are essential parts of car batteries, phosphors for lighting, catalysts for oil refining, magnets for wind turbines and other equipment, and more. Both the U.S. Department of Energy and the European Commission view rare earth elements (REEs) as essential raw materials due to their significant contribution to the modern economy. On the other hand, China produces more than 85% of the raw materials and oxides used in the production of rare earth elements (REEs) worldwide, dominating the mining, separation, refining, and manufacturing processes. The challenges associated with the supply of rare earth elements (REEs) have spurred interest in and research into recovering REEs from secondary resources like coal and fly ash as well as from used goods like lamp phosphors, nickel metal hydride batteries, and REE permanent magnets.

Coal contains rare earth elements among many other trace metal elements, and the majority of rare earth elements are present in coal. (Zhang et al., 2015; Seredin, et al., 2013) It is known to be rare earth element-s combined with inorganic minerals. The global average total concentrations of REY (lanthanides and yttrium) are 68.5 ppm and 404 ppm in coal and coal ash, respectively (Seredin et al., 2013). Recent studies have shown that the minimum concentration of rare earth oxides (REOs) in coal ash should be 800–900 ppm for profitable recovery of REE from coal (Zhang et

al., 2015). Based on this date, Zhang et al. (Zhang, et al., 2015) also estimated the limits for rare earth elements in coal to be 115-130 ppm on a whole coal basis and 677-762 ppm on an ash basis. Therefore, coal and coal byproducts are promising alternative sources for REE extraction.

The extraction of rare earth elements from coal and coal by-products is also hampered by the current limitations in the development of new conventional metal-bearing mines, the diminishing reserves of rare earth metals in conventional deposits, and the difficulty of these with modern technology. This is promising because the applications of valuable metals are increasing.

The development of processes and technologies to economically recover rare earth elements from coal and coal by-products would be innovative and beneficial, especially for countries that are highly dependent on rare earth element imports. On the other hand, incorporating rare earth element recovery processes into coal mining, processing and combustion processes can benefit society by utilizing coal by-products, thereby reducing the environmental impact of these by-products.

1.1   Problem Statement

Rare earth elements have strategic importance because they find numerous applications in various sectors of the global economy and coal is a source of them. Therefore, coal is a resource primarily used for electric power generation and the residues should be utilized. Also asphaltite is being used in electric generation plants and also a source of rare earth elements. In this study, extraction methods of rare earth elements in coal by products, mainly fly ash, of Turkey were examined. Three different coal types was used as hard coal, lignite and asphaltite and their fly ashes. By implementing different methodologies, practicability of the subject was investigated. There are several studies on hard coal and lignite fly ashes all over the world but there was a gap in the literature of Turkish fly ashes. Therefore, the study of asphaltite fly ash was a new topic to study.

CHAPTER 2

LITERATURE REVIEW

2.1   Rare Earth Elements

The Japanese call rare earth elements (REE) the "seeds of technology." Because rare earth elements (REEs) are used in high-tech permanent magnets, lasers, auto catalysts, optical fibers/superconductors, electronic devices, and green energy (Ponou et al., 2016). The continuous development of new advanced technologies has greatly increased the demand for rare earths in the international market, with emphasis on identifying new resources to ensure sufficient supply for current and future uses. These are elements that have become irreplaceable in our technological world thanks to their unique magnetic, phosphorescent, and catalytic properties (Ponou, et al. , 2016). Their atomic structure is responsible for the strong magnetic force and brightness of these elements (King, 2017).

Rare earth elements include scandium (Sc), yttrium (Y) in the third column from the left of the periodic table, and 15 elements from lanthanum (La) to lutetium (Lu) (collectively called lanthanides)17 A group of elements. These are listed under Y, but typically appear separately at the end of the table for space reasons (Figure 2.1 (Spring 8, 2018)). Scandium and yttrium are considered rare earth elements because they typically occur in the same deposits as the lanthanides and have similar chemical properties (King, 2017).

Figure 2.1 Periodic Table

Rare earth elements are not as 'rare' as their name suggests. What is unusual is that they have been discovered in sufficient quantities to support economic mineral development (King, 2017). The most common rare earth elements are cerium, yttrium, lanthanum, and neodymium (Gambogi, 2013). Although thulium and lutetium are two of the least abundant rare earth elements, the average crustal abundance of each is nearly 200 times that of gold ((Haxel, Hendrick, & Orris, 2002).

2.2   History

Rare earths were discovered between 1787 and 1941, a span of nearly 160 years (Szabadvary, 1988; Weeks, 1956). This created the problem of separating scientific and industrial use. The challenge that arose next was how to separate them for use in industry or scientific research. One of the trickiest problems with rare-earth technology has been this one. The most significant advancement was the creation of contemporary separation techniques, which made individual rare earth compounds pure and available in sufficient quantities for research into reduction processes that yield pure metals and alloys and the assessment of their properties, ((Powell & Spedding, 1959), (Beaudry & Gschneidner, Jr. , 1978)).

When the first color televisions hit the market in the middle of the 1960s, there was a sudden demand for rare earth elements. The production of color images required the use of europium (Haxel, Hendrick, & Orris, 2002). In order to achieve this, pure rare earths are being produced on a large scale and are being used in an increasing number of significant commercial applications. High purity single metals, alloys, and compounds, as well as naturally occurring oxide mixtures and products synthesized from them, are examples of the forms of rare earths that are currently available. The world has ample reserves of rare earth elements, enough to last for centuries at current rates of consumption (Krishnamurthy & Gupta, 2016).

In the early 1980s, China started to produce significant amounts of rare earth oxides, and by the early 1990s, it was one of the top producers worldwide. China kept increasing its sway over the world market for rare earth oxides in the 1990s and the first few years of the 2000s (Haxel, Hendrick, & Orris, 2002).

2.3   Applications

Numerous commonplace electronics, such as computer memory, DVDs, rechargeable batteries, cell phones, catalytic converters, magnets, and fluorescent lights, rely on rare earth metals and their alloys.

Rare earth metals are among the many products that demand metals. There were comparatively few mobile phones twenty years ago, but now there are more of them. Rare earth elements are being used in computers and in mobile phones.

Rare earth elements are used to make a lot of rechargeable batteries. Numerous pounds of rare earth compounds are found in the batteries that drive all electric and hybrid cars. As sales of electric and hybrid vehicles are driven by concerns about energy independence, climate change, and other issues, there will likely be a rise in the demand for batteries made from rare earth compounds.

Rare earths find application as abrasives, phosphorus, and catalysts. They are used to polish glass to optical quality, brighten screens in electronic devices, and purify the air.

The national defense also benefits greatly from rare earth elements. Precision-guided weapons, night vision goggles, GPS units, batteries, and other defense electronics are examples of military applications.

Rare earth metals are key ingredients in producing extremely hard alloys used in armored vehicles and projectiles that shatter on impact. The usage of each REE is shown in Figure 2.2 (Şahiner, et al., 2017) (Krishnamurthy & Gupta, 2016).
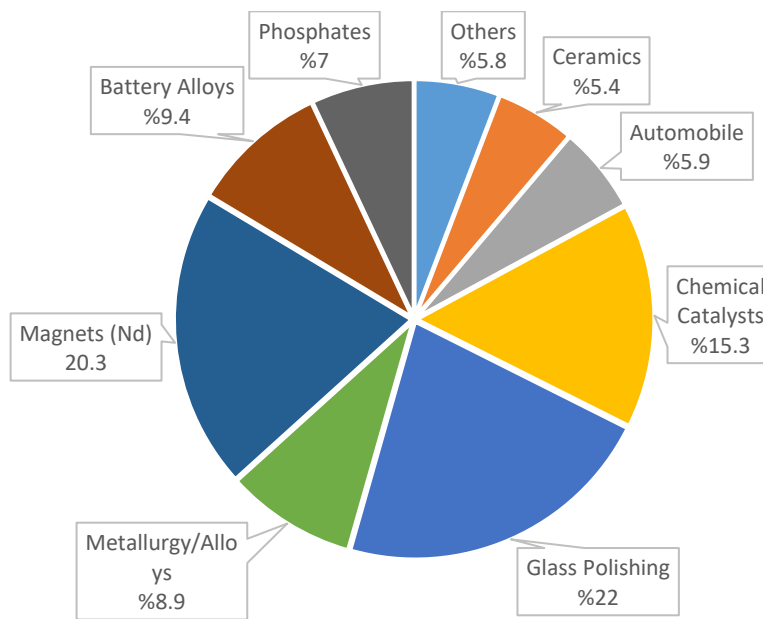
Figure 2.2 Uses of Rare Earth Elements

2.4   Sources of Rare Earth Elements

Although rare earths are relatively common in the Earth's crust, the mineable concentrations found are rarer than most other ores (Gambogi, 2013). Rare earth elements do not occur in nature as naturally occurring elemental metals, but only as

part of the chemistry of their host minerals. Rare earth minerals (REMs) are minerals that contain one or more rare earth elements as their main metallic component. Despite over 250 known rare earth-bearing minerals, only three are considered the most important rare earth minerals that are most suitable for rare earth extraction: bastnasite, xenotime, and monazite (Kumari, et al., 2015).

Bastnaesite is a carbonate mineral that is the most abundant of the three rare earth mineral ores and is primarily rich in LREEs (cerium, lanthanum, yttrium, etc.). Bastnaesite occurs in dyke deposits, contact metamorphic zones, and pegmatites. It is formed in carbonate-silicate rocks that occur in association with alkaline intrusions.

Two phosphate minerals, xenotime and monazite, can exist simultaneously but crystallize at different temperature and pressure ranges from similar magmatic environments. These minerals may contain any rare earth element (i.e., HREE or LREE), but the enrichment of a particular rare earth element is variable and a function of the temperature and pressure region in which they were formed. Monazite is often found in placer deposits. Although xenotime may occur together with monazite, it usually occurs as a minor component of this type of deposit. Phosphate rare earth ore deposits provide an opportunity to produce phosphate and rare earth element by-products. Thorium and uranium can also be used and produced as by-products and can pose significant management challenges (Kumari et al., 2015).

Monazite is generally rich in the LREEs cerium, lanthanum, and neodymium, but may also contain HREEs, especially yttrium. The predominance of LREE is due to the low crystallization temperature and pressure of this mineral. However, they typically contain more HREE than bastnaesite deposits. Occurs in acidic igneous rocks, metamorphic rocks, and some vein deposits. Monazite is weather resistant and occurs in many placer deposits when the host rock is eroded. Thorium can also be combined with monazite in varying amounts. Xenotime crystallizes at higher temperatures and pressures than monazite. Therefore, its crystal structure can easily

accommodate a higher proportion of HREE (terbium to lutetium and yttrium) than is the case with regular monazite. It is primarily a yttrium phosphate mineral, present as a minor component of granite and gneiss (Kumari et al., 2015).

There are two other important REE-containing minerals (Sadri, Rashchi, & Amini, 2017):

- Euxenite: Contains yttrium, erbium, and cerium. It is primarily found in placer deposits and occurs as tantalum oniobate (a mineral in which, for example, Ta and Nb form a compound) of titanium, rare earths, thorium, and uranium.
- Allanite is an epidote mineral that contains cerium, lanthanum, and yttrium. They occur in igneous, metamorphic, and hydrothermal environments, intercalated with pegmatites, or in vein deposits.

These five minerals are considered to be the most important deposits and potentially more important REE reserves in the United States. However, many other minerals containing rare earth elements are also produced, and deposits of these minerals have been discovered in the United States and can be profitable for mining. It is also not uncommon for rare earth elements to be produced as by-products or co-products of other mineral production (Kumari, et al., 2015).

The number of exploitable rare earth element deposits is already severely limited by rare earth geochemistry, but in recent years has also been influenced by environmental and regulatory factors. Monazite, the most abundant rare earth mineral, generally contains high levels of thorium (Haxel, Hendrick, & Orris, 2002).

2.5   Processing Techniques

There are several expensive methods to extract rare earth elements from ores, including pyrometallurgy, hydrometallurgy, etc. for high quality rare earth ores. Furthermore, various methods have been proposed for the separation and

preconcentration of low-concentration rare earth ores, including precipitation, liquid-liquid extraction, solid-liquid extraction, electrowinning, electrorefining, etc. (Ponou et al., 2016).The main stages of processing of a rare earth mineral is shown Figure 2.3 (Kumari, et al., 2015).

```
                          Ore
                           │
                           ▼
                 ┌──────────────────┐
                 │    Crushing/      │
                 └──────────────────┘
                           │
                           ▼
         Salt ───────▶┌──────────────────┐◀─────── Acid or Caustic
                      │    Roasting      │
                      └──────────────────┘
                           │
                           ▼
                 ┌──────────────────┐◀───────  Acidic/Alkali
                 │    Leaching       │
                 └──────────────────┘
                           │
                           ▼
                 ┌──────────────────┐
                 │    Filtration     │──────▶ Residue
                 └──────────────────┘
                           │
                           ▼
                 ┌──────────────────┐
                 │   Purification    │
                 └──────────────────┘
                           │
                           ▼
         ┌────────────────────────────┐           Raffinate or
         │  Precipitation/ Solvent     │──────▶
         │        Extraction           │          Barren Liquor
         └────────────────────────────┘
                           │
                           ▼
                   Rare Earth Salts
```
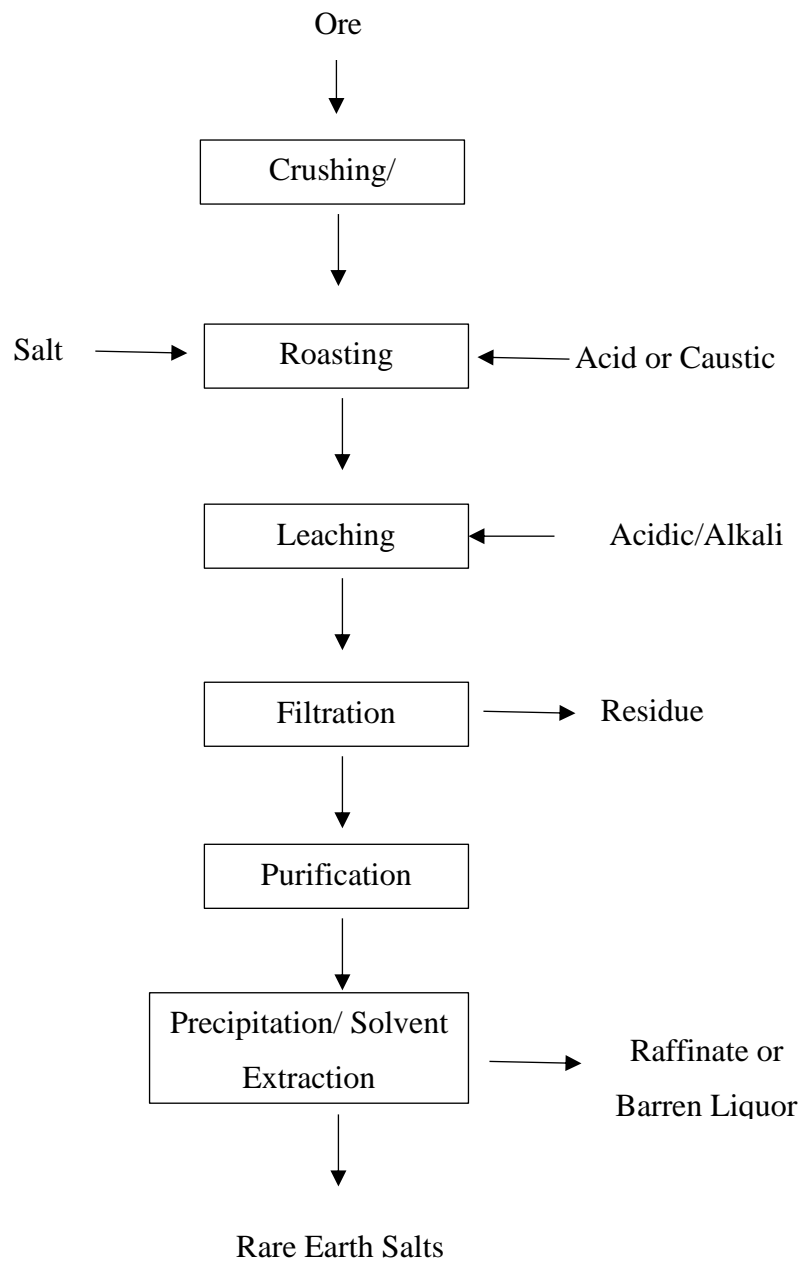
Figure 2.3 Flowsheet of a rare earth element processing (Kumari, et al., 2015)

2.5.1 Physical Beneficiation

When processing minerals for renewable energy from conventional renewable energy deposits, physical separation techniques are frequently employed in conventional processes. Particle size separation, magnetic separation, density separation (also known as gravity separation, flotation separation), electrostatic separation, and flotation sorting are the primary techniques used in this process. According to recent studies, these techniques are only sometimes used to recover rare earth elements from coal and coal byproducts. (Dai, et al., 2016).

Consequently, following coarse grinding (if required), monazite or other minerals containing rare earth elements are separated and concentrated using gravity separation, flotation, electrostatic separation, or magnetic processes. (Lin, et al., 2017).

2.5.1.1 Flotation

Depending on how easy it is to desorb the minerals before separation, phosphate esters or fatty acids can be used as scavengers in the flotation process to produce heavy mineral concentrates from fine-grained marine sand deposits (Ferron et al., 1991). Studies were conducted on the flotation of monazite using sodium oleate as a collector, as well as the effects of sodium sulfide and sodium metasilicate on the buoyancy of monazite zircon rutile and its characteristics (Kumari, et al., 2015).

According to Lin et al. (2017), the only technique available for rare earth enrichment is froth flotation. Monazite concentrate was made from fine and heavy mineral beach sand deposits by combining physical and flotation processes (Ferron et al., 1991). The concept of gravitational separation precludes this. However, since the physicochemical characteristics of monazite have not been established, more research is required to fully understand the flotation of monazite (Kumari et al., 2015).

2.5.1.2 Gravity Separation

Processing rare earth minerals (mostly monazite) frequently involves the use of gravity separation. This is due to the fact that rare earth minerals typically occur in gangue materials, particularly silicates with noticeably lower densities, and have a relatively high specific gravity (Ferron et al., 1991). The low-density vein rocks were first separated by wet gravity separation; all ferromagnetic minerals were then screened out without removing paramagnetic monazite using low-intensity magnetic separation. Additionally, rutile is extracted from paramagnetic monazite using a sequence of gravity, magnetic, and electrostatic separations, after which diamagnetic zircon is extracted using magnetic separation. The distinct characteristics of monazite, zircon, and rutile are It became evident. To create the finished concentrate, minerals are used (Kumari et al., 2015).

2.5.1.3 Electrostatic and Magnetic Separation

Electrostatic separation techniques facilitate the separation of materials according to their respective conductivities. Techniques for electrostatic separation are only employed when other methods of processing are insufficient. Electrostatic separation is used in rare earth processing to separate gangue minerals with similar specific gravity and magnetic properties from monazite and xenotime (Ferron et al., 1991). Since xenotime is not electrically conductive and ilmenite is, after magnetic separation of heavy mineral sands, xenotime—which is far more paramagnetic than monazite—can be concentrated with ilmenite. This allows ilmenite to be produced by electrostatic separation (Kumari, et al., 2015).

In the processing of rare earth minerals, magnetic separation is a widely used technique to concentrate desired paramagnetic rare earth-bearing minerals like xenotime and monazite and to remove highly magnetic vein rocks (Krishnamurthy & Gupta, 2016). In order to prepare monazite from the minerals found in beach sand, highly magnetic minerals like magnetite must be removed by gravity separation

using a magnetic separator. Additionally, it is employed in the separation of non-magnetic heavy vein materials like rutile and zircon from paramagnetic monazite (Ferron et al., 1991).

2.5.2 Processing of rare earth bearing minerals

Since rare earth metals are present in monazite, the most common rare earth-bearing mineral, extraction from such materials necessitates heat treatment followed by leaching, precipitation, and solvent extraction. After heat treatment in appropriate acidic or alkaline solutions to dissolve the metal components, the prepared concentrates are obtained directly or leached (Kumari, et al., 2015). To create the required salt or metal, metals from the leaching solution are eliminated or concentrated using techniques like precipitation, solvent extraction, ion exchange, electrolysis, etc.

2.5.3 Direct leaching of rare earth bearing minerals

Since crystalline phosphate minerals, or rare earth minerals, like monazite, are stable concentrates both chemically and thermally, dissolving them in acids or alkalis. It is not easy to accomplish. To extract composite materials or metals from minerals using acidic or alkaline solutions, the right conditions must be met (Kumari et al., 2015).

2.5.3.1 Direct leaching with acids

In order to dissolve rare earths or unwanted components and obtain concentrates, numerous studies have been conducted on the direct leaching of monazite sand using acidic solutions of sulfuric acid, hydrochloric acid, and nitric acid under various experimental conditions.

2.5.3.1.1 Leaching in sulfuric acid

Sulfuric acid is most commonly used for leaching monazite, where the sulfate (SO_4) ions of H_2SO_4 act as ligands to react with rare earths at high temperatures (Kumari et al., 2015). Below is a list of the reactions that have been documented for the sulfuric acid-bake stage's production of RE sulfate from RE phosphate and carbonate minerals (Kuppusamy & Holuszko, 2022):

$$2REPO_4 + 3H_2SO_4 \leftrightarrow (RE)_2(SO_4)_3 + 6H^+ + 2PO_4^{3-} \tag{1}$$

$$2RECO_3F + 3H_2(SO_4)_3 \rightarrow RE_2(SO_4)_3 + 2HF + 2CO_2 + 2\ H_2O \tag{2}$$
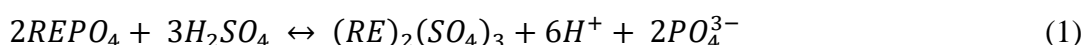
This procedure involves using sulfuric acid to break down monazite, followed by the precipitation of the RE with oxalate anions from a sulfate solution at a pH-controlled level (Welt et al., 1958).

Research has shown that REEs are found in CFA's predominant amorphous glass phase (Guoqiang et al., 2020; Hower et al., 2019; Taggart et al., 2016).

2.5.3.1.2 Leaching in hydrochloric acid

Studies using hydrochloric acid for leaching have been conducted. A batch method for separating Sm, Eu, and Gd from a hydrous lantana oxide cake made from monazite minerals was described in a study by Kumari et al., 2015. This process came about after Ce was separated from nitric acid using di-2-ethylhexyl phosphate/kerosene-hydrochloric acid. After stripping with various acid solutions of varying pH values, a concentrate with a yield of 78% and a content of 98% Sm, Eu, and Gd collectively was obtained.

Equations below present the reactions occur during the leaching process:

$$Al_2O_3 + 6HCl \rightarrow 2AlCl_3 + 3H_2O \tag{3}$$

$$Fe_2O_3 + 6HCl \rightarrow 2FeCl_3 + 3H_2O \tag{4}$$

$$CaO + 2HCl \rightarrow CaCl_2 + H_2O \tag{5}$$

$$MgO + 2HCl \rightarrow MgCl_2 + H_2O \tag{6}$$

$$TiO_2 + 2HCl \rightarrow TiOCl_2 + H_2O \tag{7}$$

$$RE_2O_3 + 6HCl \rightarrow 2RECl_3 + 3H_2O \tag{8}$$

$$Ca_2RE_8(SiO_4)_6O_2 + 28HCl \rightarrow 2CaCl_2 + 8RECl_3 + 6H_2SiO_3 + 8H_2O \tag{9}$$

Demonstrating that when the liquid-solid ratio decreases, the concentration of the H2SiO3 that is produced increases. As was already noted, a colloidal solution forms when the concentration of H_2SiO_3 rises above its saturation concentration, which lowers the leaching efficiency (Zhou et al., 2022).

2.5.3.1.3 Citric Acid Leaching

Citric acid can extract rare earth elements from magnetic fly ash because complexes can be formed. Initially, citric acid separates into its anions and H^+ ions (Li, Ge, & Wu, 2010). After then, hydrogen ions take the place of the rare earth ions, and the latter combine with anions to form soluble metal-ligand complexes (Mcdonald & Whittinghton, 2008).

$$H_3C_6H_5O_7 \leftrightarrow H_2C_6H_5O_7^- + H^+ \tag{10}$$

$$H_6C_6H_5O_7^- \leftrightarrow HC_6H_5O_7^{2-} + H^+ \tag{11}$$

$$HC_6H_5O_7^{2-} \leftrightarrow C_6H_5O_7^{3-} + H^+ \tag{12}$$

The standard complexation reaction of three valence metals can be used to derive the complexation reaction of La, Ce, and Y ions by citric acid anions.

$$La^{3+} + jH^+ + C_6H_5O_7^{3--} \leftrightarrow LaH_j(C_6H_5O_7)_k^{(3+j-3k)} \tag{13}$$

$$Ce^{3+} + jH^+ + C_6H_5O_7^{3--} \leftrightarrow CeH_j(C_6H_5O_7)_k^{(3+j-3k)} \tag{14}$$

$$Y^{3+} + jH^+ + C_6H_5O_7^{3--} \leftrightarrow YH_j(C_6H_5O_7)_k^{(3+j-3k)} \tag{15}$$
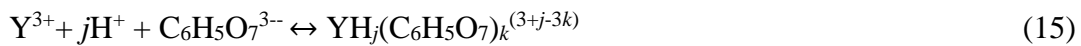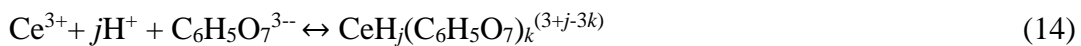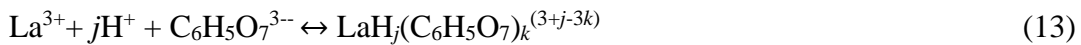
Citric acid dissociates in the solution based on the previously mentioned formulae (Prihutami et. al, 2021). The concentration of citric acid rises, which leads to an increase in the amount of anions involved in rare earth leaching. When a significant amount of citric acid is utilized, the concentration of H+ ions and anions can reach a saturation point because the dissociation of citric acid is a reversible reaction. As a result, the equilibrium moves to the left, resulting in a decrease in the concentration of anions and H^+ ions. Therefore, when an excessively high concentration of citric acid is employed, the recovery value is reduced. At lower temperatures, the impact of citric acid content is less noticeable.

By combining with organic acids to generate soluble metal-ligand complexes, rare earth elements can be extracted from magnetic fly ash. One organic acid that works really well in removing La, Ce, and Y from magnetic fly ash is citric acid (Prihutami et. al, 2021).

2.5.3.2 Leaching Mechanisms

Table 2.1 shows that all NE^{3+} ions have more negative enthalpy of hydration ($\Delta Hhyd$) ions than Na^+ and NH^{4+} ions. It is found that the first ion has a higher tendency to remain in the bulk, which explains why the next two ions are from NE of ion-adsorption clays. It explains that it is used as a solvent for the separation of 3+ ions.

Table 2.1 also shows that the radii of NE^{3+} ions decrease with increasing atomic number, and the charge density of increasing lanthanide ions increases with increasing atomic weight. This allows ions in heavy rare earth elements to be adsorbed more easily on the surface of layered clay minerals than ions from light rare earth elements and provides an explanation that ion adsorption clays are the main source of heavy rare earth elements.

Table 2.1 The relationship between the radii of the NE^{3+} ions and the atomic number (Chi & Tian, 2008)

Cation	Ion	ΔHhyd
La^{3+}	1.06	-3285
Ce^{3+}	1.03	-3340
Pr^{3+}	1.01	-3384
Nd^{3+}	0.99	-3420
Pm^{3+}	0.98	-3445
Sm^{3+}	0.96	-3465
Eu^{3+}	0.95	-3508
Gd^{3+}	0.94	-3522
Tb^{3+}	0.92	-3553
Dy^{3+}	0.91	-3577
Ho^{3+}	0.89	-3621
Er^{3+}	0.88	-3647
Tm^{3+}	0.87	-3668
Yb^{3+}	0.86	-3715
Lu^{3+}	0.85	-3668
Li^{3+}	0.68	-520
Na^{3+}	0.95	-406
NH4^{+}	1.48	-322
Cs^{+}	1.69	-276

Table 2.2 Solubility product constants of oxalates and fluorides (Zhou et al., 2022) lists the solubility product constants of the oxalate and fluoride compounds of REEs and other impurity metals. This shows that the solubility product constants of RE2(C2O4)3 are significantly lower than those of the other impurity elements. As a result, REEs can be precipitated from leachate selectively (Zhou et al., 2022).

Table 2.2 Solubility product constants of oxalates and fluorides (Zhou et al., 2022)

Species	K_{sp}
$La_2(C_2O_4)_3 \cdot 9H_2O$	2.5×10^{-27}
$Ce_2(C_2O_4)_3 \cdot 9H_2O$	3.2×10^{-26}
$La_2(C_2O_4)_3$	7.1×10^{-30}
$Ce_2(C_2O_4)_3$	6.6×10^{-31}
$Pr_2(C_2O_4)_3$	1.2×10^{-31}
$Nd_2(C_2O_4)_3$	2.7×10^{-32}
$Sm_2(C_2O_4)_3$	2.6×10^{-32}
$CaC_2O_4 \cdot H_2O$	2.32×10^{-9}
$MgC_2O_4 \cdot H_2O$	4.83×10^{-6}
$FeC_2O_4 \cdot H_2O$	3.2×10^{-7}
BaC_2O_4	1.6×10^{-7}
$BaC_2O_4 \cdot H_2O$	2.3×10^{-8}
$MnC_2O_4 \cdot 2H_2O$	1.7×10^{-7}
LaF_3	7×10^{-17}
CeF_3	8×10^{-16}
BaF_2	1.84×10^{-7}
CaF_2	5.3×10^{-9}
MgF_2	5.16×10^{-11}
FeF_2	2.36×10^{-6}

2.6 Previous Studies on Rare Earth Elements in Turkey

Özbayoğlu and Atalay done experiments in the preliminary enrichment of the bastnaezite of Beylikahir ore, washed the original ore broken up to -1.65 mm. The sample with a 50% pulp density was diluted and purified with the help of cyclone after washing for 1 hour. Pulp (cyclone overflow), which was collected in front concentrate, was obtained with a 28 %oxide rare earth element (REO) with 72.6 % efficiency. The front concentrate is fed to a mozley multiple gravitational separator

(MGS) for more improvement. As a result, a 35.5 % REO grade and 48 % yield (on the basis of original ore) were produced with a bastnaezite concentrate. The chemical analysis of the concentrate is as follows: CE, 13.75 %; La, 11.81 %; ND, 2.30 %; PR, 1 %; SM, 0.15 %; Y, 0.064 %. H_2SO_4 cure and leaching of the front concentrate with water have shown that > 75% of NTE can be included in the solution (Özbayoğlu & Atalay, 2000)

Kul et al., worked with Beylikahır (Eskişehir) Bastnazit pre-concentrate (low-grade concentrate), after cooking with sulfuric acid (0.91 kg H_2SO_4/concentrated kg, 200°C), followed by water leaning (25 ° C, k/s = 1: 4, 2 SA) and they obtained rare soil sulfates through sedimentation (90 ° C) with sodium sulfate. Acid cooking and leaching results have shown that the recovery of rare soil elements up to 90 % was easily obtained and that it is possible to recover hydrophloric acid as a by -product. Rare soil double sulfate salt from the impurities such as TH, FE, AL, and MG was properly possible with a rapid precipitation at 50 ° C using a stockiometric amount of Na_2SO_4. Total rare soil dual sulfate content > 90 % and its content is 17.3 %, 15.6 %CE, 3.2 %nd, 1.1 %PR, 0.3 cm, 0.03 %EU, 0 % , with 01 YB and 0.02 %Y, approximately 0.7 %Ca, Fe, Al, and other impurities were found. Calcium fluoride (CaF_2) in the ore is converted to gypsum ($CaSO_4$) and remains on the solid. The resulting HF gas can be earned as a by -product (Kul, Topkaya, & Karakaya, 2008).

In their study, Kurşun et al. investigated the solubility of rare earth elements (REE) such as Ce, Nd, and La in bastnasite ore in Eskişehir Kızılcaören region with sulfuric acid (H_2SO_4) and nitric acid (HNO_3). In experimental studies; The effects of pulp solid ratio, acid dosage, leaching time and leaching temperature on REE dissolution efficiency were investigated. The highest REE dissolution efficiency was 35% pulp solid rate, 400 kg/ton HNO_3 dosage, 120 min. It was obtained at leaching time and leaching temperature of 60°C, and Ce, Nd and La dissolution efficiencies were found to be 82.35%, 77.43% and 70.21%, respectively (Kurşun et al., 2017).

Kaya et al., subjected it to pressure leaching by adding H_2SO_4 and various reactive chemicals for 60 minutes at 60°C to separate the Sc element from lateritic nickel ore.

As a result of the data obtained, they determined that the Sc element was recovered with high efficiency, although it was not selective (Kaya et al., 2017).

The separation of thorium from oxalate concentrations including Th, La, Ce, Pr, Nd, Sm, Eu, and Gd was studied by Altaş et al. as part of the technological assessment of the thorium ore at Eskişehir-Beylikahir. First, by adding 100% more oxalic acid than was needed for stoichiometry, thorium-rare earth elements (REEs) oxalate concentration was precipitated from nitric acid solution. The oxalate concentrate's Th and REE contents were selected to mimic the oxalate intermediate that was previously extracted from the percolation fluid. Significant discrepancies in thorium solubility in ammonium oxalate solution serve as the basis for separating it from REEs. Central composite design (CCD) was used to examine the dissolution conditions of thorium-REEs oxalate concentrate at five different levels, with three independent variables. The study examined the impact of independent variables on the thorium dissolving efficiency (%), including contact time, precipitate amount, and ammonium oxalate (AOX) solution concentration (Altaş, et al., 2018).

As part of the technological assessment of the Eskişehir-Beylikahir Thorium-Rare Earth Elements (REE) ore, İnan et al. studied the extraction behavior of light REEs for Amberlite XAD-7 resin impregnated with Cyanex 272. Cyanex 272 that has been diluted with kerosene was impregnated onto Amberlite XAD-7 resin to create solvent impregnated resin, or SIR. The prepared SIR was examined by surface area and porosity analysis, TGA-DSC, SEM, and FTIR. It has been investigated if Cyanex 272 impregnated is useful. Based on experimental evidence, La, Pr, Nd and Sm, Eu, Gd are the two distinct groups in which REEs tend to behave. It has been found that heavier elements replace lighter elements as the load increases (İnan, et al., 2018).

Kurşunoğlu et al. studied the leaching method using HNO_3, H_2SO_4 and HCl to recover La and Cerium from bastnasite ore. As a result of the study, they observed that 85% efficiency was obtained in nitric and sulfuric acid and 90% efficiency in HCl acid (Kurşunoğlu, et al., 2020).

In an alternate study, Kurşunoğlu et al. looked into leaching a thorium-containing bastnasite ore with sulfuric acid cooking water, precipitating with oxalic acid, and thermally decomposing the oxalates to produce mixed rare earth oxide powder. The ideal cooking time for sulfuric acid was discovered to be three hours when the acid was cooked at 250 °C. After 30 minutes of leaching, 92.6% La, 86.8% Ce, 86.9% Pr, 82.3% Nd, 95.4% Th, and 31% Y were dissolved from the ore using deionized water as a solvent and baked at 25 °C. It was discovered that the final combined rare earth oxide powder had 6% ThO2 and 88.54% REO, along with trace levels of other contaminants (Kurşunoğlu, et al., 2021).

Baştürkçü and colleagues investigated the Eskişehir-Beylikova ore. Recent research on the enrichment of Eskişehir ore reported that mechanical abrasion was necessary prior to enrichment of these minerals due to REE accumulation up to 5 µm. Nevertheless, there hasn't been a good explanation of how mechanical wear impacts rare earth element behavior in fine fractions. Consequently, the goal of this study is to provide light on how mechanical etching affects rare earth element enrichment through the application of the MLA approach. As for the outcomes, following mechanical etching, the cleaned sample's -38 µm content rose by 20%, while the proportion of rare earth elements (REEs) rose from 15% to 70%. The mineral composition of REEs dropped to -38 µm, and their degree of release rose by 10–25%. Rare earth carbonate, Th-Parisite, Synschite, Carbocernaite, and Monazite were identified as rare earth minerals based on the EDS data (Baştürkcü et al., 2022).

Güneş et al.'s study investigated the processes that could be used to produce mixed rare earth oxides that don't contain thorium as well as the production technology of rare earth oxides containing barite, fluorite, rare earth elements, and thorium from the Eskişehir-Beylikova region. Roasting, leaching, solvent extraction, and precipitation techniques are the procedures used, in that order. Based on the findings of all the research, 600°C and one hour were found to be the ideal roasting temperature and time.

During the extraction stage, 5 M HCl, 1 hour of leaching time, 1/3 solid/liquid ratio, and 35°C leaching temperature produced the maximum leaching efficiency. Di-(2-ethylhexyl) phosphoric acid (D2EHPA) was used to remove thorium from the generated solution, whereas methyl tri C8-C10 ammonium chloride (Adogen 464) was employed to remove iron. Under ideal circumstances, the solution containing rare earth elements precipitated as a consequence of solvent extraction investigations. 99.65% of the product is made up of rare earth oxides after precipitation (Güneş et al., 2023).

2.7 Coal as a source of Rare Earth Elements

In addition, coal and combustion byproducts like ash, gasification slag, coal processing residue, mine waste, and the layers above and below certain coal seams contain REEs. Due to their high concentrations of heavy rare earth elements (HREEs), certain coals and coal byproducts are desirable from an economic standpoint. According to Robert L. Thompson (2017), HREEs are in short supply, have a high value, are expensive, and their demand is predicted to rise. Recent publications examining the distribution of rare earth elements in coal and coal ash and analyzing the potential for extracting rare earth elements from these resources have drawn a lot of attention, as the market conditions for alternative rare earth resources improve. (Dai et al., 2016; Lin et al., 2017; Hower et al., 2016). According to Robert L. Thompson (2017), the majority of common inorganic lanthanide compounds found in coal, such as phosphates, have high melting, boiling, and pyrolysis temperatures and can concentrate in the byproducts of gasification and combustion. It has been suggested that recovering rare earth elements from coal combustion fly ash would be an addition to mining for rare earth elements (Taggart, Hower, Dwyer, & Hsu-Kim, 2016).

According to Folgueras, Alonso, and Fernandez (2017), 41% of the world's electricity demand is satisfied by coal, which is primarily used for power generation. Rare earth elements (REEs) are strongly retained in the ash content and are

significantly enriched when coal is burned for power generation. This is in contrast to the REE content of the corresponding coking coal. Understanding the distribution of rare earth elements in coal ash is crucial for creating efficient methods of extracting these elements from this promising resource (Kolker, et al., 2017). In coal, argillaceous minerals, silicates, feldspars, oxyhydroxides, phosphates, sulfates, sulfides, and carbonate minerals are typically linked to rare earth elements. At 800 and 1100°C, La, Ce, Pr, and Nd primarily combine with silicates and aluminosilicates in coal ash. According to Folgueras, Alonso, and Fernandez (2017), the remaining rare earth elements—aside from Sm and Yb—combine with carbonates in the ash at 800°C and with sulfates at 1100°C.

Rare earth elements are mostly retained in the solid residue (ash) left over after burning coal for electricity production (Kolker et al., 2017) and do not generally enter the gas phase. Fly ash and slag, which are made from non-combustible minerals that were originally present in the coal, make up the majority of this solid content. When considering the overall mass of the coal, the ash content in commercial coal is comparatively low. Consequently, during the combustion process, REE is preferentially retained in a much smaller mass fraction (Kolker, et al., 2017).

Goldschmidt (1935) was the first to identify the partitioning of rare elements, particularly rare earth elements, in coal ash and to propose their recovery. The possibility of recovering non-energy by-products from these resources was then revisited in case studies by Seredin (1991, 1996), Seredin and Dai (2012), and Seredin et al. (2013), which provided the example of extreme enrichment of rare elements in coal and coal ash, among other things. Rare earth elements are present in trace amounts in coal (REEs). They may exist as separate minerals or as chemicals attached to organic materials. The relationship between the concentration of rare earth elements and ash yield serves as the primary basis for the method used to differentiate between the organic and inorganic associations of rare earth elements in coal (Lin, et al., 2017). Because coal combustion retains rare earth elements, coal fly ash is becoming more and more attention as a potential resource. According to earlier research, coal fly ash has different levels of rare earth element enrichment

when compared to coking coal, and the enrichment increases as the fly ash's size fraction drops (Scott et al., 2015).

Finding coals and their ashes with the highest concentrations of rare elements and developing workable extraction techniques for rare earth elements are the first steps toward the potential recovery of valuable elements from coal and coal ash (Kolker et al., 2017).

Rare metal concentrations in common coal ash and coal-associated sedimentary rocks (Dai et al., 2016; Hower et al., 2016), and concentrations in the ash of some metal-bearing coals are either higher or comparable to those in conventional rare metal ores (Seredin and Dai, 2012). As a result, there has been a lot of interest in coal that contains metals (Dai et al., 2016). Additionally, a global average of 445 ppm of REE is estimated to be present in coal fly ash (CFA) (Blissett, Smalley, & Rowson, 2013).

As a result, the rare earth element content of coal fly ash has been the subject of numerous additional studies. Brissett et al. (2014) looked into fly ash from three bituminous coals in Poland, one anthracite, and two bituminous coals in the UK. All of the coals examined had a similar distribution of rare earth elements in their fly ash, but the British coal's fly ash had the highest concentrations (which were also economically viable) (Blissett & Smalley, 2014). In a 200 MW power plant, Dai et al. (2016) investigated the variation in REE concentration between the coarsest and finest portions of fly ash made from highly volatile bituminous coal from China. They discovered that finer fly ash had a higher concentration of all rare earth elements (Dai, et al., 2016). Additionally, they noted that some fly ash glass phase minerals contained La, Ce, Pr, and Nd (Dai, et al., 2016).

Fly ash from burning lignite and hard coal was examined by Franas et al. (2015), noted that there is a correlation between the content of silica and aluminum and REE. In a similar vein, Querol et al. (1995) discovered that fly ash and slag contain glassy aluminosilicate regions where REE is present. In fly ash from coal, rare earth elements have also been discovered bound to minerals like carbonates and

phosphates. Thus, selmonazite (Ce,La,Nd,Sm,Th,U) was found in the ash of a coal-fired power plant in Poland, and Dai et al. Smolka-Danielowska (2010) found rare earth-bearing calcite in fly ash. (PO_4) was found.

According to a 2005 study by Vassilev and Menendez, pre-separating coal fly ash from thermal power plants in Spain is a more environmentally friendly method of separation than using a lot of highly heterogeneous fly ash. It has been demonstrated that recovering Ce, Gd, and Tb can be done in an environmentally responsible way. According to Scott et al.'s (2015) research, the limited material fractions available at this size make it more difficult to separate smaller fly ash fractions, making them less practical below ~10μm.

According to Lin et al. (2017), the total He REE concentrations across the coal base and the He LREE/HREE ratio both rise with increasing ash yield, but the sum of the He REE concentrations within the ash base increases significantly.

The extraction of rare earth elements (REEs) and other valuable trace elements can be done with a growing supply of raw materials from the combustion of fly ash from coal and coal combined with other fuels like petroleum coke, tires, biomass, etc. (Hower et al., 2013).

The newly formed glass, minerals, and carbon found in fly ash from coal combustion are combined with the mineral matter of the coking coal, the combustion process, and the types of ash, as well as minerals and macerals that pass through the boiler (hower) largely intact. The REE contents of these glasses vary; those rich in Ca and/or Fe have comparable or higher REE contents than those of the main sample, while aluminosilicates, which are made up of Al and Si and lack other major components, typically have REE contents similar to or slightly lower than those of the main sample. Compared to the bulk sample, this has a higher rare earth enrichment. The fly ash components with the highest rare earth contents are typically co-occurring fused silica and/or high silica glasses, which have significantly lower rare earth contents than aluminosilicate glasses. Compared to aluminosilicate

24

glasses, the REE content of iron oxide magnetospheres is more variable, indicating different ratios of light rare earths (LREEs) and heavy rare earths (HREEs).

According to Dai et al. (2017), the majority of rare earth elements that are currently available are extracted from the aluminosilicate glass fraction in coal ash. For this reason, this fraction is crucial to ongoing efforts to recover rare earth elements from coal fly ash.

According to Phuoc, Wang, and McIntyre (2015), burning coal for energy production results in high concentrations of non-volatile minerals in coal ash waste. As a result, the concentration of rare earth elements in coal ash can be concentrated to the level of ore deposits. Therefore, in order to identify and assess ash sources that are candidates for rare earth recovery, it is necessary to analyze the concentration of rare earths in ash waste from coal-fired power plants. To identify rare earth elements in coal and coal byproducts, various techniques such as laser ablation, inductively coupled plasma mass spectrometry (LA-ICP-MS), X-ray powder diffraction (XRD), bulk mineral composition analysis, and chemical analysis (diagnostic leaching) are employed (Thompson, et al., 2018).

2.7.1 Opportunities

Compared to traditional REE ores, fly ash extraction of REE offers a number of benefits. First of all, it is a waste product that is easily accessible, has a sizable market for advantageous reuse, and strong environmental incentives. Secondly, fly ash eliminates the need for large-scale excavation, which can be costly and environmentally hazardous. Large volumes of waste rock with high uranium and thorium contents can be produced by rare earth mineral mines, which presents a problem in terms of radioactive waste. Lastly, chemical processing can be performed with fly ash because it is a fine powder that eliminates the need for several expensive ore processing steps.

Advantages of using coal and coal by-products for the production of rare earth elements can be summarized as follows:

1) Large and reliable resources,
2) Already mined material (no new mining permit required),
3) New mining is prohibited due to potential environmental and health benefits.
4) Using the waste material.

2.7.2   Challenges

Rare earth elements (REEs) are only found in host minerals and do not exist as elemental metals in nature. Because of this, the extraction of rare earth metals (REMs) needs to be done with sophisticated processing techniques that break down the minerals that contain REEs chemically (Gambogi, 2013)).

The difficulty of separating and gathering rare earth elements is one of the difficulties in using them. When using certain rare earth elements, the desired element must be extracted from the mixture because the elements naturally occur in mixtures with ores. Generally speaking, chemical properties like melting and boiling points are used to separate substances. It is challenging to distinguish between rare earth elements because of their similar chemical characteristics.

Solvent extraction is the separation technique currently in use. This process involves mixing an organic solvent solution with an ore that contains rare earth elements. The rare earth elements are then extracted twice: once from the organic phase and again from the aqueous phase (Krishnamurthy & Gupta, 2016).

2.8   Previous Studies on Rare Earth Elements Extraction from Coal by-Products

Seredin et al. (2013) investigated the recovery of rare earth elements (REEs) from coal fly ash using hydrometallurgical processes. The study utilized hydrochloric acid (HCl) and nitric acid (HNO_3) with acid concentrations ranging from 1 to 6 M, temperatures between 60 and 90°C, and leaching times of 2 to 6 hours. The results demonstrated REE recovery rates of up to 70% under optimized conditions, with solvent extraction techniques further purifying the recovered REEs to over 90%. Hydrochloric acid showed the highest recovery rates among the acids tested (Seredin et al., 2013).

Vassilev et al. (2016) conducted a comprehensive review on the presence of REEs in coal and coal fly ash. This study compiled data from various sources and did not specify particular acids or conditions, as it aimed to provide an overview. The results indicated that REE concentrations in fly ash ranged from 200 to 500 ppm, depending on the coal source and combustion conditions. It was found that heavy REEs (HREEs) were more enriched in fly ash compared to light REEs (LREEs), providing detailed geochemical profiles for targeted extraction strategies (Vassilev et al., 2016).

Jiang et al. (2019) explored the extraction of REEs from fly ash using a combined approach of alkali fusion followed by acid leaching. The study employed sodium hydroxide (NaOH) at high temperatures (300-600°C) for alkali fusion, followed by leaching with hydrochloric acid (HCl) at concentrations of 3 to 6 M and leaching times of 2 to 4 hours. The results showed that this combined method achieved REE recovery rates of over 80%. Sodium hydroxide treatment effectively broke down the fly ash matrix, enhancing the subsequent acid leaching efficiency and achieving high selectivity for REEs while minimizing the extraction of unwanted elements (Jianget al., 2019).

Tang et al. (2020) focused on the selective recovery of REEs from coal fly ash using environmentally benign processes. The study investigated bioleaching, utilizing microorganisms without specific acids, and ionic liquids as environmentally friendly solvents. Bioleaching conditions included pH 1.5-2.0, temperatures between 30 and 50°C, and durations of 10 to 20 days, while ionic liquid conditions varied based on specific compositions. Bioleaching achieved REE recovery rates of approximately 50-60%, with a lower environmental impact compared to traditional acid leaching. Ionic liquids showed high selectivity for REEs, with recovery rates around 70%. Both methods demonstrated potential for sustainable and environmentally friendly REE extraction (Tang et al., 2020).

Zhang et al. (2021) provided an overview of hydrometallurgical processing techniques for REE extraction from coal fly ash. The study reviewed the use of sulfuric acid (H_2SO_4), hydrochloric acid (HCl), and nitric acid (HNO_3), with acid concentrations ranging from 1 to 6 M, temperatures between 60 and 90°C, and leaching times of 2 to 8 hours. The results indicated that acid leaching with sulfuric and hydrochloric acids yielded the highest REE recovery rates, ranging from 60 to 80%. Alkaline leaching with sodium hydroxide also showed promising results for certain REEs. The study emphasized the importance of optimizing leaching parameters to maximize recovery while minimizing environmental impact (Zhang et al., 2021).

Shaw et al. (2022) conducted pilot-scale testing of an integrated process for the extraction of REEs from coal fly ash. The study used hydrochloric acid (HCl) and sulfuric acid (H_2SO_4) with acid concentrations of 2 to 4 M, temperatures between 60 and 80°C, and leaching times of 4 to 6 hours. The pilot-scale testing achieved overall REE recovery rates of 75-85%. The integrated process demonstrated scalability and potential for commercial application, with consistent recovery rates across different fly ash samples. The multi-stage approach, combining physical pre-concentration, acid leaching, and solvent extraction, proved effective in maximizing REE recovery and purity (Shaw, Nash, & Miller, 2022).

Zhang et al. (2015) explored the extraction of rare earth elements (REEs) from coal fly ash using supercritical carbon dioxide (scCO$_2$) and chelating agents such as diethylenetriaminepentaacetic acid (DTPA). The experimental conditions included pressures of 10-20 MPa, temperatures of 40-80°C, and extraction times of 1-5 hours. The method achieved REE recovery rates of up to 65%, demonstrating that scCO$_2$ and chelating agents were effective in selectively extracting REEs with minimal co-extraction of other elements (Zhang et al., 2015).

Li et al. (2017) investigated the recovery of REEs from fly ash using a combination of magnetic separation and acid leaching. The study employed hydrochloric acid (HCl) and sulfuric acid (H$_2$SO$_4$) with acid concentrations of 2-5 M, temperatures of 70-90°C, and leaching times of 2-6 hours. The combined process achieved REE recovery rates of approximately 75%, with hydrochloric acid proving more effective than sulfuric acid in leaching REEs from the magnetically separated fraction (Li, Wang, & Yu, 2017).

Wu et al. (2018) examined the effects of thermal treatment followed by acid leaching to enhance the recovery of REEs from coal fly ash. The study utilized hydrochloric acid (HCl) for leaching, with thermal treatment conducted at 600-800°C, followed by leaching with 3-6 M HCl at 60-90°C for 2-4 hours. The results showed that thermal treatment significantly improved leaching efficiency, leading to REE recovery rates of up to 80%. This demonstrated the potential of pre-treatment processes in enhancing REE extraction yields (Wu et al., 2018).

Ribeiro et al. (2019) researched the use of amino acids as leaching agents for the recovery of REEs from coal fly ash. The study used amino acids such as glycine and glutamic acid, with leaching agent concentrations of 0.5-2 M, temperatures of 50-70°C, and leaching times of 4-8 hours. The results indicated REE recovery rates of 55-65%, suggesting that amino acids could serve as an environmentally friendly alternative to traditional acids for REE extraction (Ribeiro, Silva, & Ferreira, 2019).

Kang et al. (2020) investigated the enhancement of REE extraction from coal fly ash through ultrasonic-assisted leaching. The study used hydrochloric acid (HCl) with

acid concentrations of 3-6 M, ultrasonic frequencies of 20-40 kHz, temperatures of 50-80°C, and leaching times of 1-3 hours. The ultrasonic-assisted method increased REE recovery rates to around 70-80%, significantly reducing leaching time and improving extraction efficiency (Kang, Zhang, & Wang, 2020).

CHAPTER 3

MATERIALS AND METHOD

3.1   Materials

In this study, Lignite Fly Ash (SFA), Asphaltite Fly Ash (AFA), and Hard Coal Fly Ash (HFA) were used in order to extract rare earth elements (REE). Approximately 100 kg of Fly Ash samples delivered to the laboratory were first prepared in accordance with standard representative sample preparation methods in order to obtain samples to be used in chemical characterization and hydrometallurgy tests.

3.1.1   Sample Preparation

First of all, representative sample preparation processes were carried out for the chemical characterization of Fly Ash samples and their preparation for hydrometallurgical leaching tests.

From the approximately 100 kg sample received (SFA, AFA, and HFA), representative samples were prepared to be used in characterization and hydrometallurgical leaching tests using standard cone - quartering processes and Jones Riffles of various sizes, since the particle size was suitable for representative sample preparation processes.

A large sample can be divided into many kilogram samples using the cone and quartering method. On a spotless surface, the material is blended and heaped into a cone form. The cone is flattened to form a frustum. The upper surface of the frustum was divided into four equal sections using a hard stick or a straight cross (Figure 3.1). Two of the opposing quarters are taken out with a shovel, while the remaining two are joined, piled, flattened, and divided into four new quarters. Repeat coning

and quartering until the necessary sample size from large bulks is fairly representative.

Figure 3.1 Cone and Quartering

The V-shaped chute riffler is composed of an equal number of chute apertures of corresponding sizes that are alternately placed on both sides. The material enters a chute riffler trough, where it is split approximately in half and placed onto two trays on either side of the apparatus Figure 3.2. With each cycle through the device, the sample size is halved until the required sample size is obtained. With this apparatus, head samples weighing less than one kilogram can be divided. It is more effective than the cone and quartering approach.

Figure 3.2 Chute Riffler

In order to check the representativeness of the samples at the end of the sample preparation, number of samples are selected randomly and tested.

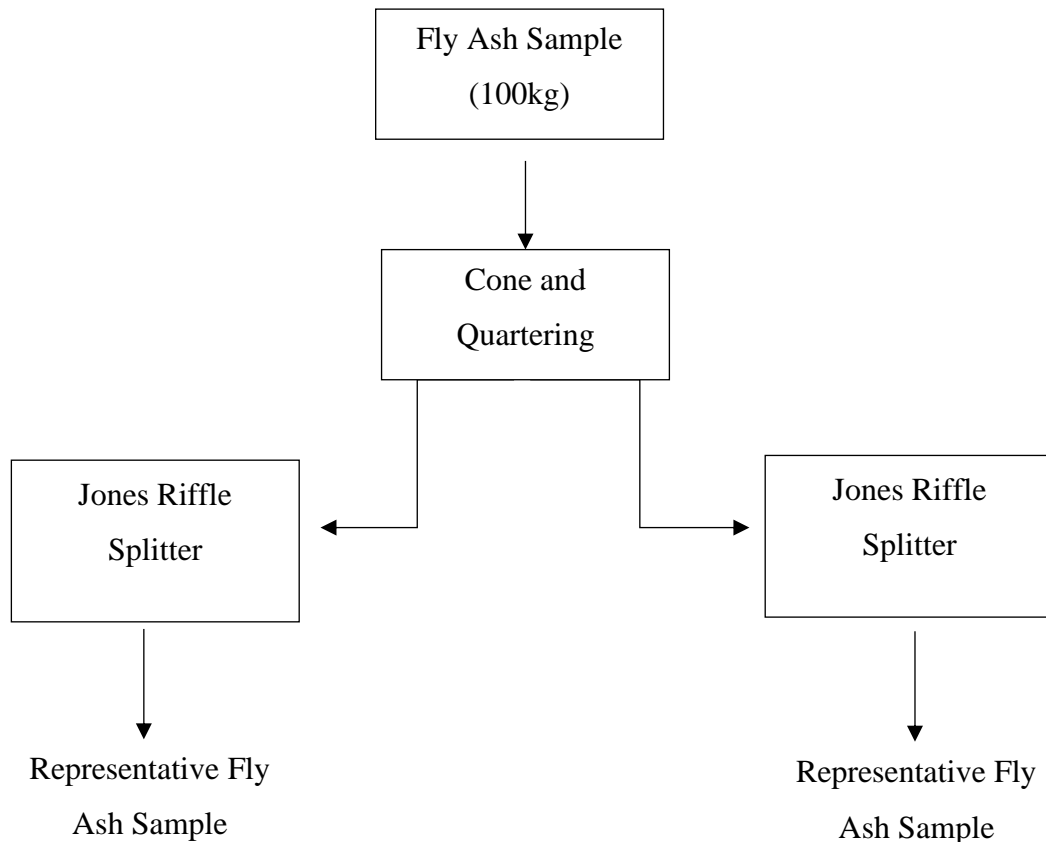Basic flowsheet for the representative sample preparation is shown in Figure 3.3.

```
                    ┌─────────────────┐
                    │  Fly Ash Sample │
                    │     (100kg)     │
                    └─────────────────┘
                             │
                             ▼
                    ┌─────────────────┐
                    │    Cone and     │
                    │   Quartering    │
                    └─────────────────┘
              ┌──────────┘         └──────────┐
              ▼                                 ▼
    ┌─────────────────┐              ┌─────────────────┐
    │   Jones Riffle  │              │   Jones Riffle  │
    │    Splitter     │              │    Splitter     │
    └─────────────────┘              └─────────────────┘
              │                                 │
              ▼                                 ▼
    Representative Fly               Representative Fly
      Ash Sample                       Ash Sample
```

Figure 3.3 Flowsheet of Sample Preparation

3.1.2   Characterization of the Samples

Representative feed samples were subjected to chemical analysis to determine their elemental composition, specifically Rare Earth Elements (REE) contents. Chemical analyzes of the samples were performed using Inductivity Couples Plasma - Mass Spectroscopy (ICP-MS) device. Three parallel analyzes were performed on all samples and the results were averaged. The mineral phases determined by X-ray Diffraction (XRD) analysis. Size analysis done by Mastersizer Particle Size analyzer.

SEM (Scanning electron microscopy) analysis has shown the elemental composition, morphology, and microstructure of samples by high resolution images. The chemical content of each feed material is given in further sections below.

3.1.2.1   Lignite Fly Ash

Lignite fly ash came from the thermal power plant located in Soma district of Manisa province. The coal has 2,400 kcal/kg calories, 32% ash content, and 21% moisture content.

The chemical characterization data is shown in Table 3.1. Based on the chemical characterization results, it was determined that the total rare earth grade of the feed material was 364.82 ppm. In addition, it was observed that the material had 13.85% Ca, 10.65% Al, 13.85% Si and 4.15% Fe content as the main impurity elements. It is a silicocalcic type fly ash.

The X-ray diffraction of the mineralogical composition of the lignite fly ash is given in Figure 3.4. According to that, volatile ash generally contains crystal phases and glassy structure. Crystallized phases were 63% Anhydrate ($CaSO_4$), 17% Quartz (SiO_2), 12% Albite ($Na(AlSi_3O_8)$) and impurities (i.e. hematite (Fe_2O_3)).

It has been seen that the lignite fly ash consists of spherical and angular particles of dimensions ranging from 1-50 microns as a result of morphological examination. It has been found that small particles with 1-20 micron diameter in particular are mostly spherical structure (Figure 3.5 & Figure 3.6).

Based on the particle size analysis (Figure 3.7 & Figure 3.8) results feed material was having 82 % of -45µm size and 18.4µm d_{50}.

Table 3.1 Compositional Characteristics of Lignite Fly Ash

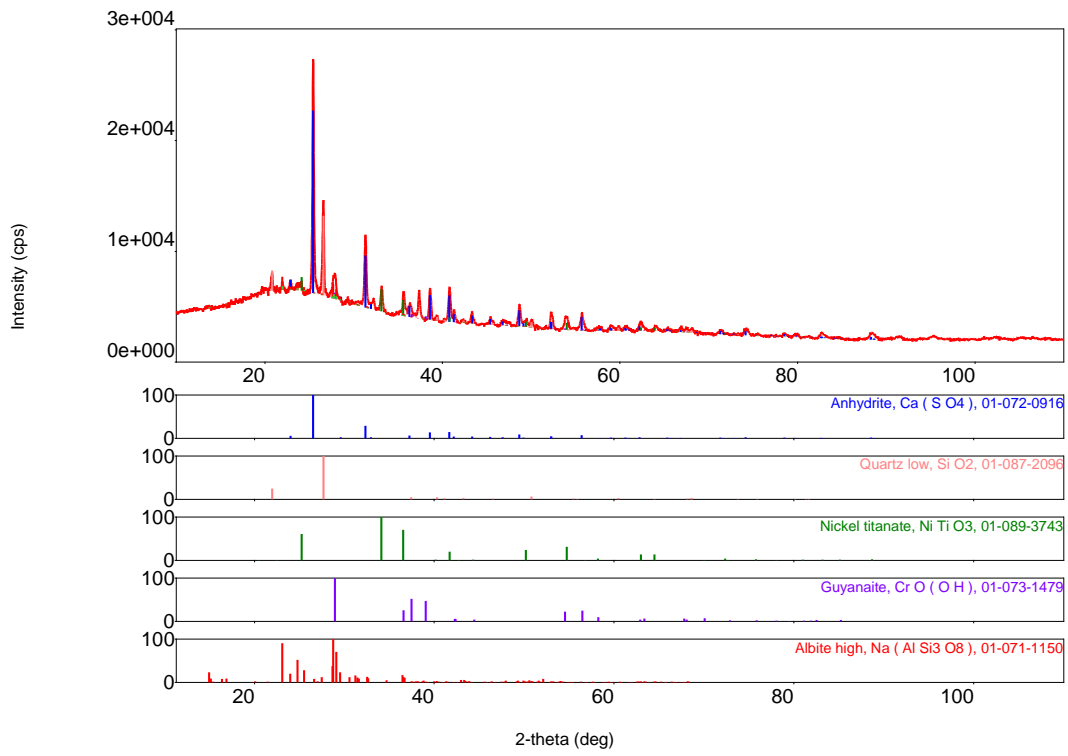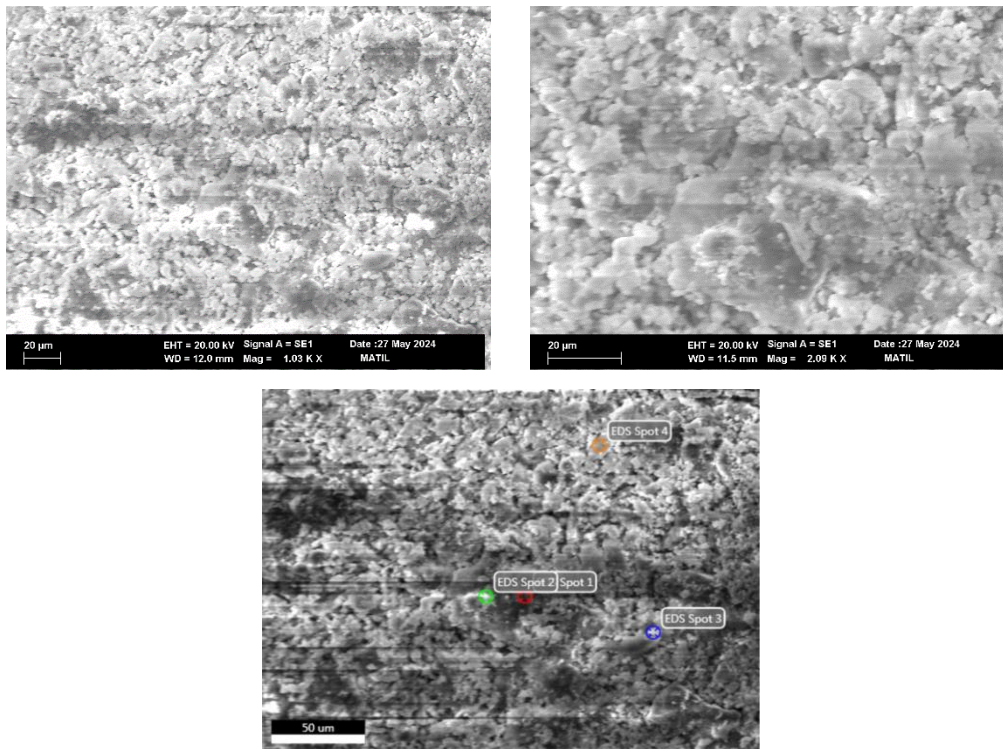| Element	Concentration	Unit
Al	10.65	%
Si	13.85	%
Ca	13.85	%
Fe	4.15	%
Sc	27	ppm
Y	48.5	ppm
La	66.5	ppm
Ce	116	ppm
Pr	14	ppm
Nd	50	ppm
Sm	9.65	ppm
Eu	2.2	ppm
Gd	9.2	ppm
Tb	1.3	ppm
Dy	7.7	ppm
Ho	1.6	ppm
Er	4.85	ppm
Tm	0.7	ppm
Yb	4.85	ppm
Lu	0.77	ppm
Th	34.5	ppm
V	1100	ppm
Sr	263.5	ppm
U	71.5	ppm

Figure 3.4 XRD Analysis of Lignite Fly Ash

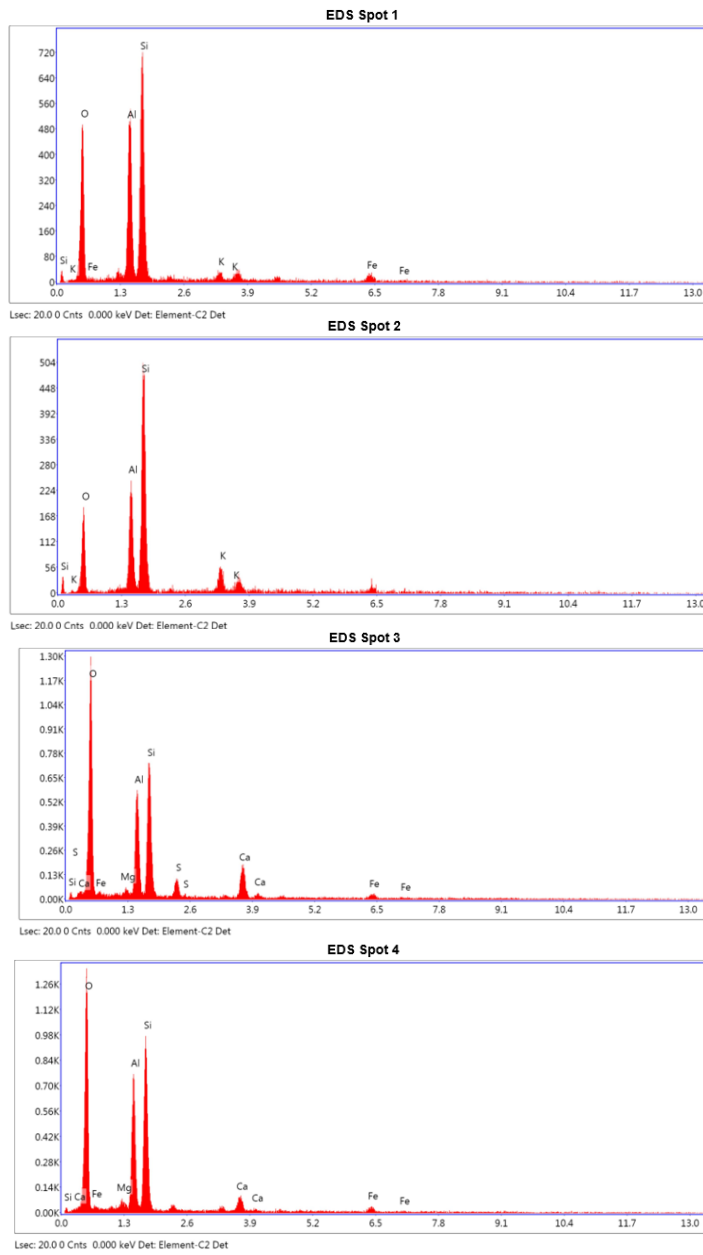Figure 3.5 SEM Images of Lignite Fly Ash

Figure 3.6 EDS analysis of the different spots of Lignite Fly Ash

Table 3.2 Size Analysis of Lignite Fly Ash

Particle Size (μm)	Weight (%)	Cum. Undersize (%)	Cum. Oversize (%)
+850	0.00	100.00	0.00
-850+600	0.00	100.00	0.00
-600+425	0.00	100.00	0.00
-425+300	0.00	100.00	0.00
-300+212	0.00	100.00	0.00
-212+150	0.00	100.00	0.00
-150+106	0.68	99.32	0.68
-106+75	3.72	95.60	4.40
-75+53	8.47	87.13	12.87
-53+38	11.64	75.49	24.51
-10+38	40.60	6.71	65.11
-10+0	34.89		100.00

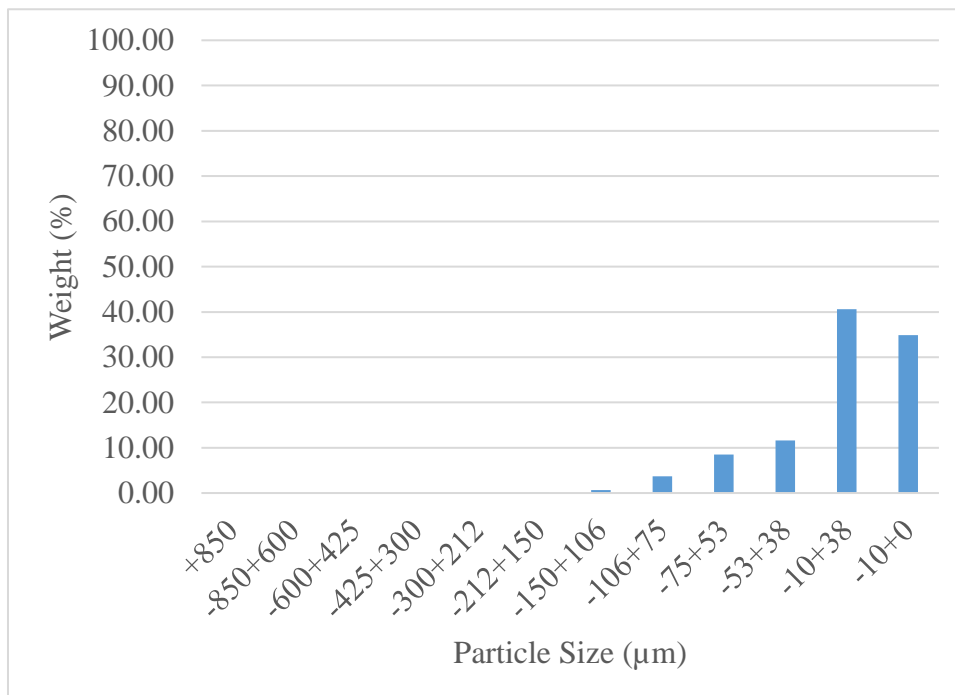|	
D_{10} (μm)	2.22
D_{50} (μm)	18.4
D_{90} (μm)	58.4

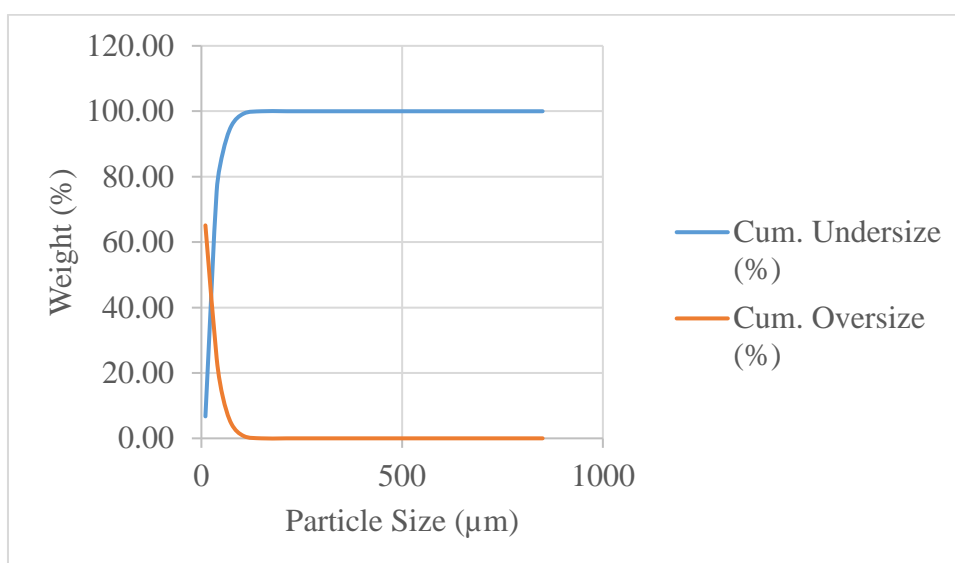Figure 3.7 Size Analysis of Lignite Fly Ash

Figure 3.8 Particle size distribution of Lignite Fly Ash

3.1.2.2   Asphaltite Fly Ash

Asphaltite fly ash came from the thermal power plant located in Silopi, Şırnak. Asphaltite has 5500 kcal/kg calories, 35% ash content, and 4-7% sulfur content.

The chemical characterization data is shown in Table 3.3. Based on the chemical characterization results, it was determined that the total rare earth grade of the feed material was 380.99 ppm. In addition, it was observed that the material had 2.2% Ca, 12.6% Al, 26.0% Si and 4.6% Fe content as the main impurity elements. It is a silicoaluminus type fly ash.

The XRD of the asphaltite fly ash is given in Figure 3.9. According to that, volatile ash generally contains crystal phases and glassy structure. Based on the XRD results, fly ash contains 41% Calcium Sulfate ($CaSO_4$), 20% Akermanite-gehlinite ($Ca_2(MgO_5Al_{0.5})(Si_{1.5}Al_{0.5}O_7)$), 23% Orthoclase ($K(AlSi_3)O_8$), and impurities.

It has been seen that the lignite fly ash consists of spherical and needle type particles of dimensions ranging from 1-50 microns as a result of morphological examination (Figure 3.10 & Figure 3.11).

Based on the particle size analysis results (Figure 3.12 & Figure 3.13) feed material was having 86 % of -45µm size and 8µm d_{50}.

Table 3.3 Compositional Characteristics of Asphaltite Fly Ash

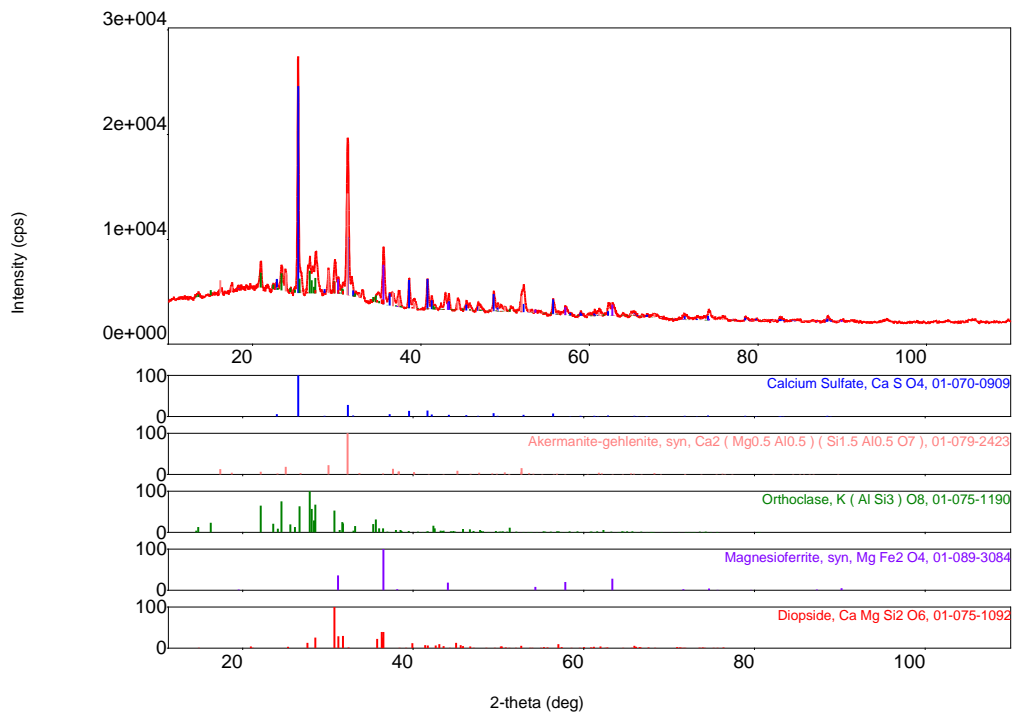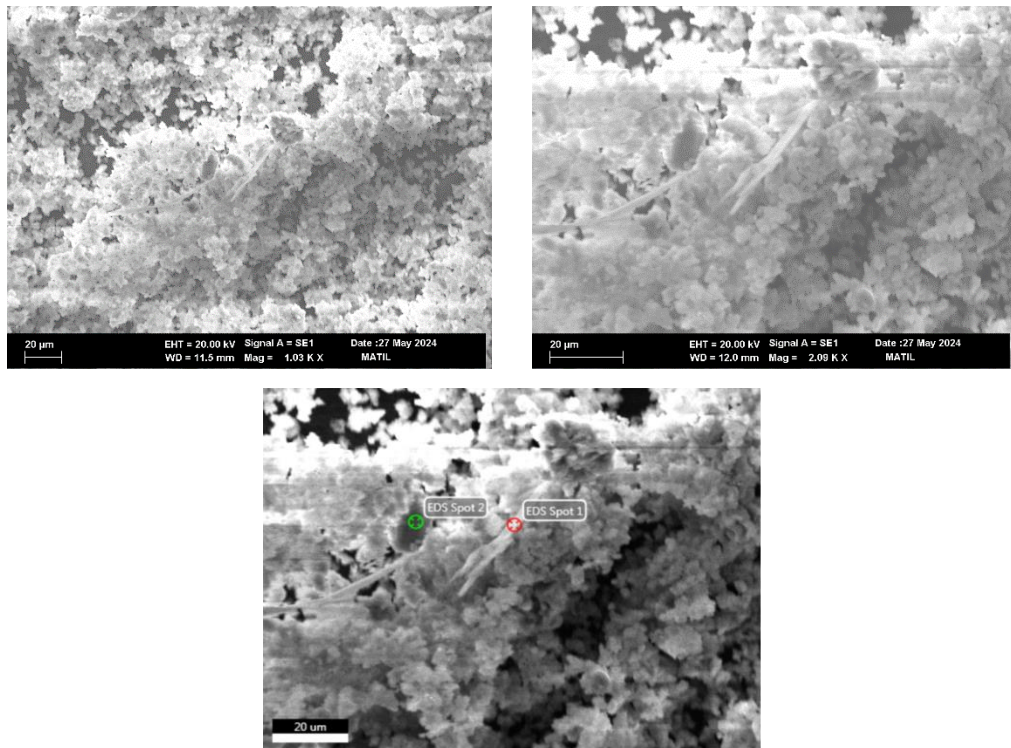| Element	Concentration	Unit
Al	12.60	%
Si	26.00	%
Ca	2.20	%
Fe	4.60	%
Sc	29.00	ppm
Y	118.27	ppm
La	61.01	ppm
Ce	43.13	ppm
Pr	13.01	ppm
Nd	55.30	ppm
Sm	10.68	ppm
Eu	2.62	ppm
Gd	13.71	ppm
Tb	1.93	ppm
Dy	12.03	ppm
Ho	3.25	ppm
Er	8.38	ppm
Tm	1.11	ppm
Yb	6.59	ppm
Lu	0.97	ppm
V	6784.82	ppm
Sr	637.02	ppm
U	236.49	ppm
Th	5.90	ppm

Figure 3.9 XRD Analysis of Asphaltite Fly Ash

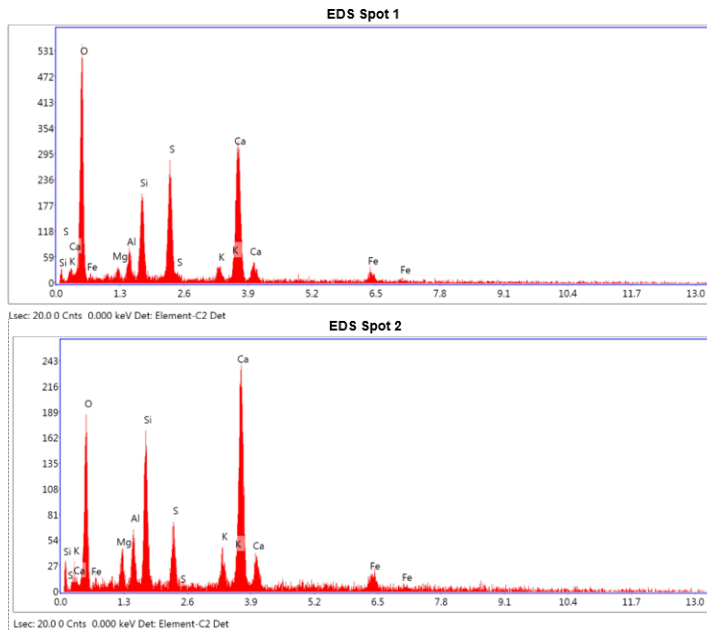Figure 3.10 SEM Images of Asphaltite Fly Ash

Figure 3.11 EDS analysis of the different spots of Asphaltite Fly Ash

Table 3.4 Size Analysis of Asphaltite Fly Ash

Particle Size (μm)	Weight (%)	Cum. Undersize (%)	Cum. Oversize (%)
+850	0.00	100.00	0.00
-850+600	0.00	100.00	0.00
-600+425	0.00	100.00	0.00
-425+300	0.00	100.00	0.00
-300+212	0.03	99.97	0.03
-212+150	0.36	99.61	0.39
-150+106	1.43	98.18	1.82
-106+75	3.45	94.73	5.27
-75+53	5.43	89.30	10.70
-53+38	6.32	82.98	17.02
-10+38	26.98	6.71	44.00
-10+0	56.00		100.00

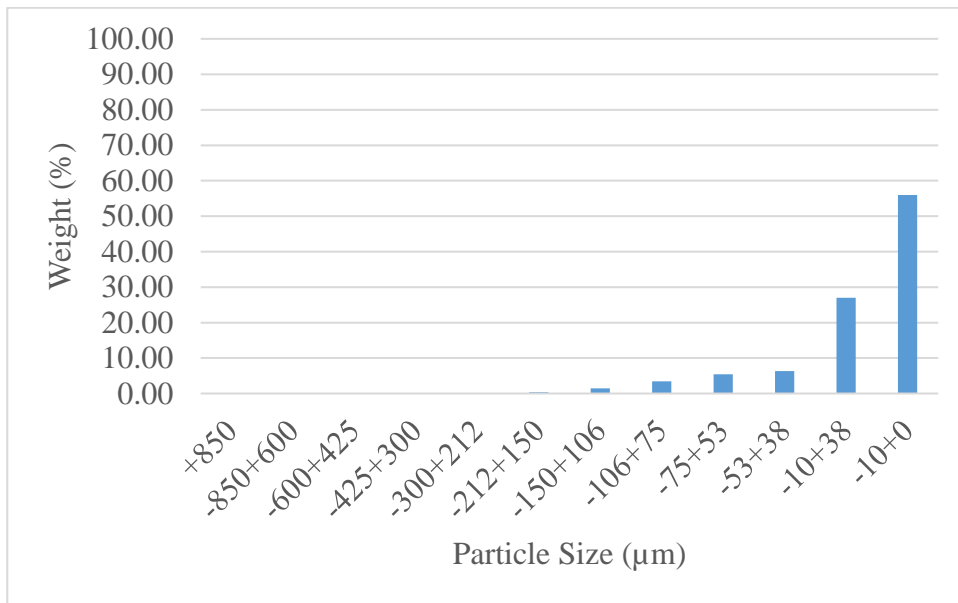| Particle Size	Weight (%)
D_{10} (μm)	1.87
D_{50} (μm)	8.01
D_{90} (μm)	55.2

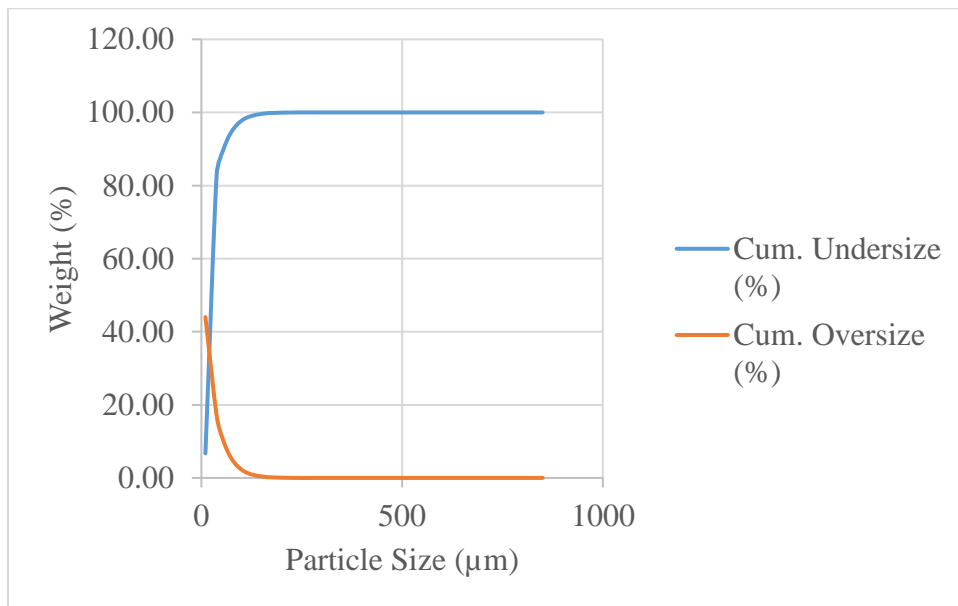Figure 3.12 Size Analysis of Asphaltite Fly Ash

Figure 3.13 Particle size distribution of Asphaltite Fly Ash

3.1.2.3　Hard Coal Fly Ash

Hard Coal fly ash came from the Çatalağzı Thermal Power Plant located in Zonguldak. The coal has 3,300 kcal/kg calories, 45% ash content, and 18% moisture content.

The chemical characterization data is shown in Table 3.5. According to the chemical characterization results, it was determined that the total rare earth grade of the feed material was 464.61 ppm. In addition, it was observed that the material had 16.5% Ca, 5.5% Al, 14.8% Si and 4.4% Fe content as the main impurity elements. It is a silicocalcic type fly ash.

The X-ray differentials of the Hard Coal fly ash mixture samples are given in Figure 3.14. Accordingly, the fly ash is generally composed of glassy structure and less crystal phases Crystallized phases were detected as 57% Quartz (SiO_2) and 43% Mullite ($Al_{4.52}Si_{1.48}O_{9.74}$). This analysis shows that the glassy phase is in the silicon-rich alumino-silicate composition.

It has been seen that the Hard Coal fly ash consists of spherical particles of 1-120 microns as a result of morphological examination. In particular, small particles with 5-15 microns diameter have been found to be full spherical structure (Figure 3.15 & Figure 3.16).

Based on the particle size analysis results (Figure 3.17 & Figure 3.18) feed material was having 66 % of -45µm size and 20.1µm d_{50}.

Table 3.5 Compositional Characteristics of Hard Coal Fly Ash

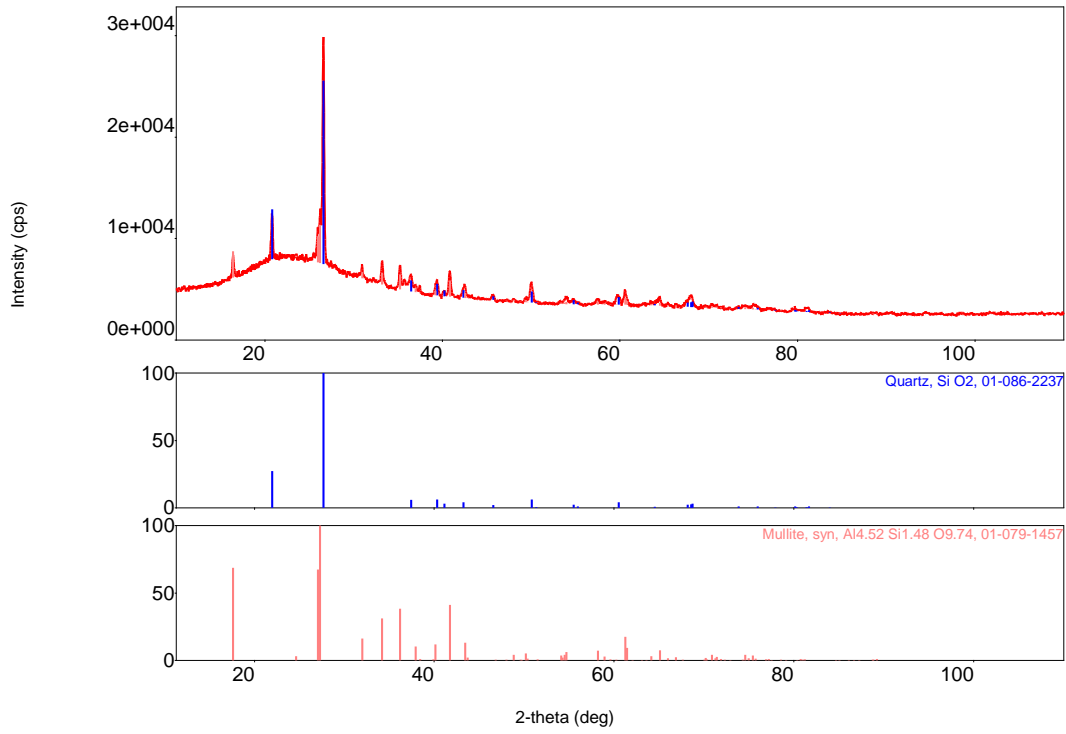| Element	Concentration	Unit
Al	5.50	%
Si	14.80	%
Ca	16.50	%
Fe	4.40	%
Sc	29.57	ppm
Y	111.14	ppm
La	62.66	ppm
Ce	126.20	ppm
Pr	11.69	ppm
Nd	54.65	ppm
Sm	11.66	ppm
Eu	2.72	ppm
Gd	23.15	ppm
Tb	1.75	ppm
Dy	11.77	ppm
Ho	2.53	ppm
Er	7.44	ppm
Tm	0.97	ppm
Yb	5.81	ppm
Lu	0.90	ppm
Th	6.80	ppm
V	5278.01	ppm
Sr	568.02	ppm
U	204.23	ppm

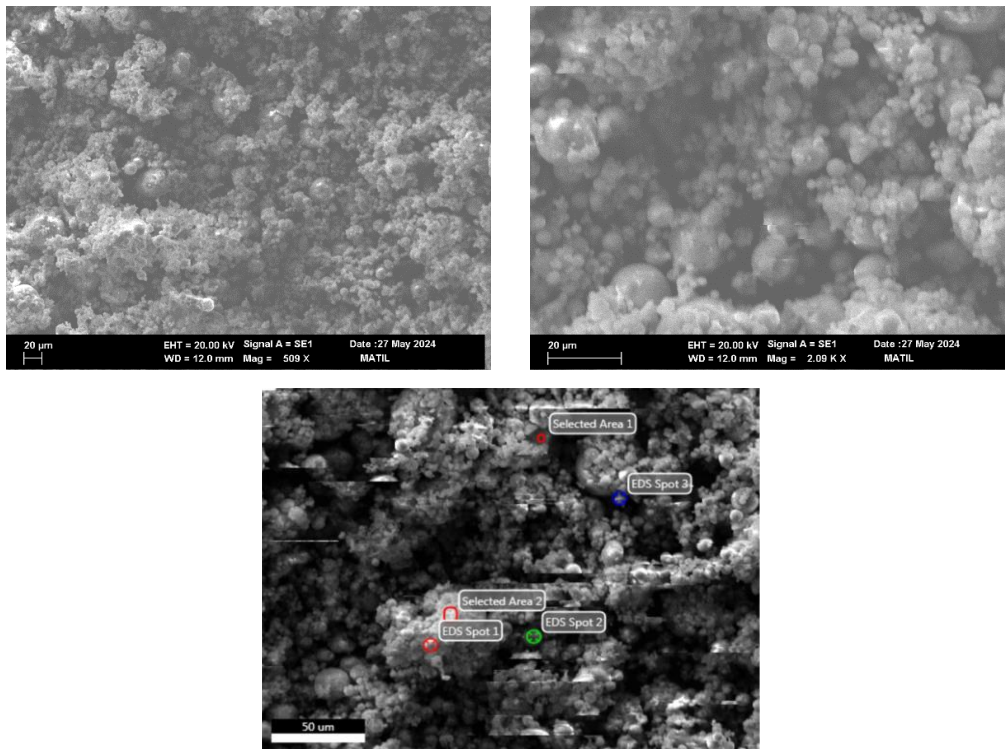Figure 3.14 XRD Analysis of Hard Coal Fly Ash
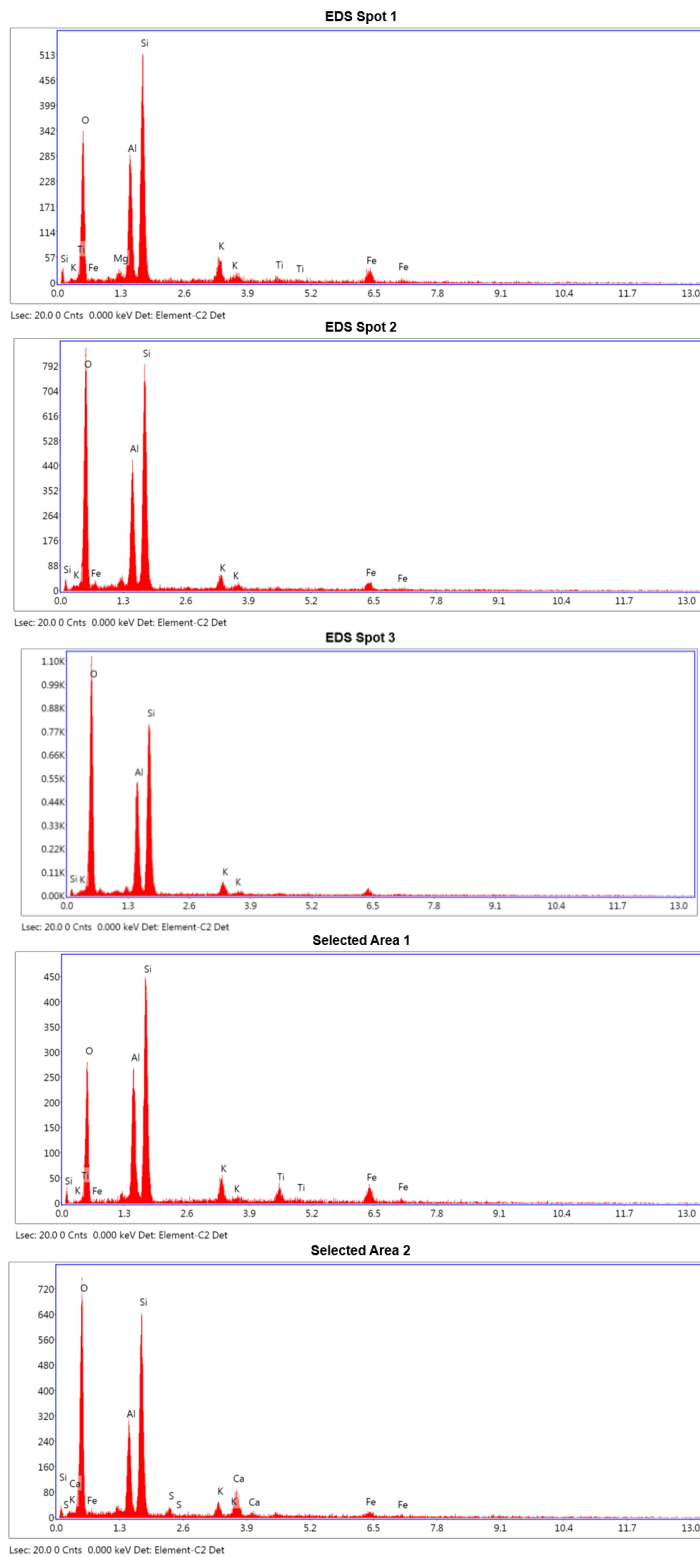

Figure 3.15 SEM Images of Hard Coal Fly Ash

Figure 3.16 EDS analysis of the different spots and areas of Hard Coal Fly Ash

Table 3.6 Size Analysis of Hard Coal Fly Ash

Particle Size (µm)	Weight (%)	Cum. Undersize (%)	Cum. Oversize (%)
+850	0.00	100.00	0.00
-850+600	0.04	99.96	0.04
-600+425	1.02	98.94	1.06
-425+300	3.44	95.50	4.50
-300+212	5.10	90.40	9.60
-212+150	5.44	84.96	15.04
-150+106	5.10	79.86	20.14
-106+75	5.28	74.58	25.42
-75+53	5.44	69.14	30.86
-53+38	5.79	63.35	36.65
-10+38	31.77	6.71	68.42
-10+0	31.58		100.00

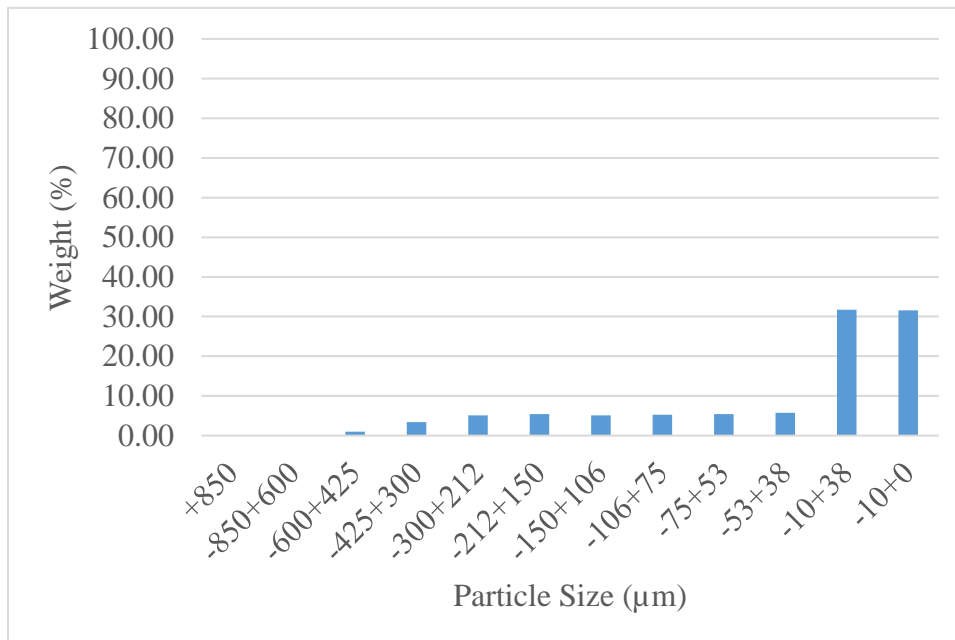|	
D_{10} (µm)	4
D_{50} (µm)	20.1
D_{90} (µm)	207

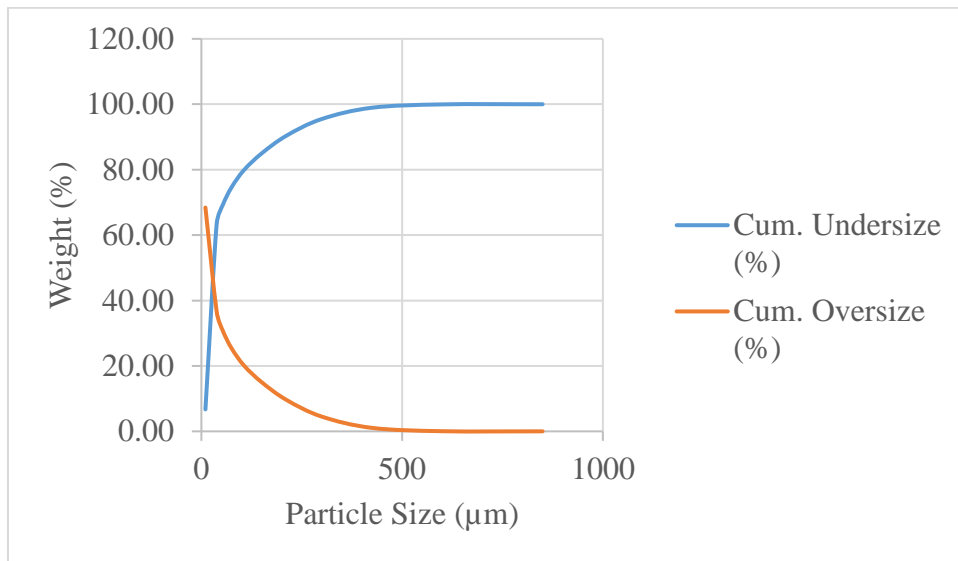Figure 3.17 Size Analysis of Hard Coal Fly Ash

Figure 3.18 Particle size distribution of Hard Coal Fly Ash

3.2 Method

After the chemical characterization of the feed material, based on the structure of the material, it is aimed to extract the rare earth element contents by taking them into the solution phase through hydrometallurgical leaching processes and thus to recover them. The purpose of leaching is chemical demineralization of coal fly ash and concentrate the rare earth minerals by using acidic solutions. Demineralization of the fly ashes were investigated by ICP-MS and the results were compared.

Hydrometallurgical leaching tests were carried out under atmospheric conditions in 3 liter double-walled beakers using temperature-controlled mechanical stirrers (Figure 3.19). During the leaching tests, previously prepared representative feed samples (75 gr.) were used and mechanical mixing was applied to provide a homogeneous mixture to increase the leaching efficiency. The tests were carried out at a solid-liquid ratio of 1/10, and the ore was fed following heating of the acid solution to the targeted temperature before each test. A controlled leaching process was ensured by measuring the pH values of the solution both at the beginning and at the end. After experiments slurry was filtered in a press filter in order to separate the

leach residue and leach solution obtained after the leaching processes, and thus to enable solid/liquid separation. The leach residue obtained after filtration was washed using distilled water and dried in a laboratory type oven at 100°C. Following the drying process, the products were weighed and the samples were prepared for chemical analysis. For all the tests three parallel experiments were performed and the results were averaged.

Figure 3.19 Leaching Tests Experimental Setup

The recovery of Rare Earth Elements was calculated by using following formula (Mokoena, Mokhahlane, & Clarke, 2022):

$$R\% = \frac{VC_2}{MC_1} x100\%$$

where, R% = REE Recovery %

    V = volume of leachate, ml

    M = mass of fly ash sample, g

    C_1 = the element content in sample, ppm

    C_2 = the element concentration in leachate, ppm

In this context, the first focus was taking the rare earth elements into the solution during hydrometallurgical leaching. The second focus was on obtaining a precipitate relatively enriched in rare earth elements by removing the basic impurities of the material during hydrometallurgical leaching and neutralization - selective precipitation processes.

3.2.1 Direct Leaching with Inorganic Acids

By feed materials chemical characterization, direct leaching experiments first conducted to SFA, AFA and HFA samples using Sulfuric (H_2SO_4) and Hydrochloric (HCl) Acids. The reason to select these two acids are they were being used in the literature to extract rare earth elements. Also, the concentrations and leaching duration are chosen according to the previous studies. After 90°C it is needed to be use autoclave and pressure for the leaching process. So that, the temperature is chosen as 30, 60 and 90°C. All the experiments done in three parallels and the final results obtained by the average of the results. Hydrometallurgical Leach Parameters of direct leaching is shown in Table 3.7.

Table 3.7 Leaching Parameters of Inorganic Acids

Variable Name	Parameters
Lixiviant type	Hydrochloric Acid, HCl Sulfuric Acid, H_2SO_4
Lixiviant Concentration	10%, 20%, 30%
Temperature	30°C, 60° C, 90° C
Leach time	6 h, 12h, 24h

Fixed parameters were:

- Solid-Liquid ratio (1/10)
- Mixing speed and rotation

In direct leaching test, 75 grams of solid and 750 ml of lixiviant were put in 3 liter double walled glass container. Between two walls of class container, heated water travels. To prevent precipitation of the sample mechanical mixer was used in a fixed speed of 600 rpm. Flowsheet of direct leaching experiments is shown in Figure 3.20.
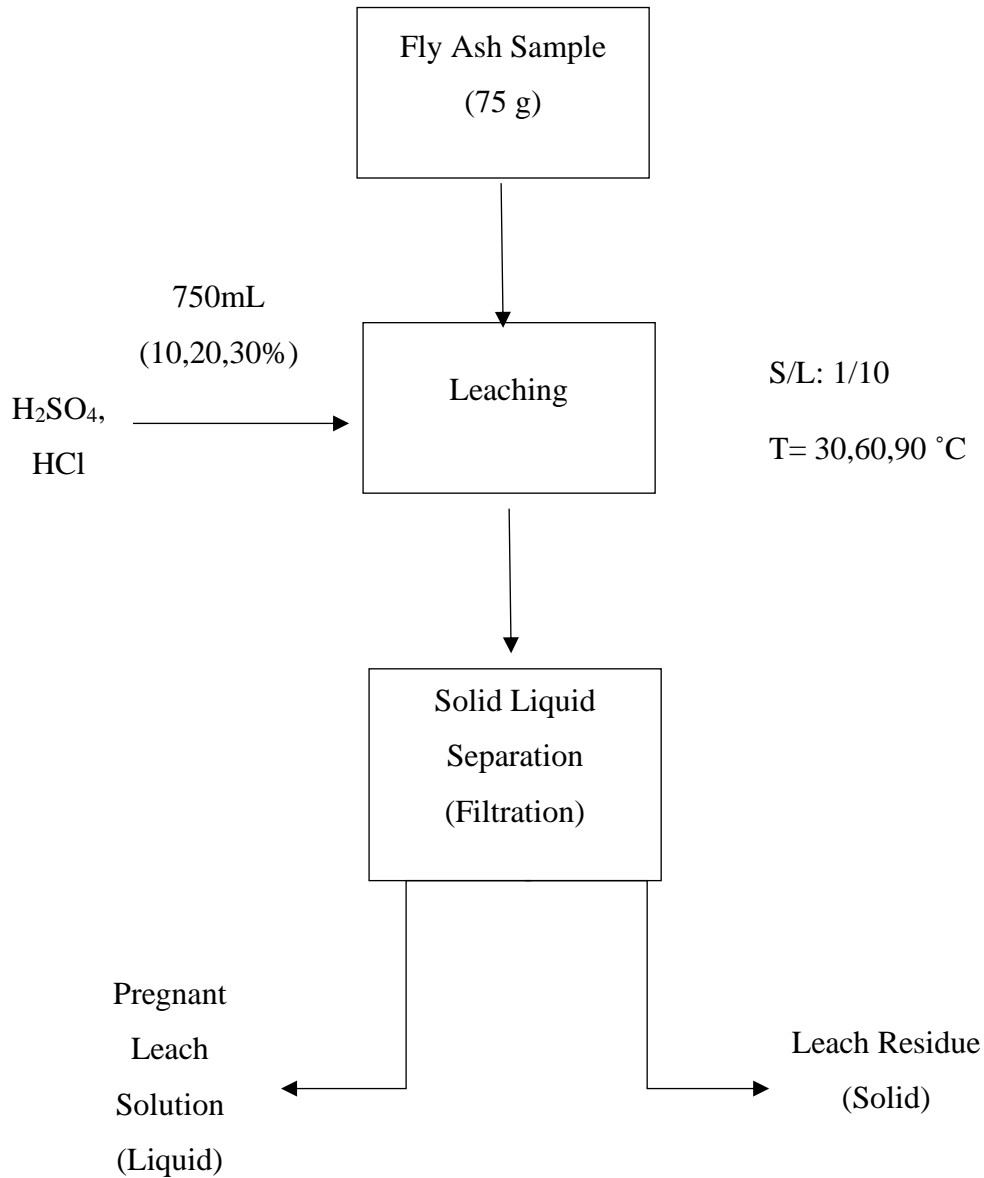
```
                        ┌──────────────────────┐
                        │   Fly Ash Sample     │
                        │       (75 g)         │
                        └──────────────────────┘
                                   │
                                   ▼
       750mL            ┌──────────────────────┐
     (10,20,30%)        │                      │        S/L: 1/10
                        │      Leaching        │
   H₂SO₄,  ──────────▶  │                      │        T= 30,60,90 ˚C
     HCl                └──────────────────────┘
                                   │
                                   ▼
                        ┌──────────────────────┐
                        │    Solid Liquid      │
                        │     Separation       │
                        │    (Filtration)      │
                        └──────────────────────┘
                           │               │
             Pregnant      │               │      Leach Residue
              Leach     ◀──┘               └──▶      (Solid)
             Solution
             (Liquid)
```

Figure 3.20 Flowsheet of Direct Leaching (Inorganic Acids)

3.2.2   Direct Leaching with Organic Acids

Second direct leaching experiments conducted to SFA, AFA and HFA samples using Citric Acid. The reason to select citric acid is it has been used in the previous studies to extract rare earth elements and it is a cheap organic acid that can be found easily. The other parameters were selected the same with the direct leaching with inorganic acids. All the experiments done in three parallels and the final results obtained by the average of the results. Hydrometallurgical Leach Parameters of direct leaching is shown in Table 3.8.

Table 3.8 Leaching Parameters of Organic Acid (Citric Acid)

Variable Name	Parameters		
Lixiviant type	Citric Acid		
Lixiviant Concentration	10%	20%	30%
Temperature	30° C	60° C	90° C
Leach time	6 h	12 h	24 h

Fixed parameters were:

- Solid-Liquid ratio (1/10)
- Mixing speed and rotation

Flowsheet of organic acid leaching experiments is shown in Figure 3.21.
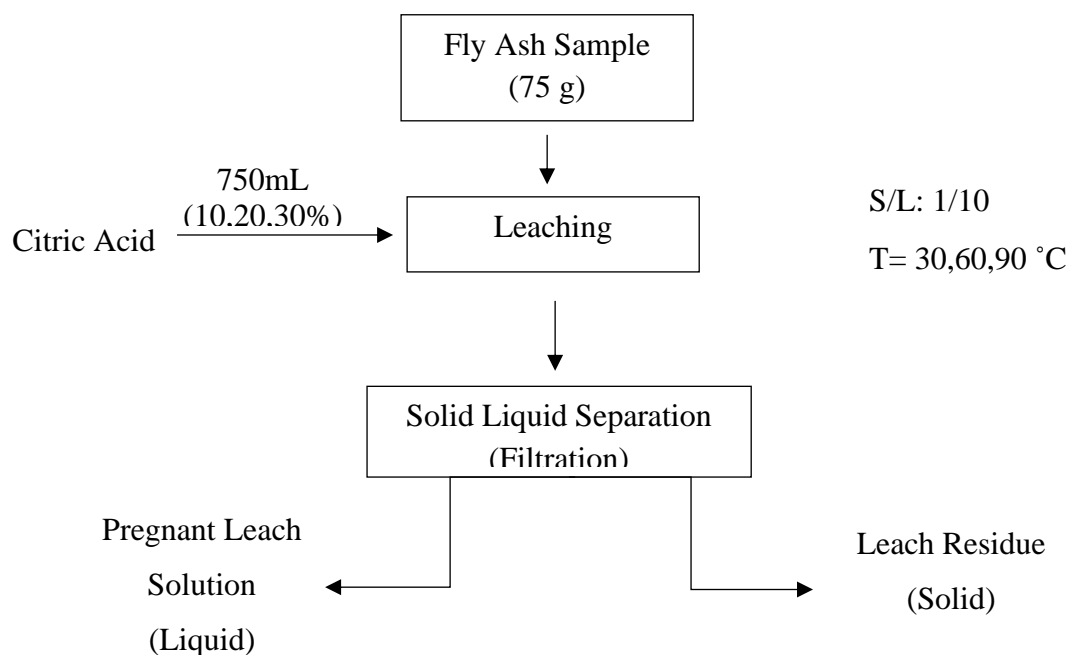
Figure 3.21 Flowsheet of Direct Leaching (Organic Acid)

3.2.3 Sequential Leaching with Inorganic Acids

Second experiment group was sequential leaching to SFA, AFA, and HFA samples using Sulfuric (H_2SO_4) and Hydrochloric (HCl) Acids. Sequential Leach Parameters of direct leaching is shown in Table 3.9. Solid-Liquid ratio is fixed to 1/10 (s/l). Same equipment was used with direct leaching.

Table 3.9 Sequential Leaching Parameters

Experiment Order	Lixiviant	Lixiviant Concentration (%)	Leach time (hour)
1	H_2SO_4	10	6
2	HCl	30	24

The reason in sequential leaching is to extract maximum rare earth minerals by using acidic solutions. Demineralization of the fly ashes were investigated by ICP-MS and the results were compared.

Flowsheet of sequential leaching experiments is shown in Figure 3.22.
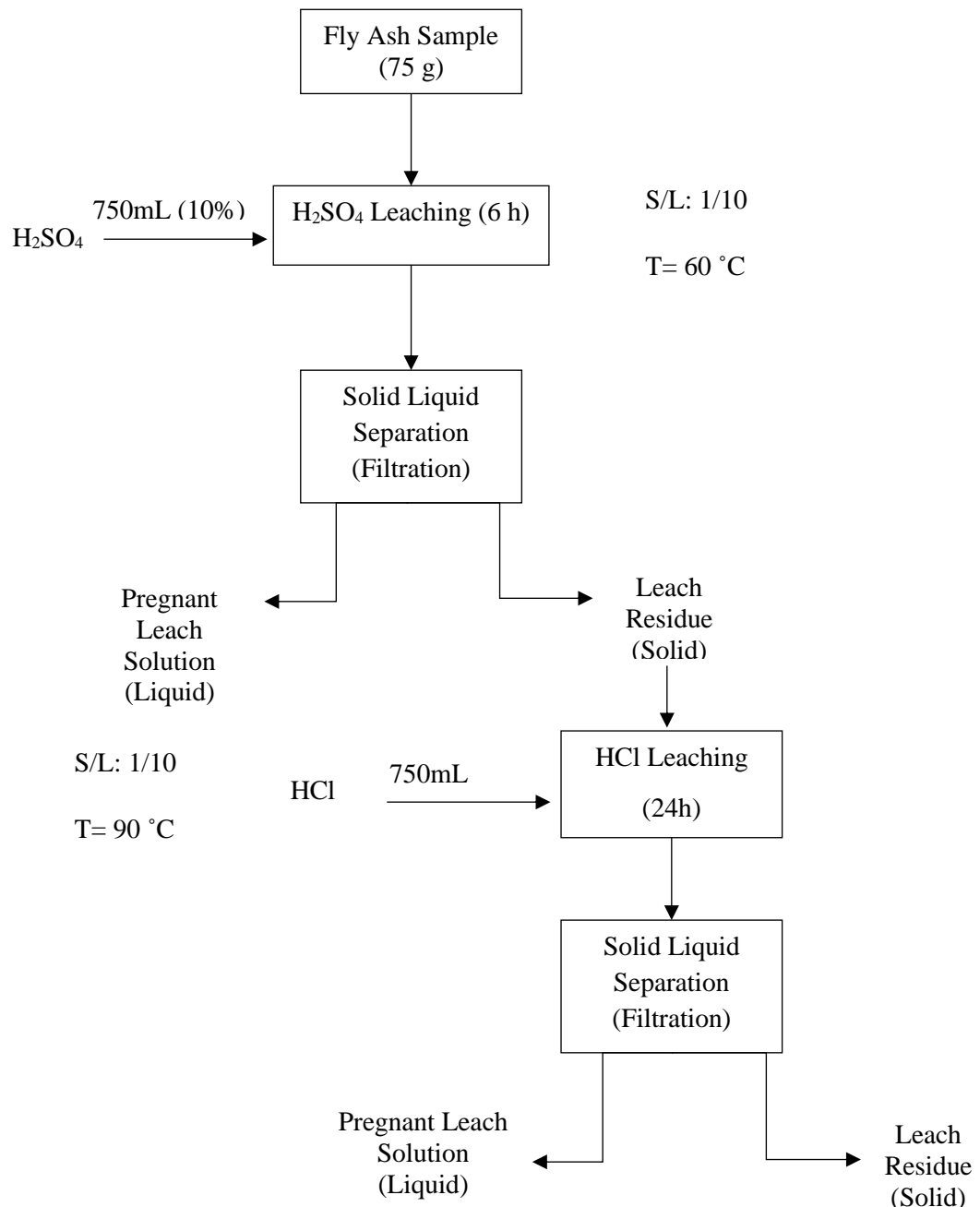
Figure 3.22 Flowsheet of Sequential Leaching

3.2.4   Neutralization - Selective Precipitation Tests

Within the scope of neutralization - selective precipitation tests, it was aimed to obtain a precipitate (cake) with total rare earth element content at an economically salable grade by precipitating the rare earth elements that were transferred to the solution phase as a result of hydrometallurgical leaching processes. The main motivation for neutralization - selective precipitation tests is that the elements contained in the leach solution previously obtained from hydrometallurgical leaching tests show precipitation behavior at different pH values. In this context, precipitation of precious metals was achieved at different pH values. Based on both literature research and test results, it is known that aluminum content of the pregnant solution shows precipitation behavior approximately in the pH = 3-5 range and rare earth content shows precipitation behavior in the pH = 6-9. Also calcium content precipitates in the pH=12-14.

Selective precipitation tests were carried out under atmospheric conditions in 1 liter beakers using magnetic stirrers (Figure 3.23). During the tests, previously obtained pregnant leaching solutions (500 mL) were used and the pH values were increased with different concentrations of sodium hydroxide (Merck) solutions to precipitate the valuable elements contained in the solutions. During the tests, pH values were constantly checked and a controlled precipitation was ensured. The material was filtered through a press filter in order to separate the precipitate (cake) and solution obtained after the selective precipitation processes, and thus to enable solid/liquid separation. The precipitate obtained after filtration was washed using distilled water in order to wash the neutralization solution it contained, and the solid precipitate (cake) obtained after washing was dried at 105 °C in a laboratory type oven. Following the drying process, the products were weighed and the samples were prepared for chemical analysis. The chemical reagents used during selective precipitation tests and the applied flowsheet are given in Figure 3.24.

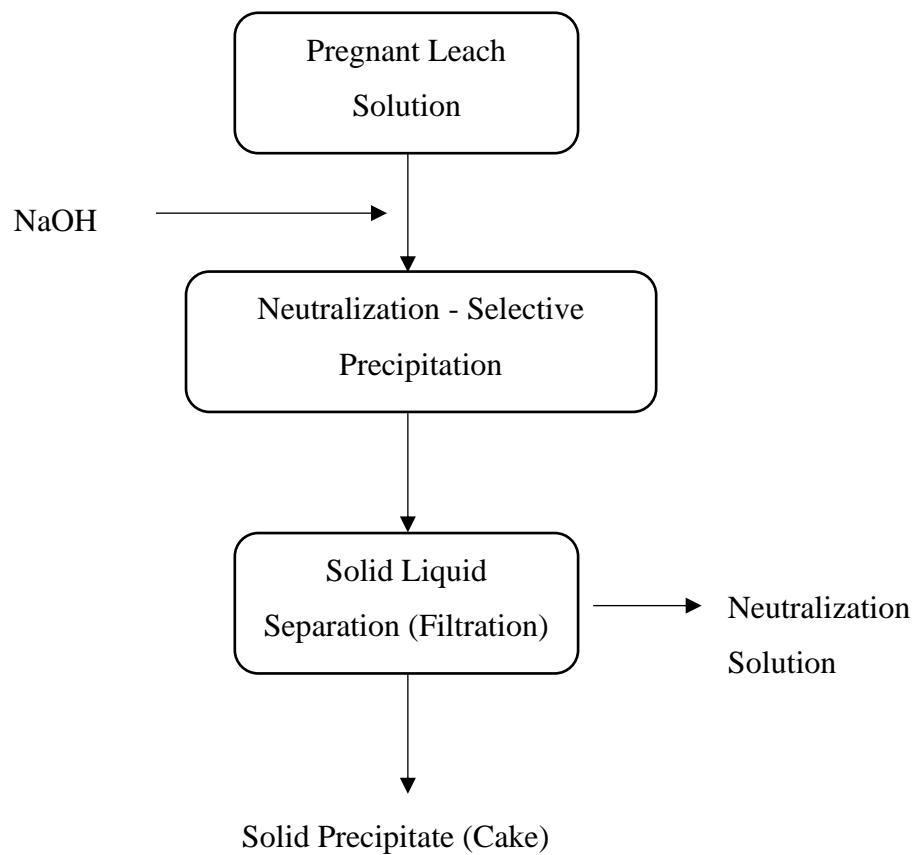Figure 3.23 Neutralization - Selective Precipitation Tests Experimental Setup

Figure 3.24 Neutralization - Selective Precipitation Tests Experimental Procedure

CHAPTER 4

RESULTS AND DISCUSSION

4.1   Leaching Experiments

After the chemical characterization of the feed material, based on the structure of the material, it is aimed to extract the rare earth minerals by taking them into the solution phase through hydrometallurgical leaching processes and thus to recover them. Acidic leaching processes were applied using technical sulfuric acid, hydrochloric acid, and citric acid to recover the rare earth contents of the material.

All the experiments planned by two factorial design and each experiment had three parallel. An experimental design known as a two-factor factorial design gathers data for every possible combination of the two factors of interest's levels. In the thesis work Full factorial design made for 3 factors. Design Summary is shown in Table 4.1.

Table 4.1 Two Factorial Design Summary

Factors: 3	Base Design:	3, 8
Runs: 16	Replicates:	2
Blocks: 1	Center pts (total):	0

After experiment results found with ICP-MS, Minitab software was used for the statistical assessment.

The results given in the Chapter 4 are the average of that parallel experiments.

4.1.1 Direct Leaching with Inorganic Acids

Direct leaching with inorganic acids experiments were performed for each sample (SFA, AFA and HFA). Half of them were leached by using sulfuric acid and the other half were by using hydrochloric acid. The main purpose of sulfuric acid and hydrochloric acid leaching tests, which are carried out as the first step of hydrometallurgical studies, is to recover the rare earth elements contained in the fly ash material by passing them into the solution phase. At the same time, it is aimed to remove impurities such as Ca and Si contained in the feed material.

4.1.1.1 Lignite Fly Ash

According to the characterization of lignite fly ash, it is a silicaocalcic type fly ash consisting aluminosilicate glass phase. By using inorganic acids, that glassy phase had been broken and rare earth elements had been extracted. The results are shown in latter two sections.

4.1.1.1.1 Sulfuric Acid Leaching

As a result of hydrometallurgical leaching tests with sulfuric acid of lignite fly ash, the rare earth element contents of the feed material were obtained by passing them into the solution phase. Even though Scandium recovery is up to 73% (Figure 4.1), the total rare earth element yield was obtained maximum 43.62%. Best recoveries obtained in high temperature (90°C). The best results are shown in Table 4.2.

Table 4.2 Best Results of Sulfuric Acid Leaching Experiments on Lignite Fly Ash

Conditions	Total REE Recovery (%)
20%H_2SO_4, 60°C, 12h	40.15
30% H_2SO_4, 90°C, 6h	43.07
30% H_2SO_4, 90°C, 24h	43.62

Recoveries of 5 rare earth minerals (Sc, Y, La, Ce & Nd) results were investigated in Figure 4.1.
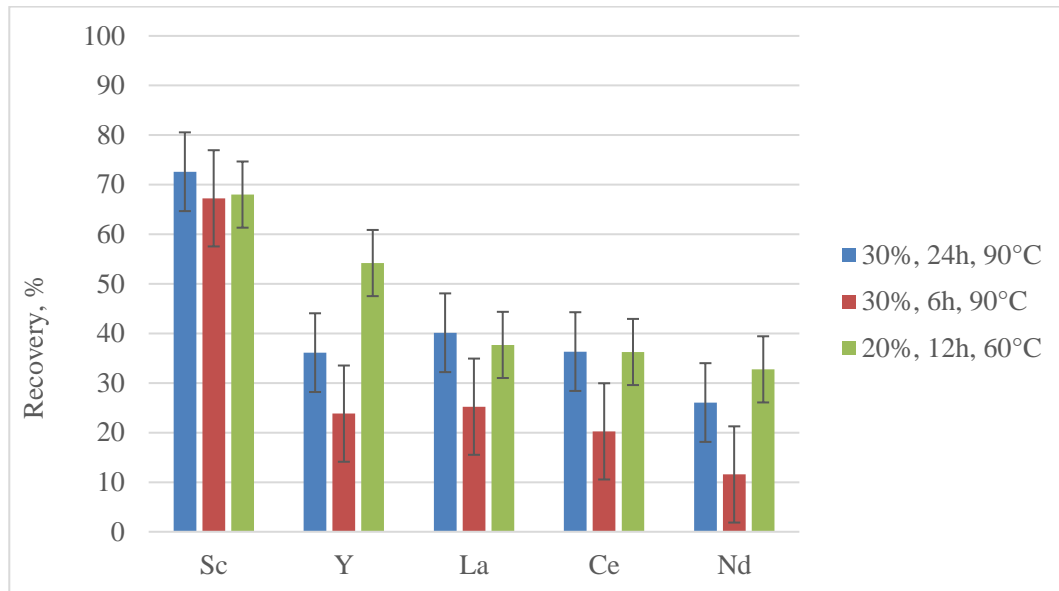

Figure 4.1 Recoveries of Sc, Y, La, Ce, Nd of Lignite Fly Ash after Sulfuric Acid Leaching Experiments

The test results are statistically examined by two factorial design by using Minitab software and contour graphs drawn by the analysis (Figure 4.2).

Contour graphs show the relation between the leach parameters. Acid concentration vs Time graph shows that time higher efficiencies obtained with increased time and it shows the highest efficiency in 10% acid concentration with 24 hours leach time. Therefore, the relationship of time vs temperature is directly proportional. Both increasing time and temperature reduces the total REE efficiency. Lastly, in the acid concentration vs temperature contour graph best efficiency obtained in the middle values.
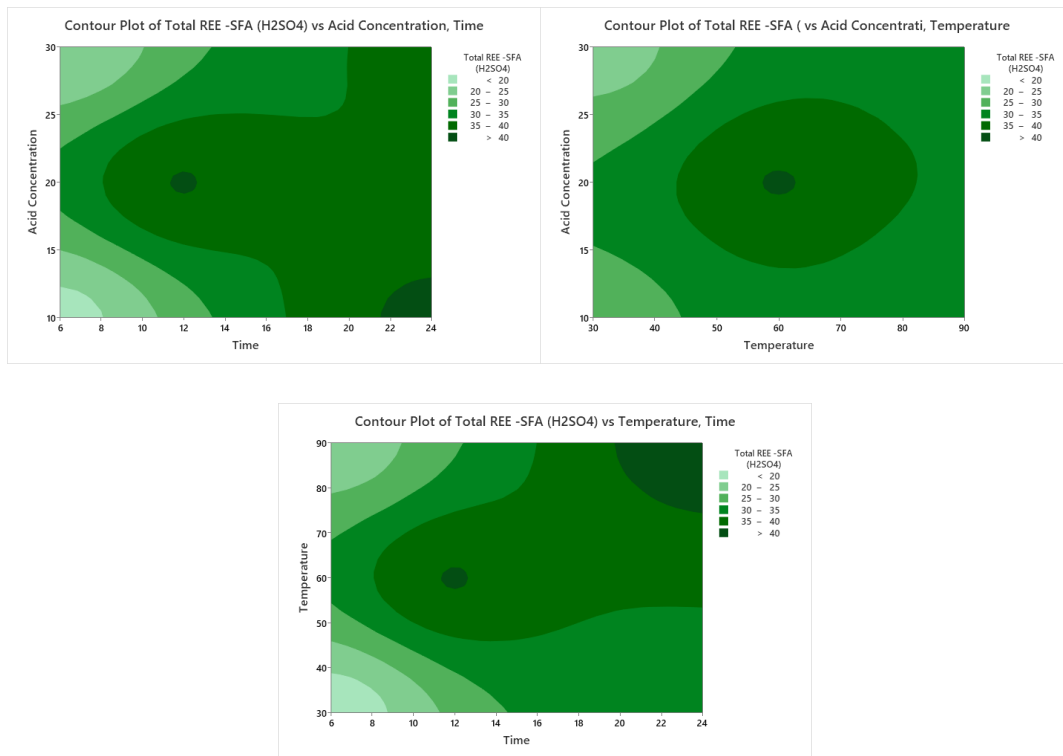
Figure 4.2 Contour Graphs of Lignite Fly Ash after Sulfuric Acid Leaching
Experiments (Minitab Software)

As a result of hydrometallurgical leaching tests and statistical analysis, optimum condition is selected 10% sulfuric acid in 90°C for 24 h. In optimum conditions, pregnant leach solution with 110 ppm total rare earth element content was obtained with 42.12% yield. When the resulting pregnant leach solution is examined in terms of basic impurities, it is seen that it contains Al, Fe, Mg, Si, and Ca. In this context, it was aimed to remove these impurities and leave them in the solution phase during neutralization - selective precipitation tests.

The experimental results of the selected condition are given in Figure 4.3.
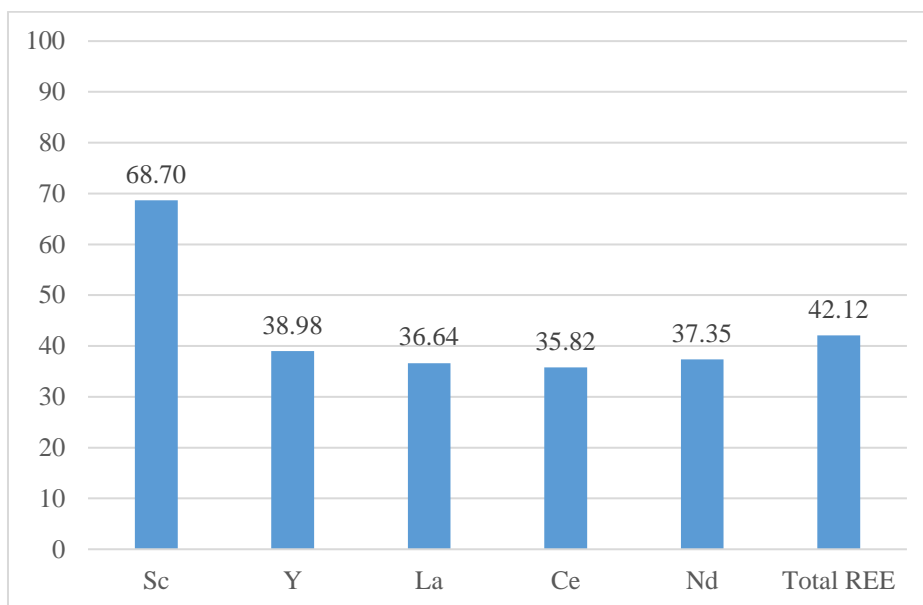
Figure 4.3 Recoveries of Sc, Y, La, Ce, Nd, and Total REE of Lignite Fly Ash
subjected to 10% Sulfuric Acid leaching in 90℃ for 24 h
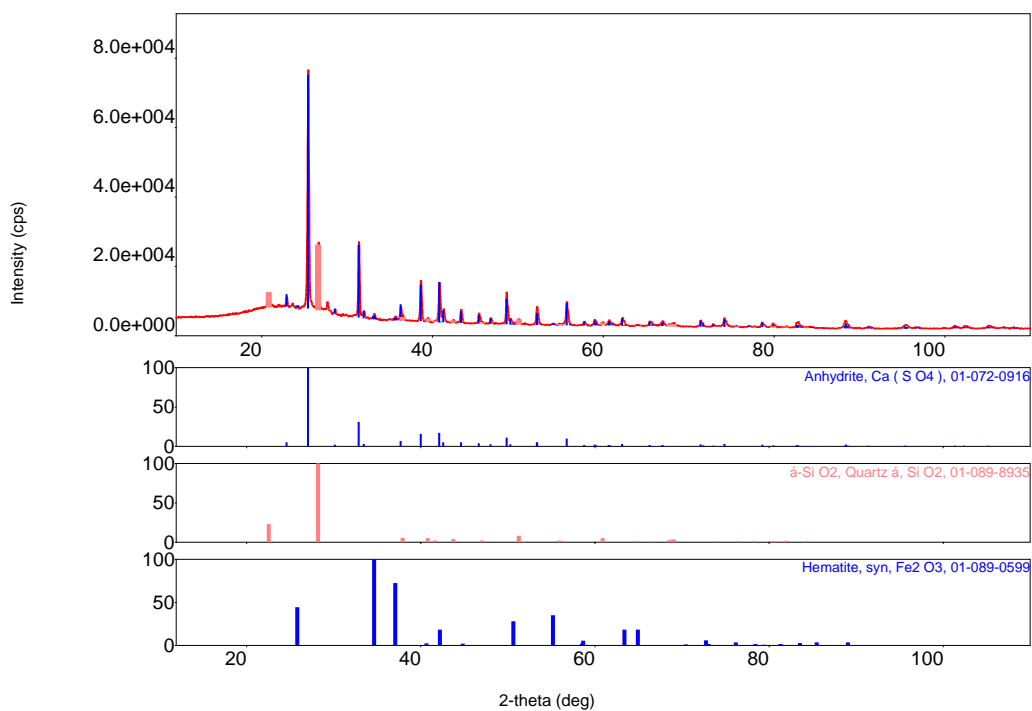
Figure 4.4 XRD Results of Lignite Fly Ash after Sulfuric Acid Leaching
Experiments

63

XRD analysis done in order to examine the results of the optimum condition and in resulted that the minerology is changed during leaching experiments. Based on the XRD results, fly ash contains 84.9% Anhydrate ($CaSO_4$), 13.8% Quartz (SiO_2) and 1.36% Hematite (Fe_2O_3). Studies have shown that REE occurs in the main amorphous glass phase of fly ash (Guoqiang et al., 2020; Hower et al., 2019; Taggart et al., 2016). XRD result showed that feed materials aluminosilicate phase was broken and rare earth minerals can be leached by acid (Figure 4.4).

4.1.1.1.2 Hydrochloric Acid Leaching

In Lignite Fly Ash, after the experiments, it is seen that hydrochloric acid better dissolved the rare earth elements than sulfuric acid. Best cases were 20%HCl, 60°C, 12h; 30%HCl, 90°C, 6h and 30%HCl, 90°C, 24h (Table 4.3).

Recoveries of 5 rare earth minerals (Sc, Y, La, Ce & Nd) results were investigated in Figure 4.5.

Table 4.3 Best Results of Direct Leaching with HCl Experiments on Lignite Fly Ash

Conditions	Total REE Recovery (%)
20%HCl, 60°C, 12h	67.36
30%HCl, 90°C, 6h	70.88
30%HCl, 90°C, 24h	76.57

Because Sc content of the feed material is very low, there was an error in ICP-MS results of 30%, 6h and 90°C results. Even though it is seen in higher than the 24 hour leaching in Figure 4.5, 22ppm of Sc is obtained in that experiments and in 6 hour leaching 26 ppm of Sc is recovered.
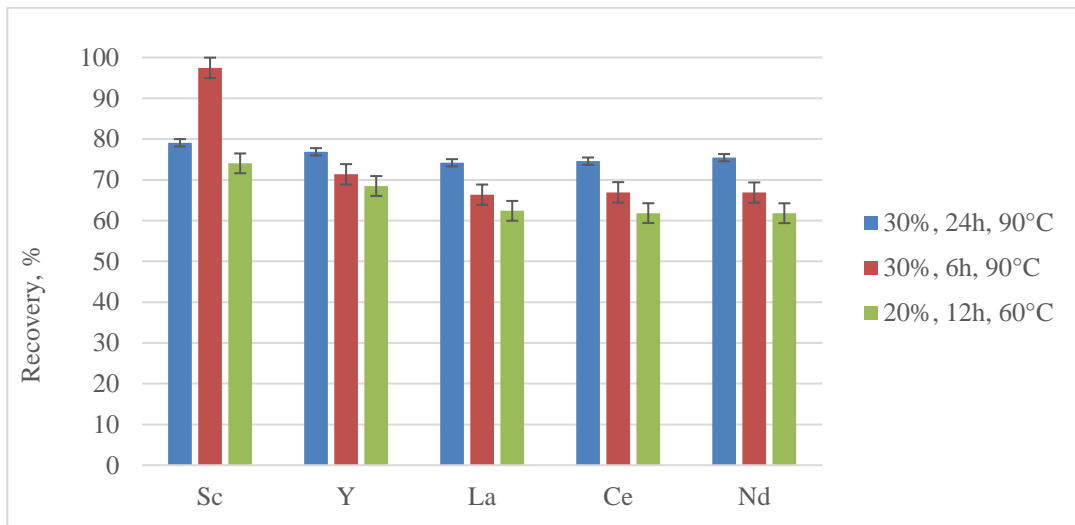
Figure 4.5 Recoveries of Sc, Y, La, Ce, Nd of Lignite Fly Ash after Hydrochloric
Acid Leaching Experiments

The test results are statistically examined by two factorial design by using Minitab
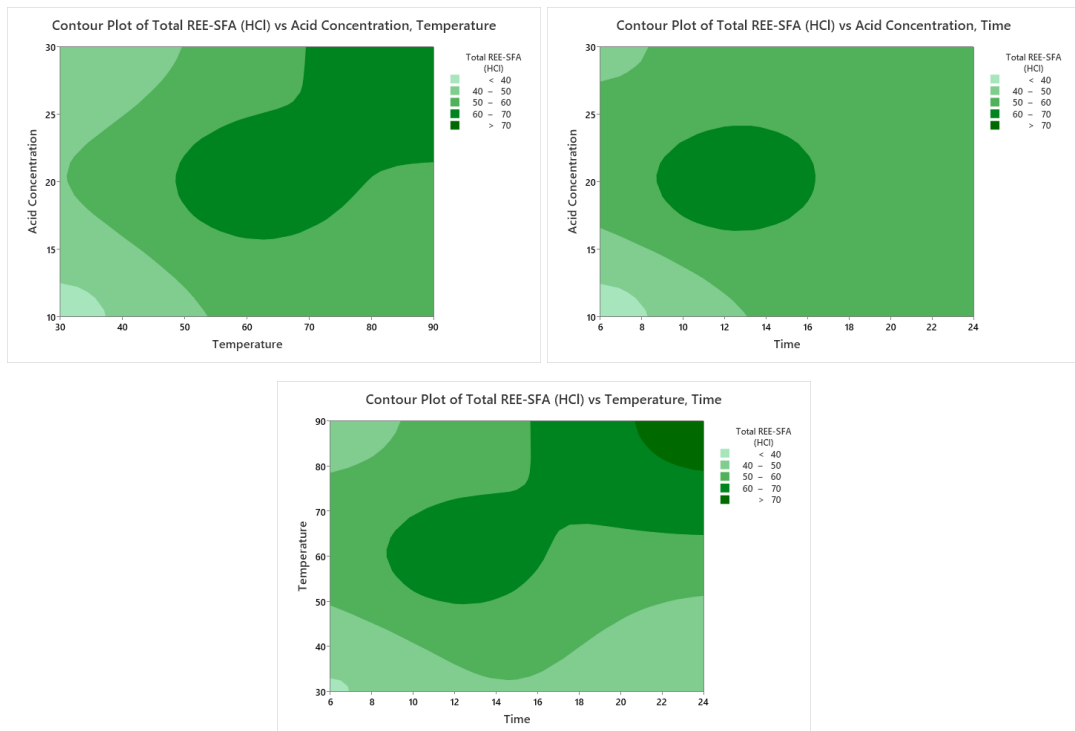software and contour graphs drawn by the analysis (Figure 4.6).

Figure 4.6 Contour Graphs of Lignite Fly Ash after Hydrochloric Acid Leaching
Experiments (Minitab Software)

Acid concentration vs Temperature graph shows that they are directly proportional and by increasing time and temperature better efficiencies could be obtained. Also, Time and temperature were having a similar relationship. Therefore, the relationship of acid concentration vs temperature shows best efficiency obtained in the middle values.

As a result of hydrometallurgical leaching tests and statistical analysis, optimum condition is selected 10% hydrochloric acid in 90°C for 24 h. Although with higher acid concentrations higher efficiencies can be achieved, because of the price of the acid is the highest in the leaching operations lowest concentration is chosen. Also, by using the higher concentrations of HCl there can be a safety issue due to the danger of the HCl vaporization or spilling risk etc. In optimum conditions, pregnant leach solution with 258 ppm total rare earth element content was obtained with 70.77% yield. When the resulting pregnant leach solution is examined in terms of basic impurities, it is seen that it contains Al, Fe, Mg, Si, and Ca. In this context, it was aimed to remove these impurities and leave them in the solution phase during neutralization - selective precipitation tests.

The experimental results of the selected condition are given in Figure 4.7.

XRD analysis done in order to examine the results of the optimum condition and in resulted that the minerology is changed during leaching experiments like sulfuric acid leaching tests. Based on the XRD results, fly ash contains 39.4% Anhydrate ($CaSO_4$), 46% Quartz (SiO_2) and 14.6% Hematite (Fe_2O_3). XRD result showed that feed materials aluminosilicate phase was broken and rare earth minerals can be leached by acid (Figure 4.8).
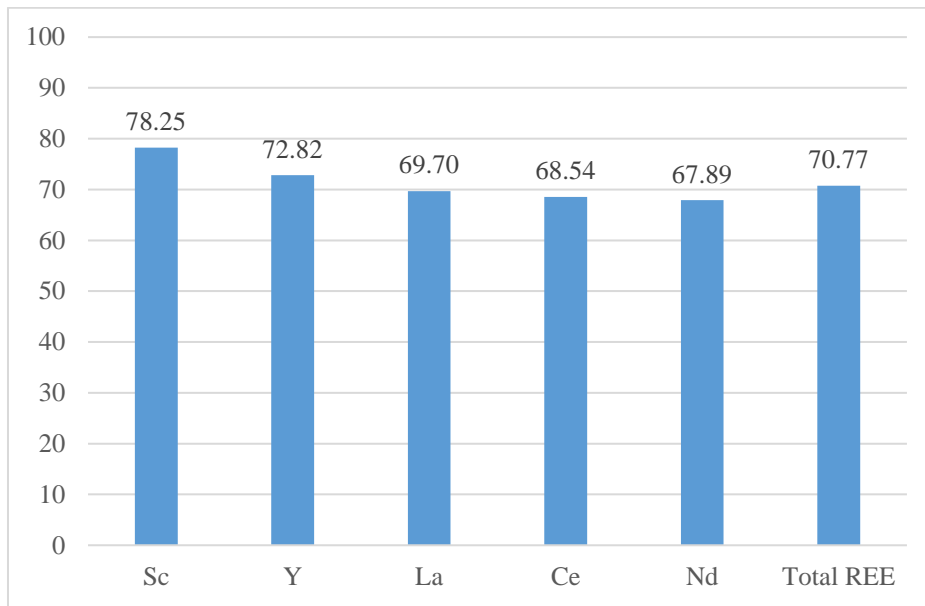
Figure 4.7 Recoveries of Sc, Y, La, Ce, Nd, and Total REE of Lignite Fly Ash

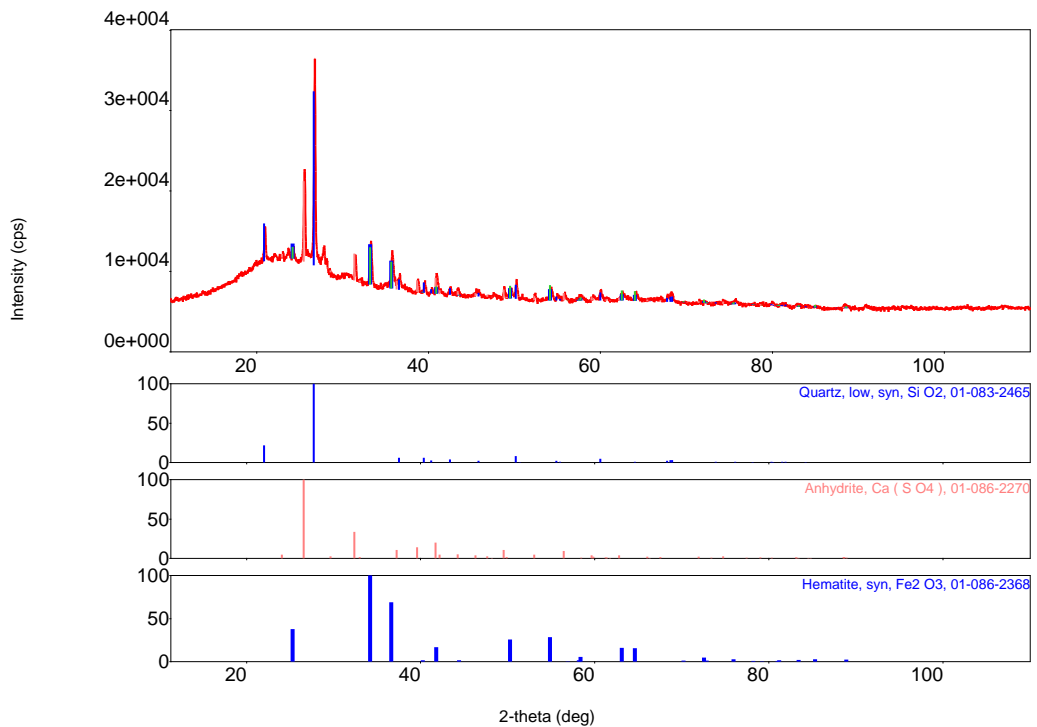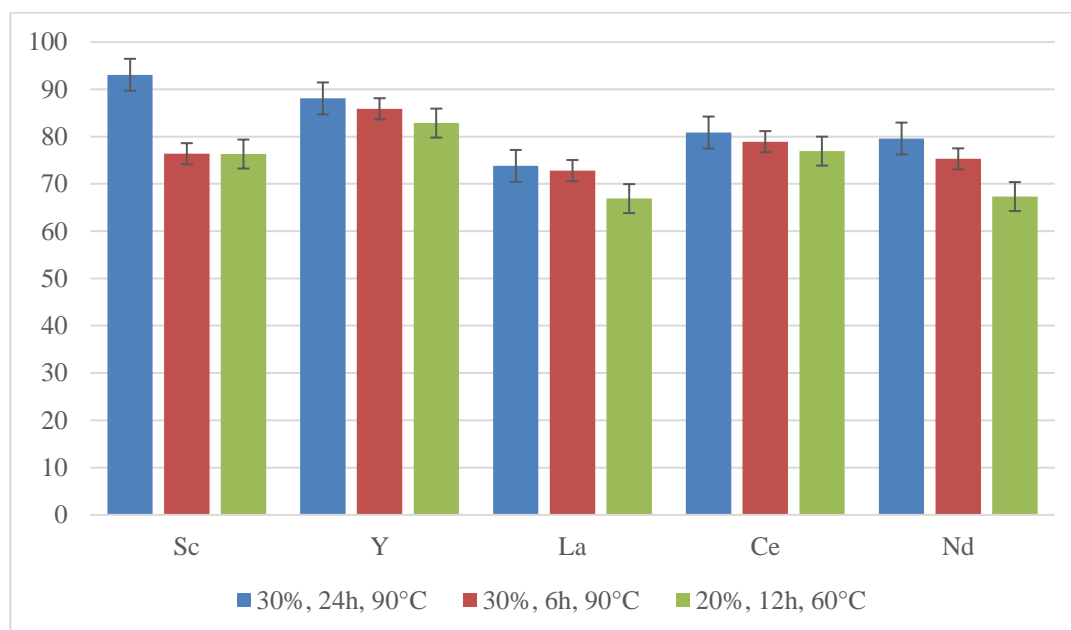subjected to 10% Hydrochloric Acid leaching in 90℃ for 24 h

Figure 4.8 XRD Results of Lignite Fly Ash after Hydrochloric Acid Leaching

Experiments

4.1.1.2   Asphaltite Fly Ash

According to the characterization of asphaltite fly ash, it is a silicoaluminus type fly ash consisting aluminosilicate glass phase and calcium sulfite crystals. with inorganic acids leaching, that glassy phase had been broken and rare earth elements had been extracted. The results are shown in following two sections.

4.1.1.2.1   Sulfuric Acid Leaching

The same procedure was applied to asphaltite fly ash sample and results of hydrometallurgical leaching tests with sulfuric acid showed that the rare earth element contents of the feed material were obtained by recovering them into the solution phase. Best recoveries obtained in high temperature (90°C) like Lignite fly ash but the recoveries are higher. The best results are shown in Table 4.4

Table 4.4 Best Results of Sulfuric Acid Leaching Experiments on Asphaltite Fly Ash

Conditions	Total REE Recovery (%)
20%H_2SO_4, 60°C, 12h	64.68
30% H_2SO_4, 90°C, 6h	76.46
30% H_2SO_4, 90°C, 24h	78.08

Recoveries of 5 rare earth minerals (Sc, Y, La, Ce & Nd) results were investigated in Figure 4.9.

The test results are statistically examined by two factorial design by using Minitab software and contour graphs drawn by the analysis (Figure 4.10).

According the statistical analysis and drawn contour graphs, all the parameters (Acid concentration, time and temperature vs total REE recovery) are directly proportional and best results could be reached at maximum conditions of the experiments done. By increasing the temperature better results can be obtained but higher than 100°C autoclave needed.

As a result of hydrometallurgical leaching tests, optimum condition is selected 10% sulfuric acid in 90°C for 24 h. In optimum conditions, pregnant leach solution with 283 ppm total rare earth element content was obtained with 77.86% yield. When the resulting pregnant leach solution is examined in terms of basic impurities, it is seen that it contains Al, Fe, Mg, Si and Ca. In this context, it was aimed to remove these impurities and leave them in the solution phase during neutralization - selective precipitation tests.

The experimental results of the selected conditions are given in Figure 4.11

XRD analysis done in order to examine the results of the optimum condition and in resulted that the minerology is changed during leaching experiments. Based on the XRD results, fly ash contains 95% Anhydrate ($CaSO_4$). XRD result showed that feed materials aluminosilicate phase was broken and rare earth minerals can be leached by acid (Figure 4.12).

Figure 4.9 Recoveries of Sc, Y, La, Ce & Nd of Asphaltite Fly Ash after Sulfuric Acid Leaching Experiments
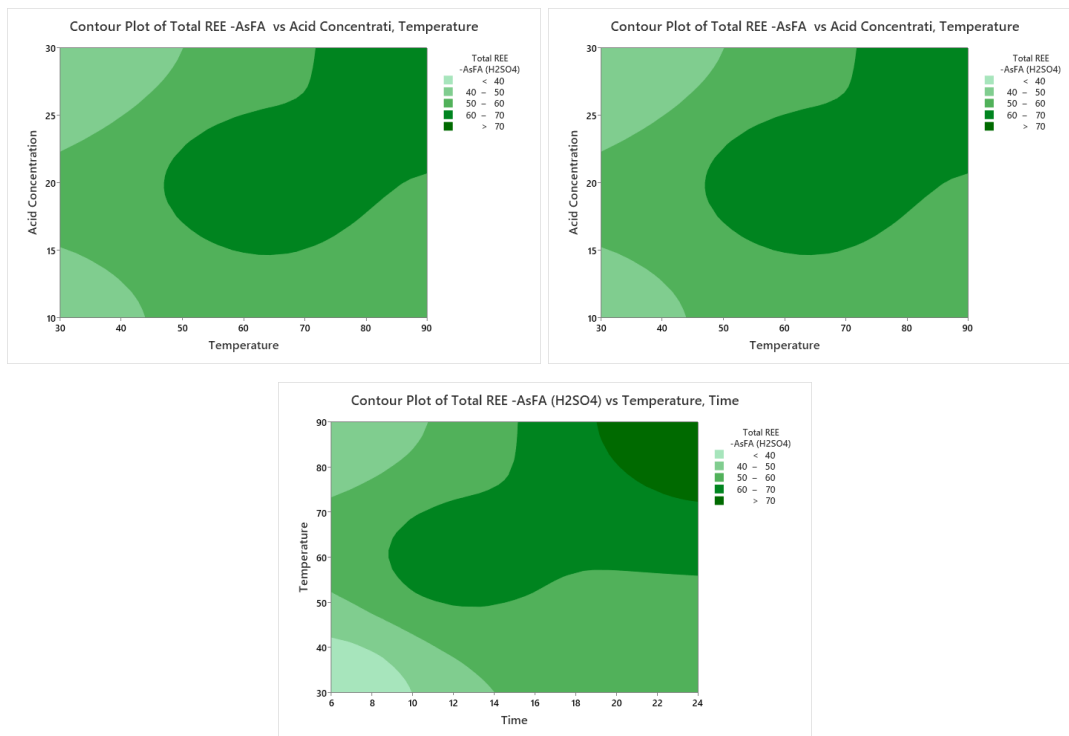
Figure 4.10 Contour Graphs of Asphaltite Fly Ash after Sulfuric Acid Leaching Experiments (Minitab Software)
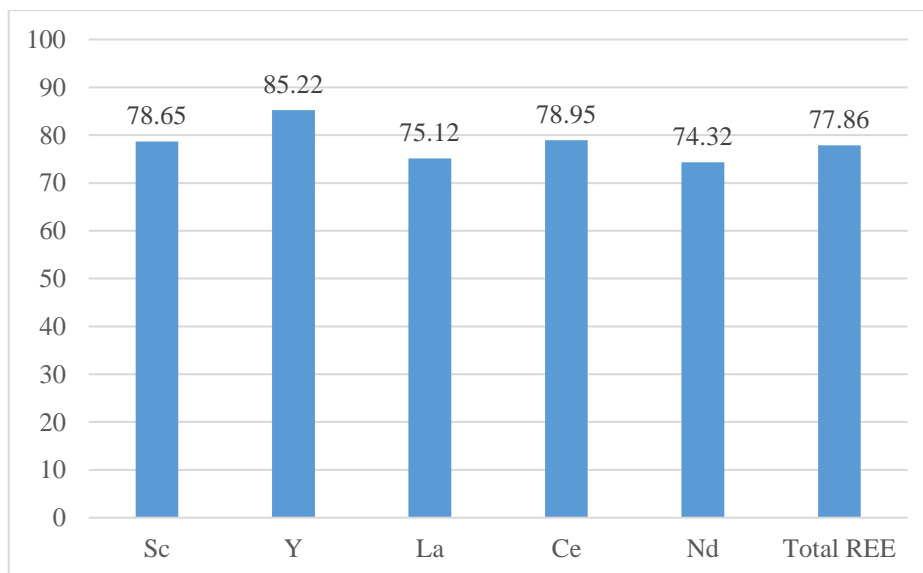

Figure 4.11 Recoveries of Sc, Y, La, Ce, Nd, and Total REE of Asphaltite Fly Ash subjected to 10% Sulfuric Acid leaching in 90℃ for 24 h
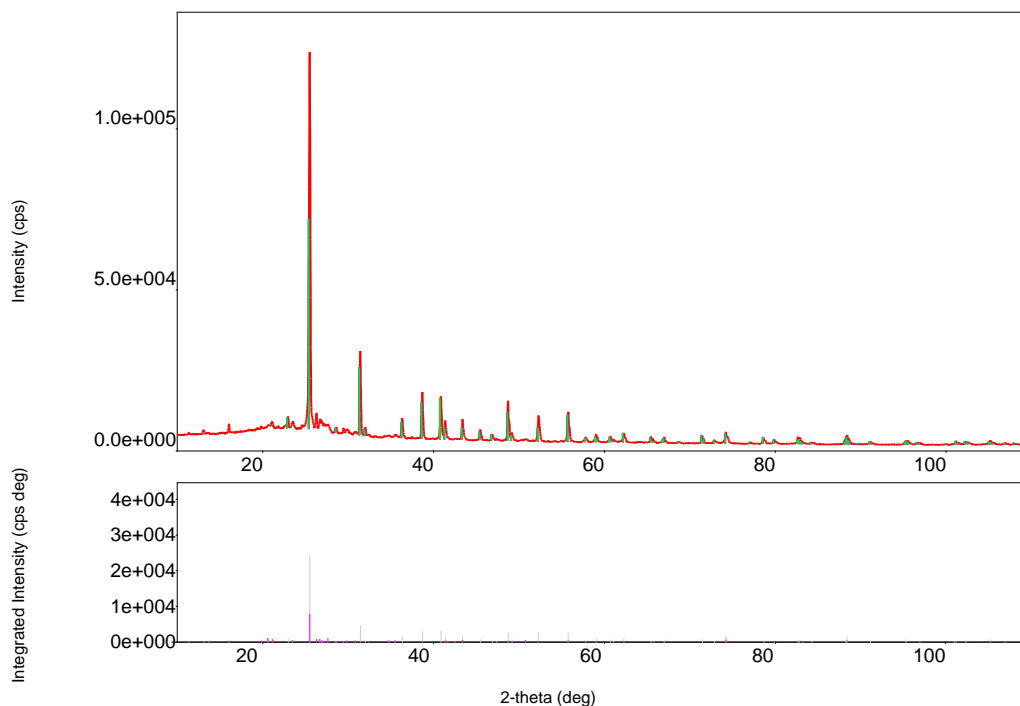
Figure 4.12 XRD Results of Asphaltite Fly Ash after Sulfuric Acid Leaching
Experiments

4.1.1.2.2   Hydrochloric Acid Leaching

In Asphaltite Fly Ash, after the experiments, it is seen that hydrochloric acid better dissolved the rare earth elements than sulfuric acid like lignite fly ash. Overall, hydrochloric acid was found to be the most effective leaching agent, leaching more than 90% of REEs. However, the concentrations of Ca ions in the leachate were also high, which would complicate recovery of the REEs. Best cases were 20%HCl, 60℃, 12h; 30%HCl, 90℃, 6h and 30%HCl, 90℃, 24h (Table 4.5).

Table 4.5 Best Results of HCl Leaching Experiments on Asphaltite Fly Ash

Conditions	Total REE Recovery (%)
20%HCl, 60℃, 12h	75.15
30%HCl, 90℃, 6h	80.14
30%HCl, 90℃, 24h	82.85

By initial concentrations and the final recoveries of 5 rare earth minerals (Sc, Y, La, Ce, Nd) results were investigated (Figure 4.13).
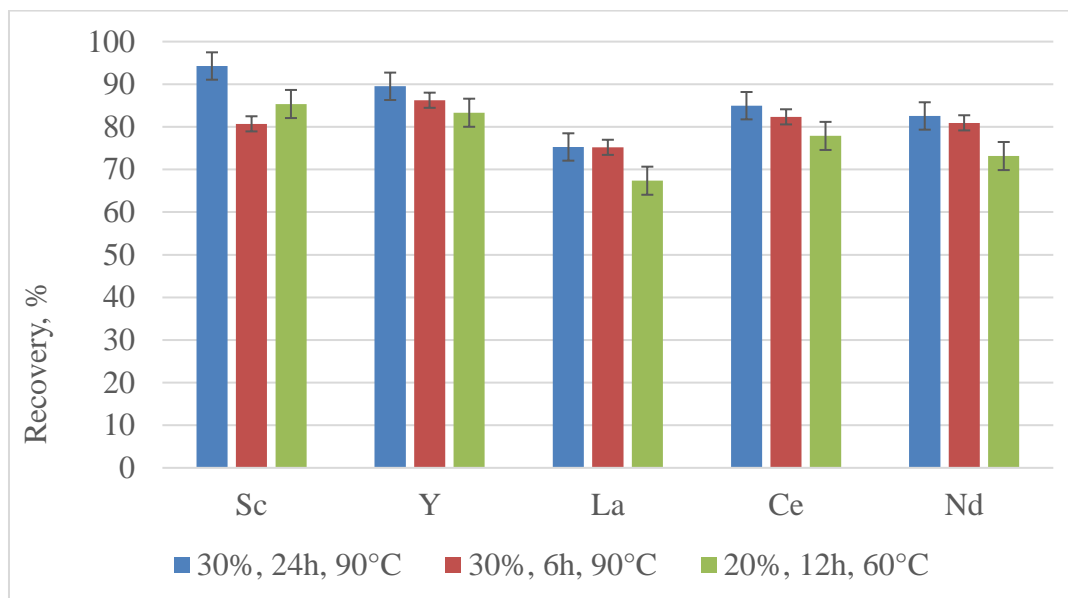
Figure 4.13 Recoveries of Sc, Y, La, Ce & Nd of Asphaltite Fly Ash after Hydrochloric Acid Leaching Experiments

The test results are statistically examined by two factorial design by using Minitab software and contour graphs drawn by the analysis (Figure 4.14).

The contour graphs shown that acid concentrations are directly proportional with recovery. Also by the time and temperature increases, recovery increases.

As a result of hydrometallurgical leaching tests and statistical analysis, optimum condition is selected 10% hydrochloric acid in 90°C for 24 h. Like Lignite fly ash even though higher acid concentrations results in higher efficiencies, due the economic and safety reasons in operation lowest concentration is chosen. In optimum conditions, pregnant leach solution with 287 ppm total rare earth element content was obtained with 79.21% yield. When the resulting pregnant leach solution is examined in terms of basic impurities, it is seen that it contains Al, Fe, Mg, Si and Ca. In this context, it was aimed to remove these impurities and leave them in the solution phase during neutralization - selective precipitation tests.
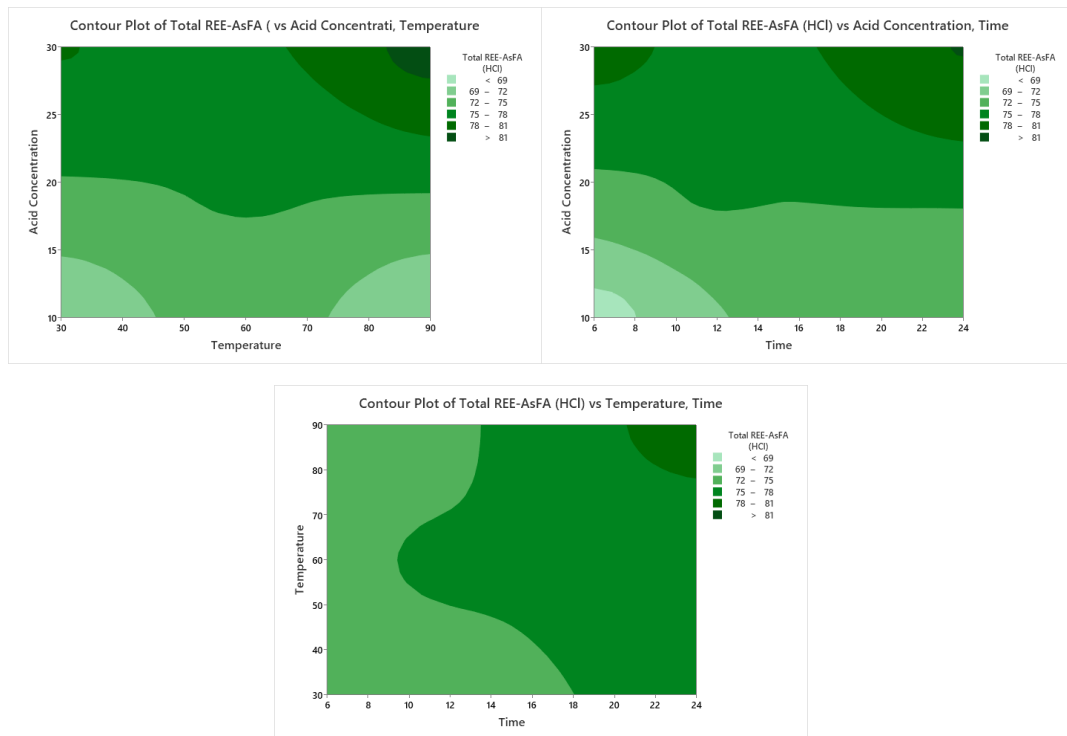
Figure 4.14 Contour Graphs of Asphaltite Fly Ash after Hydrochloric Acid
Leaching Experiments (Minitab Software)

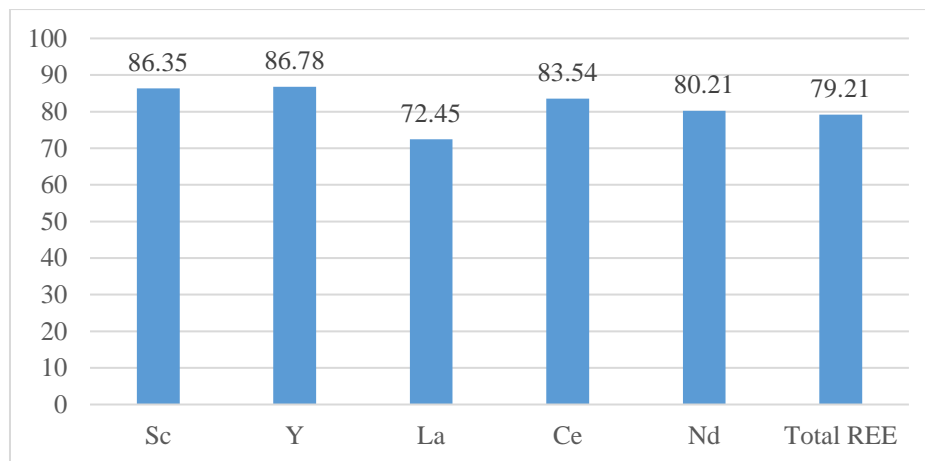The experimental results of the selected conditions are given in Figure 4.15

Figure 4.15 Recoveries of Sc, Y, La, Ce, Nd, and Total REE of Asphaltite Fly Ash
subjected to 10% Hydrochloric Acid leaching in 90℃ for 24 h

XRD analysis done in order to examine the results of the optimum condition and in resulted that the minerology is changed during leaching experiments like sulfuric acid leaching tests. Based on the XRD results, fly ash contains 37% Calcium Sulfate hydrate ($CaSO_4$), 60% Microline and 3.1% Magnesium Aluminum Iron Oxide. XRD result showed that feed materials aluminosilicate phase was broken and rare earth minerals can be leached by acid (Figure 4.16).
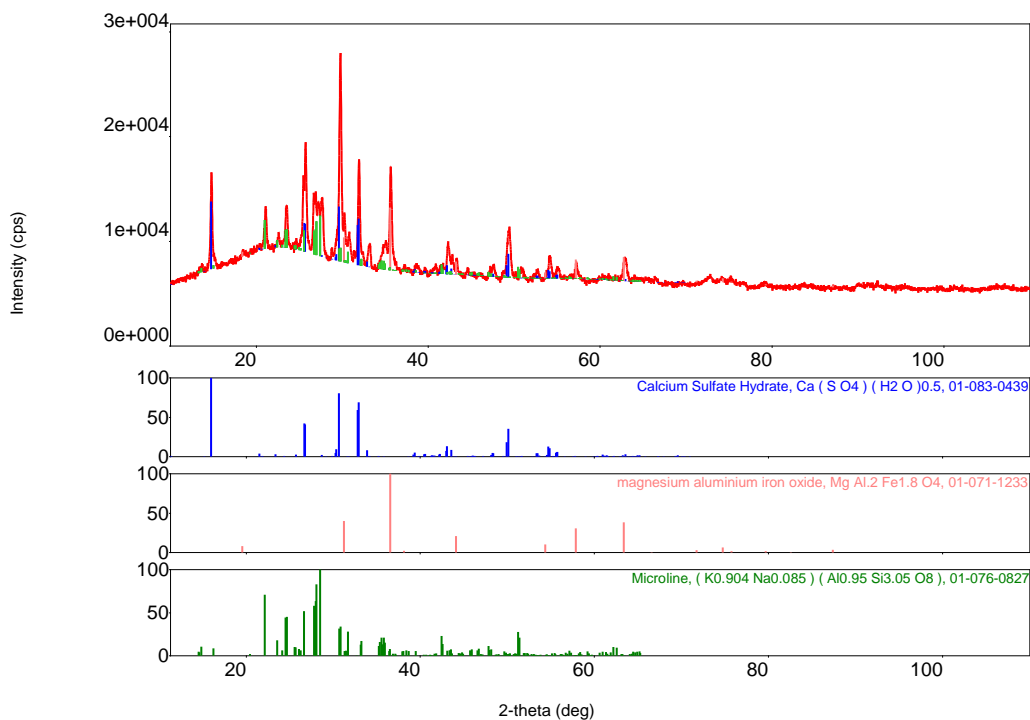

Figure 4.16 XRD Results of Lignite Fly Ash after Hydrochloric Acid Leaching Experiments

4.1.1.3   Hard Coal Fly Ash

According to the characterization of hard coal fly ash, it is a silicaocalcic type fly ash consisting aluminosilicate glass phase. By using inorganic acids, rare earth elements had been extracted. The results are shown in following two sections.

4.1.1.3.1 Sulfuric Acid Leaching

The same procedure was applied to hard coal fly ash sample and results of direct leaching tests with sulfuric acid showed that the rare earth element contents of the feed material were obtained by recovering them into the solution phase. Best recoveries obtained in high temperature (90°C) like lignite and asphaltite fly ash but the recoveries are lower than the values of the both fly ashes. The best results are shown in Table 4.6.

Table 4.6 Best Results of Sulfuric Acid Leaching Experiments on Hard Coal Fly Ash

Conditions	Total REE Recovery (%)
20% H_2SO_4, 60°C, 12h	64.35
30% H_2SO_4, 90°C, 6h	65.24
30% H_2SO_4, 90°C, 24h	65.81

Recoveries of 5 rare earth minerals (Sc, Y, La, Ce & Nd) results were investigated in Figure 4.17.
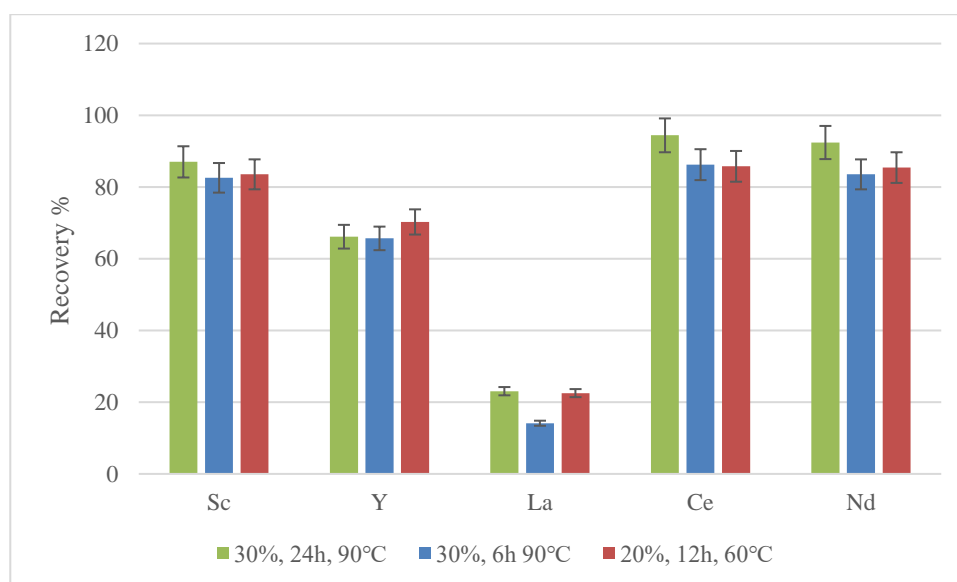

Figure 4.17 Recoveries of Sc, Y, La, Ce & Nd of Hard Coal Fly Ash after Sulfuric Acid Leaching Experiments

La recovery of Hard Coal fly ash is much lower than the recoveries of other fly ashes.

The test results are statistically examined by two factorial design by using Minitab software and contour graphs drawn by the analysis Figure 4.18.
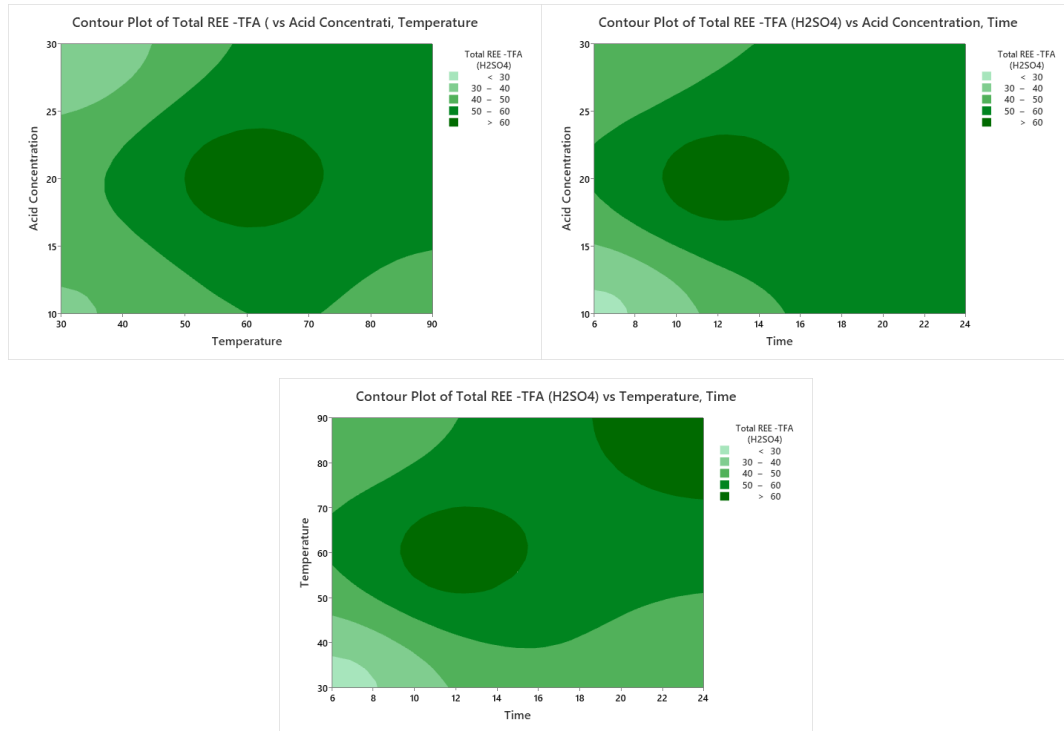

Figure 4.18 Contour Graphs of Hard Coal Fly Ash after Sulfuric Acid Leaching Experiments (Minitab Software)

The relationship of acid concentration vs temperature and acid concentration vs time shows best efficiency obtained in the middle values. Therefore, the relationship of time vs temperature is directly proportional. Both increasing time and temperature increase the total REE efficiency.

As a result of hydrometallurgical leaching tests, optimum condition is selected 10% sulfuric acid in 90°C for 24 h. In optimum conditions, pregnant leach solution with 282 ppm total rare earth element content was obtained with 64.18% yield. When the resulting pregnant leach solution is examined in terms of basic impurities, it is seen that it contains Al, Fe, Mg, Si and Ca. In this context, it was aimed to remove these

impurities and leave them in the solution phase during neutralization - selective precipitation tests.

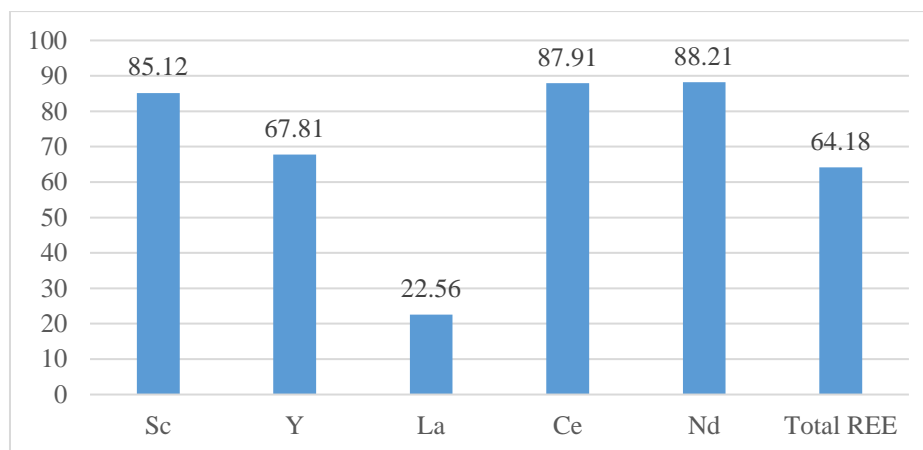The experimental results of the selected conditions are given in Figure 4.19

Figure 4.19 Recoveries of Sc, Y, La, Ce, Nd, and Total REE of Hard Coal Fly Ash subjected to 10% Sulfuric Acid leaching in 90℃ for 24 h
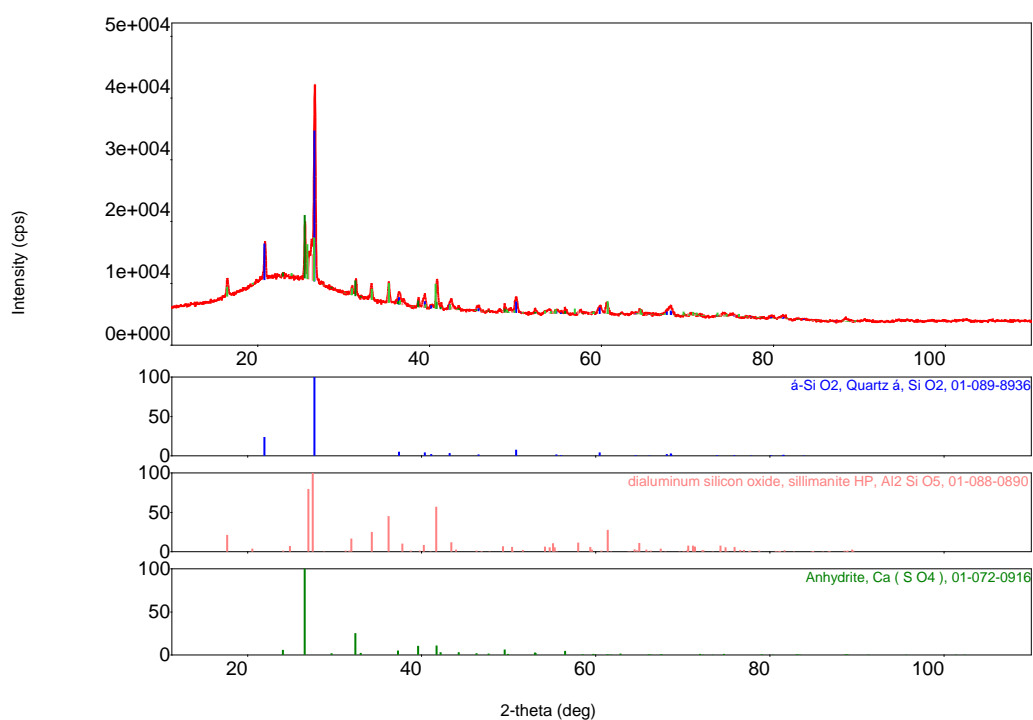

Figure 4.20 XRD Results of Hard Coal Fly Ash after Sulfuric Acid Leaching Experiments

XRD analysis done in order to examine the results of the optimum condition and in resulted that the minerology is changed during leaching experiments. Based on the XRD results, fly ash contains 11.8% Anhydrate, 35% Quartz and 53% Sillimanite (Figure 4.20). Results showed that feed material's minerology was not changed, only slightly change of the contents changed, so the recovery of the rare earth minerals are lower than the other types of fly ashes used in this thesis.

4.1.1.3.2   Hydrochloric Acid Leaching

After the hydrochloric acid leaching experiments, it is seen that the results of hydrochloric acid nearly the same with sulfuric acid unlike like previous fly ashes. Best cases were 20%HCl, 60°C, 12h; 30%HCl, 90°C, 6h and 30%HCl, 90°C, 24h (Table 4.7).

Table 4.7 Best Results of HCl Leaching Experiments on Hard Coal Fly Ash

Conditions	Total REE Recovery (%)
20%HCl, 60°C, 12h	63.81
30%HCl, 90°C, 6h	63.24
30%HCl, 90°C, 24h	64,35

By initial concentrations and the final recoveries of 5 rare earth minerals (Sc, Y, La, Ce, Nd) results were investigated (Figure 4.21).

The test results are statistically examined by two factorial design by using Minitab software and contour graphs drawn by the analysis Figure 4.22.

Similar with the sulfuric acid leaching the relationship of acid concentration vs temperature and acid concentration vs time have given the best efficiency in the middle values. Moreover, the relationship of time vs temperature is directly proportional. So that, increasing in both time and temperature enhance the total REE efficiency.
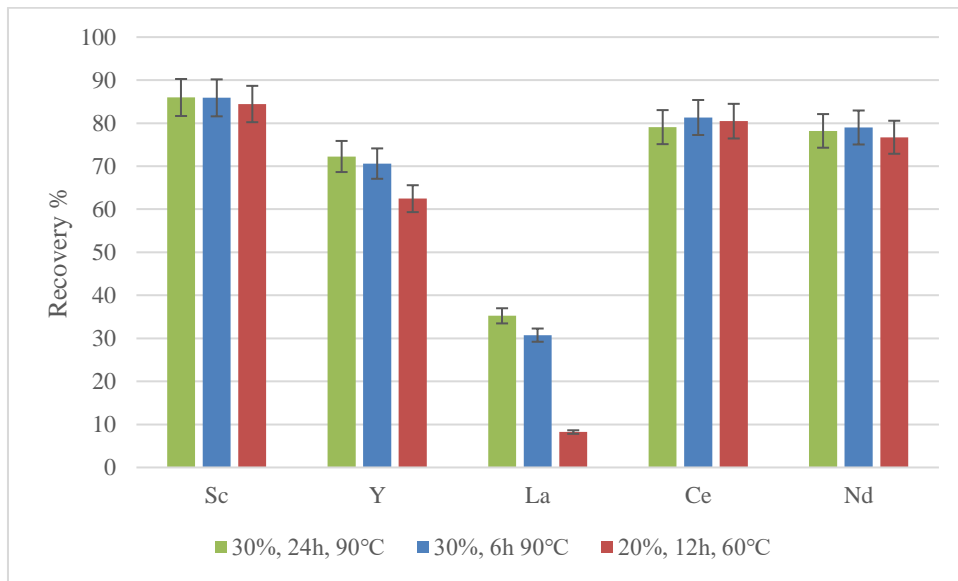
Figure 4.21 Recoveries of Sc, Y, La, Ce & Nd of Hard Coal Fly Ash after
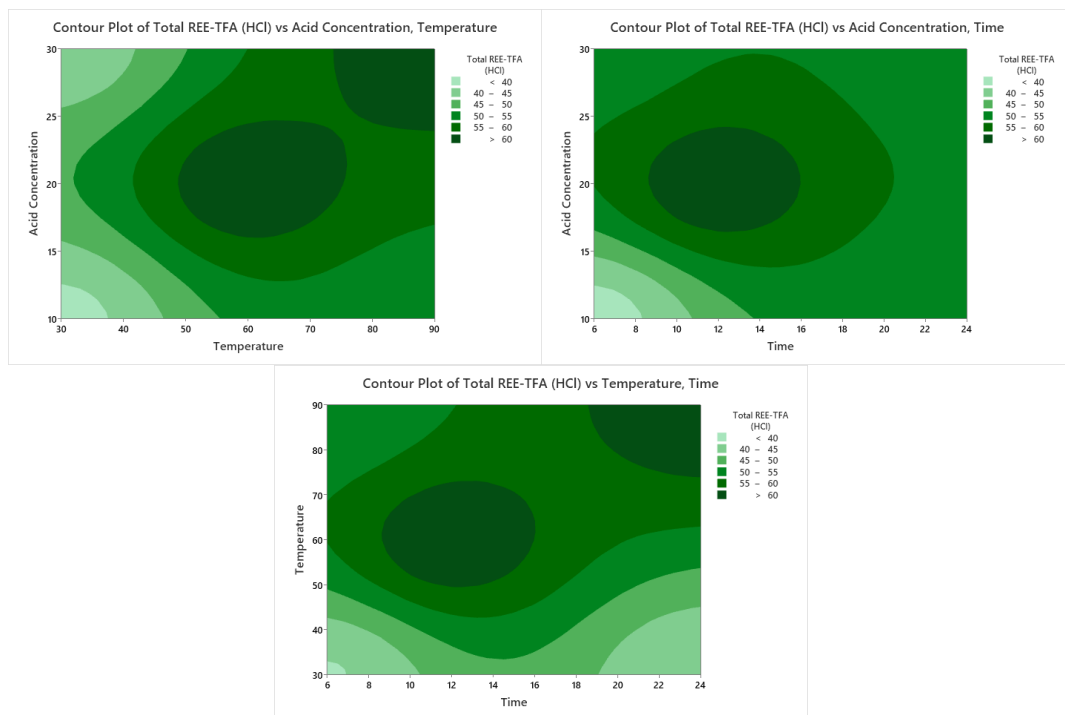Hydrochloric Acid Leaching Experiments

Figure 4.22 Contour Graphs of Hard Coal Fly Ash after Hydrochloric Acid
Leaching Experiments (Minitab Software)

As a result of hydrometallurgical leaching tests, optimum condition is selected 10% sulfuric acid in 90°C for 24 h. In optimum conditions, pregnant leach solution with 275 ppm total rare earth element content was obtained with 62.64% yield. When the resulting pregnant leach solution is examined in terms of basic impurities, it is seen that it contains Al, Fe, Mg, Si and Ca like the others. In this context, it was aimed to remove these impurities and leave them in the solution phase during neutralization - selective precipitation tests.

The experimental results of the selected conditions are given in Figure 4.23
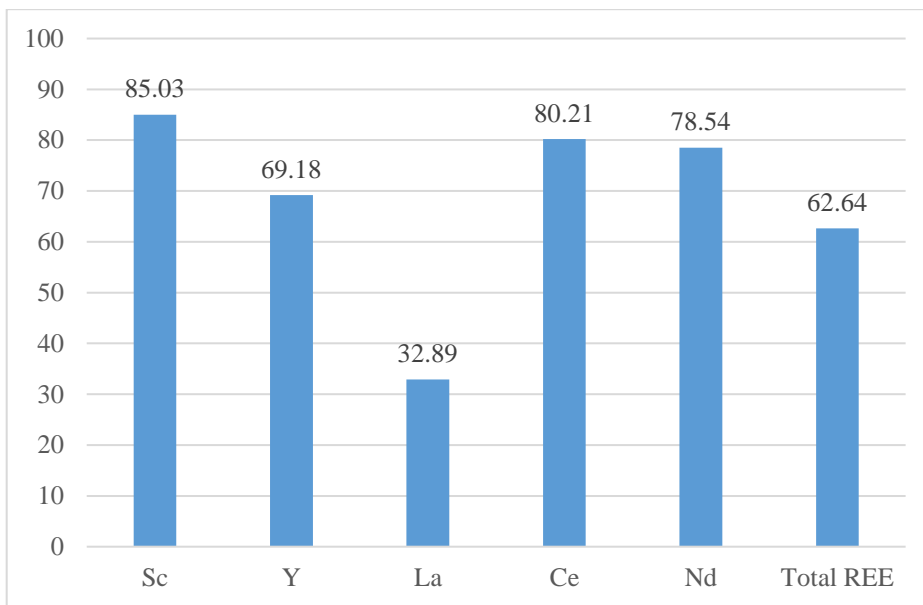

Figure 4.23 Recoveries of Sc, Y, La, Ce, Nd, and Total REE of Hard Coal Fly Ash subjected to 10% Hydrochloric Acid leaching in 90°C for 24 h

XRD analysis done in order to examine the results of the optimum condition and in resulted that the minerology is changed during leaching experiments like sulfuric acid leaching tests. Based on the XRD results, fly ash contains 65% Quartz and 35% Silimanite (Figure 4.24). Result showed that feed material's minerology was not changed, only slightly change of the contents changed, so the recovery of the rare earth minerals are lower than the other types of fly ashes used in this thesis.
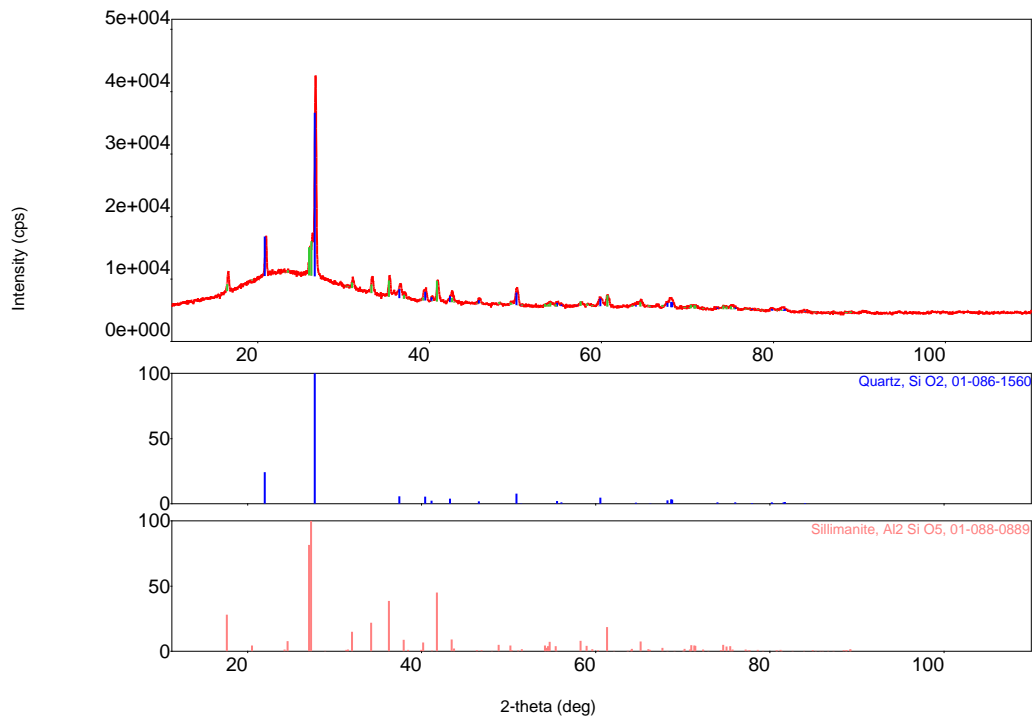
80

Figure 4.24 XRD Results of Hard Coal Fly Ash after Hydrochloric Acid Leaching Experiments

4.1.2 Direct Leaching with Organic Acids

In direct leaching tests experiments were done for each sample (SFA, AFA and HFA). The organic acid used for the leaching tests is citric acid.

4.1.2.1 Lignite Fly Ash

In citric acid leaching tests of Lignite fly ash, obtained efficiencies were lower than inorganic acids. By increasing temperature better results are obtained. Best cases were 30%Citric Acid, 90°C, 3h; 10%Citric Acid, 90°C, 1h and 20%Citric Acid, 60°C, 2h (Table 4.8).

Table 4.8 Best Resulted Direct Leaching Experiments on Lignite Fly Ash

Conditions	Total REE Recovery (%)
30%Citric Acid, 90℃, 24h	41.26
30%Citric Acid, 90℃, 6h	37.58
20%Citric Acid, 60℃, 12h	36.85

By initial concentrations and the final recoveries 5 rare earth minerals (Sc, Y, La, Ce & Nd) results were investigated (Figure 4.25).
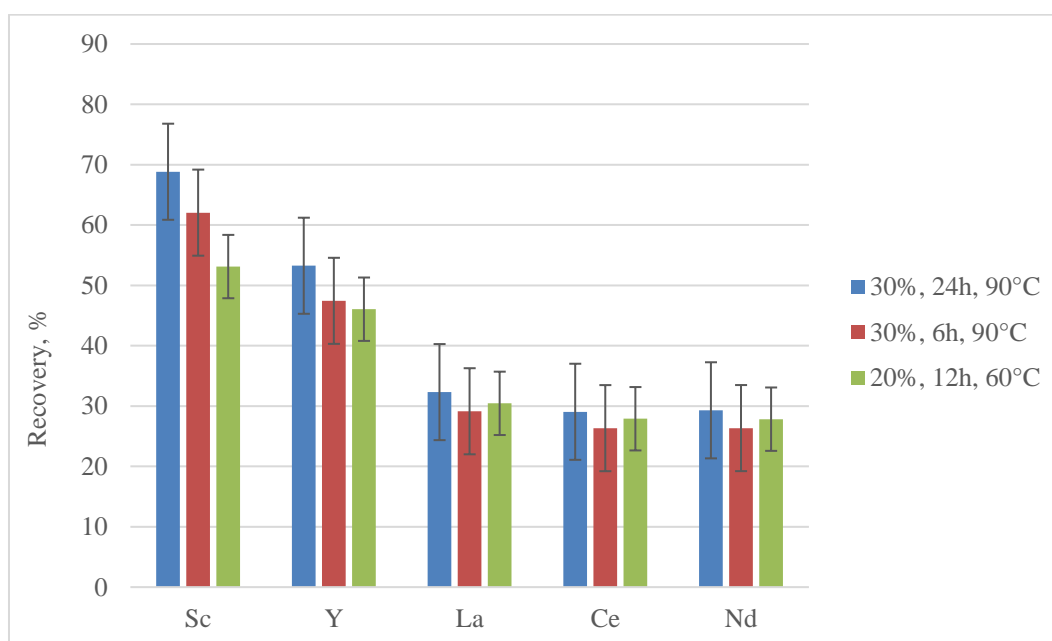

Figure 4.25 Recoveries of Sc, Y, La, Ce & Nd of Lignite Fly Ash after Citric Acid Leaching Experiments

The test results are statistically examined by two factorial design by using Minitab software and contour graphs drawn by the analysis Figure 4.26.

Acid concentration vs Temperature graph shows that temperature is very important, higher the temperature better the efficiencies. Also, similar relationship is occurred in time and temperature contour, temperature should be highest. Therefore, the

relationship of acid concentration vs time shows best efficiency obtained in the middle values.
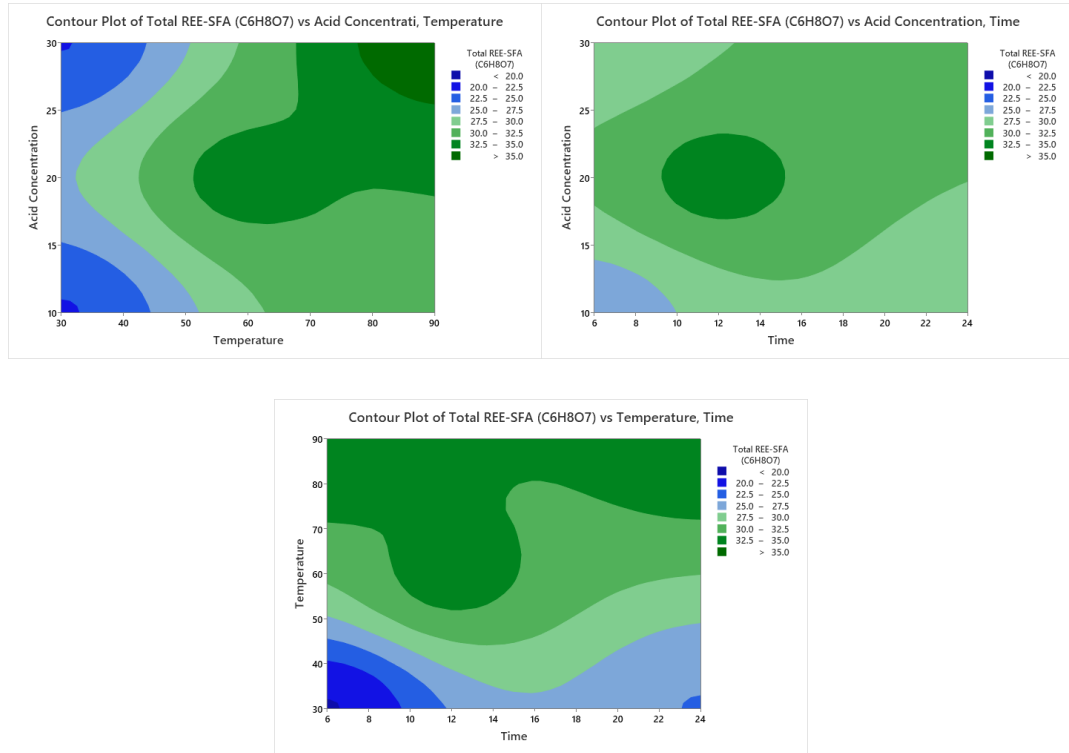

Figure 4.26 Contour Graphs of Lignite Fly Ash after Sulfuric Acid Leaching
Experiments (Minitab Software)

As a result of hydrometallurgical leaching tests and contour graphs, optimum condition is selected 30% citric acid in 90°C for 24 h which is also the best condition. In optimum conditions, pregnant leach solution with 150 ppm total rare earth element content was obtained with 41.26% yield.
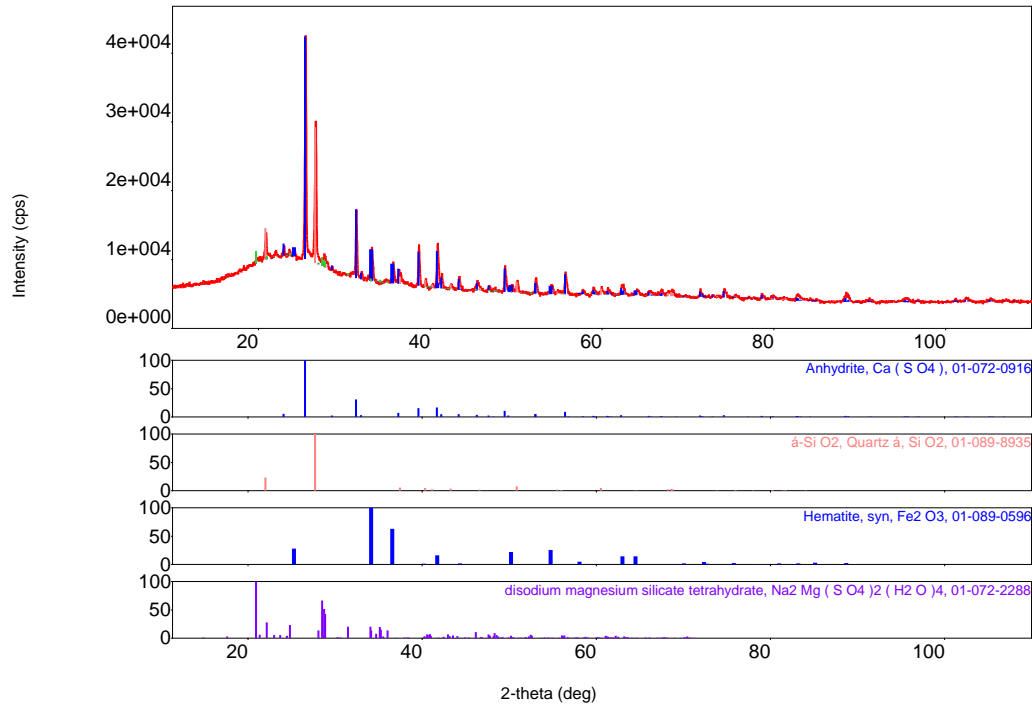
Figure 4.27 XRD Results of Lignite Fly Ash after Citric Acid Leaching Experiments

XRD analysis done in order to examine the results of the optimum condition and in resulted that the minerology is changed during leaching experiments. Based on the XRD results, fly ash contains 42.3% Anhydrate, 18.3% Quartz, 35% Disodium Magnesium Silicate Tetrahydrate and 4.6% Hematite (Fe_2O_3). XRD result showed that feed materials aluminosilicate phase was slightly broken and rare earth minerals could be leached by citric acid (Figure 4.27).

4.1.2.2   Asphaltite Fly Ash

In Asphaltite Fly Ash, by increasing the lixiviant concentration, better results are obtained. Best cases were 30%Citric Acid, 90°C, 3h; 30%Citric Acid, 90°C, 1h and 20%Citric Acid, 60°C, 2h (Table 4.9).

Table 4.9 Best Resulted Direct Leach Experiments on Asphaltite Fly Ash

Conditions	Total REE Recovery (%)
30% Citric Acid, 90°C, 24h	75.74
30% Citric Acid, 90°C, 6h	74.66
20% Citric Acid, 60°C, 12h	63.53

By initial concentrations and the final recoveries 5 rare earth minerals (Sc, Y, La, Ce & Nd) results were investigated (Figure 4.28).
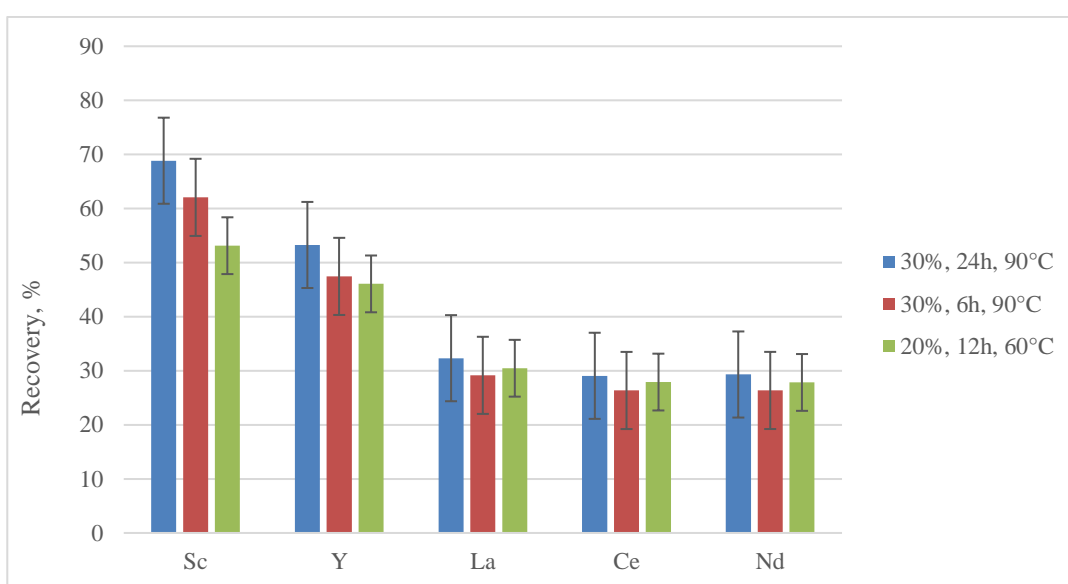

Figure 4.28 Recoveries of Sc, Y, La, Ce & Nd of Asphaltite Fly Ash after Citric Acid Leaching Experiments

The test results are statistically examined by two factorial design by using Minitab software and contour graphs drawn by the analysis Figure 4.29.

The contour graphs above shows that best recovery could be achieved in highest acid concentration, temperature and time. They are all directly related. So, optimum condition is selected the best condition 30% citric acid in 90°C for 24 h. In optimum conditions, pregnant leach solution with 218 ppm total rare earth element content was obtained with 75.74% yield.
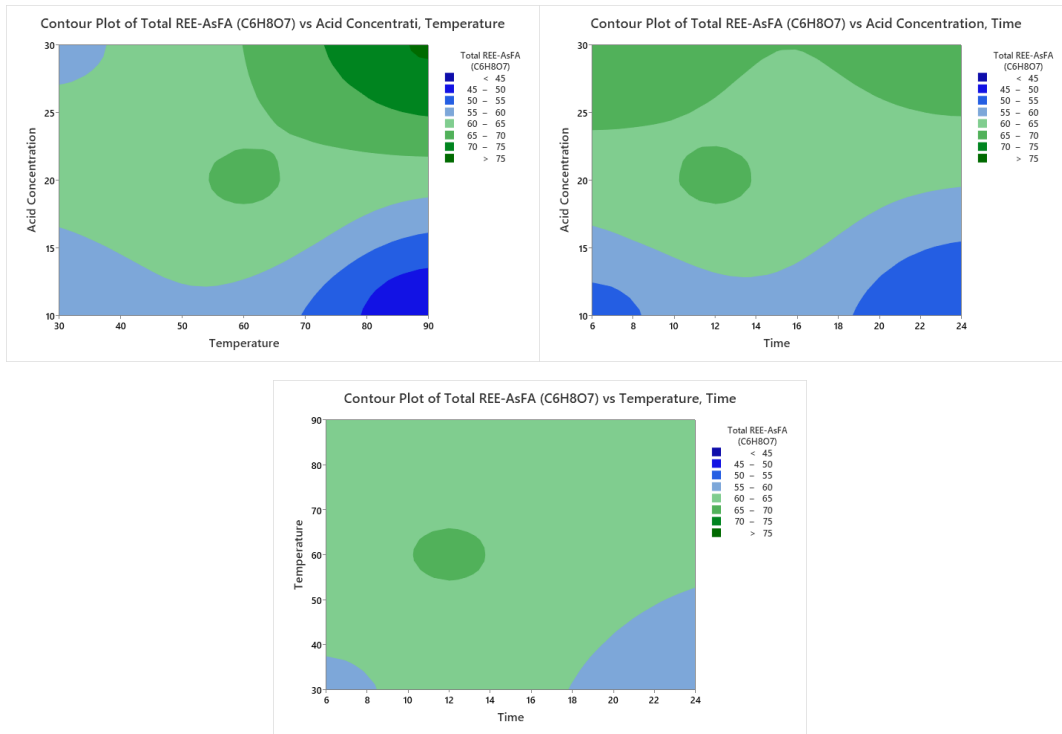
Figure 4.29 Contour Graphs of Asphaltite Fly Ash after Citric Acid Leaching
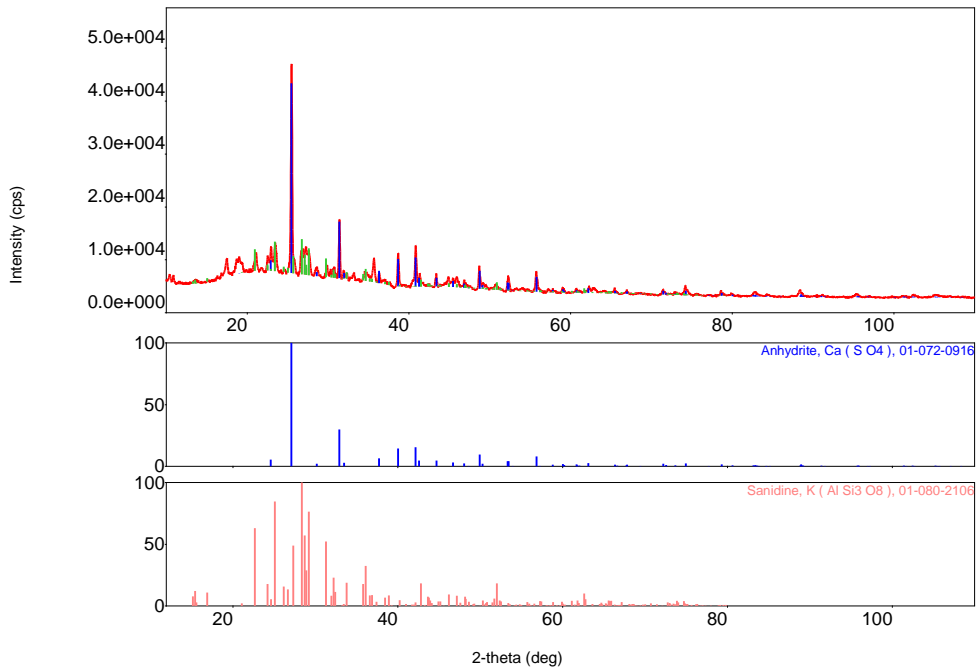Experiments (Minitab Software)

Figure 4.30 XRD Results of Asphaltite Fly Ash after Citric Acid Leaching
Experiments

XRD analysis done in order to examine the results of the optimum condition and in resulted that the minerology is changed during leaching experiments. Based on the XRD results, fly ash contains 57% Anhydrate, and 43.4% Sanidine. XRD result showed that feed materials aluminosilicate phase was slightly broken and rare earth minerals could be leached by citric acid (Figure 4.30).

4.1.2.3   Hard Coal Fly Ash

Citric acid leaching of hard coal fly ash has similar results with asphaltite fly ash. Best cases were 30%Citric Acid, 90°C, 3h; 30%Citric Acid, 90°C, 1h and 20%Citric Acid, 60°C, 2h (Table 4.10).

Table 4.10 Best Resulted Citric Acid Leaching Experiments on Hard Coal Fly Ash

Conditions	Total REE Recovery (%)
30% Citric Acid, 90°C, 24h	64.58
30% Citric Acid, 90°C, 6h	64.50
20% Citric Acid, 60°C, 12h	64.22

By initial concentrations and the final recoveries 5 rare earth minerals (Sc, Y, La, Ce & Nd) results were investigated (Figure 4.31).
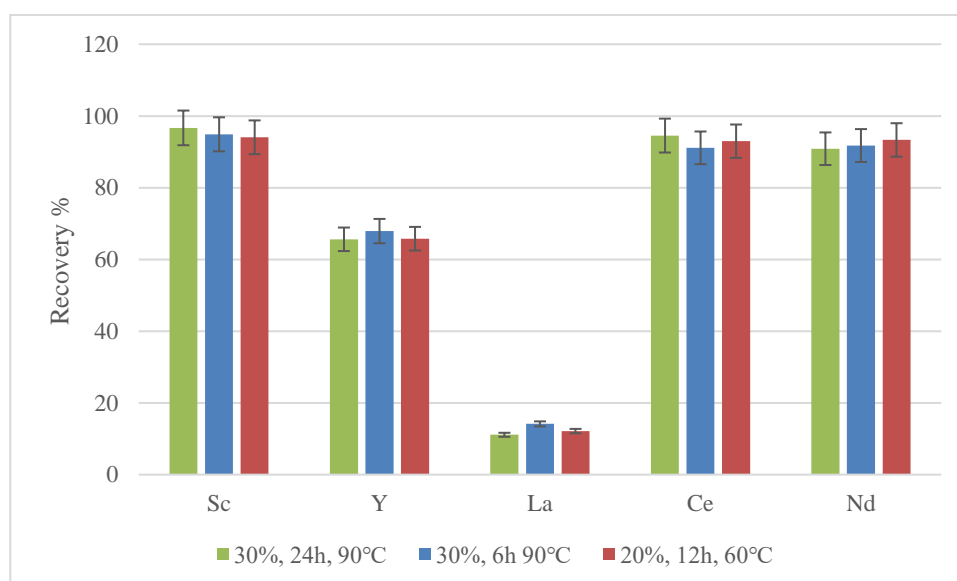
Figure 4.31 Recoveries of Sc, Y, La, Ce & Nd of Hard Coal Fly Ash after Citric
Acid Leaching Experiments

The test results are statistically examined by two factorial design by using Minitab
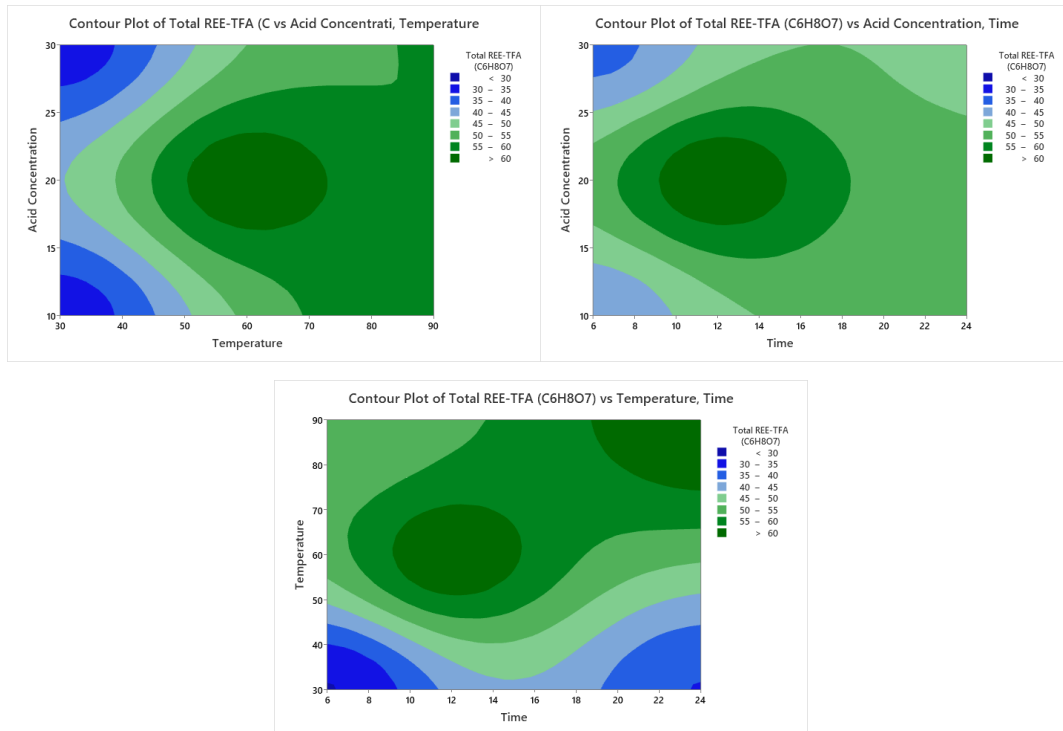software and contour graphs drawn by the analysis Figure 4.32.

Figure 4.32 Contour Graphs of Hard Coal Fly Ash after Citric Acid Leaching
Experiments (Minitab Software)

Contour graphs shows that as the temperature increases, recovery increases. The
relationship of acid concentration vs temperature and acid concentration vs time
shows best efficiency obtained in the middle values.

As a result of hydrometallurgical leaching tests, optimum condition is selected 30%
citric acid in 90°C for 24 h. Like as Lignite and asphaltite fly ashes that is also the
best condition. In optimum conditions, pregnant leach solution with 283 ppm total
rare earth element content was obtained with 64.58% yield.

XRD analysis done in order to examine the results of the optimum condition and in
resulted that the minerology is changed during leaching experiments. Based on the
XRD results, fly ash contains 60% Quartz and 40% Silimanite (Figure 4.33). Results

showed that feed material's minerology was not changed, only slightly change of the contents changed, so the recovery of the rare earth minerals are lower than the other types of fly ashes used in this thesis.
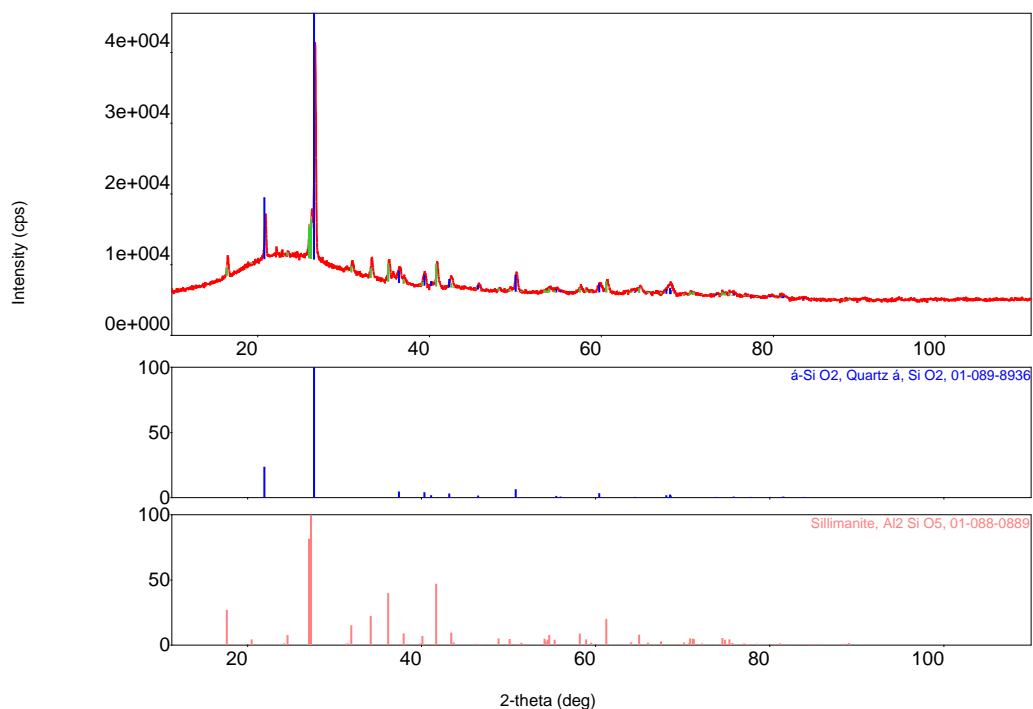

Figure 4.33 XRD Results of Hard Coal Fly Ash after Citric Acid Leaching Experiments

4.1.3   Sequential Leaching with Inorganic Acids

In line with the results of sulfuric acid and hydrochloric acid leaching performed on fly ash material before, it was thought that the application of the Sequential Leaching process would carry the test results further. In this context, the metallurgical leaching efficiencies of hydrochloric acid leaching carried out on the leach residue of hydrochloric acid leaching following sulfuric acid leaching.

Within the scope of sequential leaching tests, the main purpose of the sulfuric acid leaching carried out in the first stage is the selective recovery of elements with relatively similar metallurgical behavior such as scandium, yttrium and neodymium

while leaving as much of the rare earth elements in the leach residue as possible. The main purpose of hydrochloric acid leaching carried out in the second stage was to recover rare earth elements by leaching the leach residue, which was purified from scandium, yttrium and the other rare earth element contents, and alumina-silicate bonds containing rare earth elements were weakened as much as possible with hydrochloric acid.

4.1.3.1 Lignite Fly Ash

As a result of the leaching tests carried out for 6 hours at 60 °C and 1/10 solid-liquid ratio using 10% sulfuric acid solution within the scope of the first stage leaching tests, 63.35% of the Scandium content, 51.86% of yttrium content and 45.31% of the total rare earth content of the fly ash material was recovered in the leach solution.

At the second stage as a result of the leaching tests carried out on the leach residue produced from sulfuric acid leaching, using 30% Hydrochloric acid solution, at 90 °C and 1/10 solid-liquid ratio for 24 hours, the Lanthanum content of the material is 71.88%, the Cerium content is 68.01%, Praseodymium 66.64% of the content and 75.50% of the total rare earth element content was recovered in the leach solution.

In this context, the total leaching efficiencies obtained as a result of the sequential leaching process are as follows;

- Scandium Leach Yield: 85.78%
- Yttrium Leach Yield: 86.22%
- Lanthanum Leach Yield: 80.82 %
- Cerium Leach Yield: 77.15%
- Praseodymium Leach Yield: 75.92%
- Neodymium Leach Yield: 76.82%
- Total Rare Earth Leach Yield: 86.05%

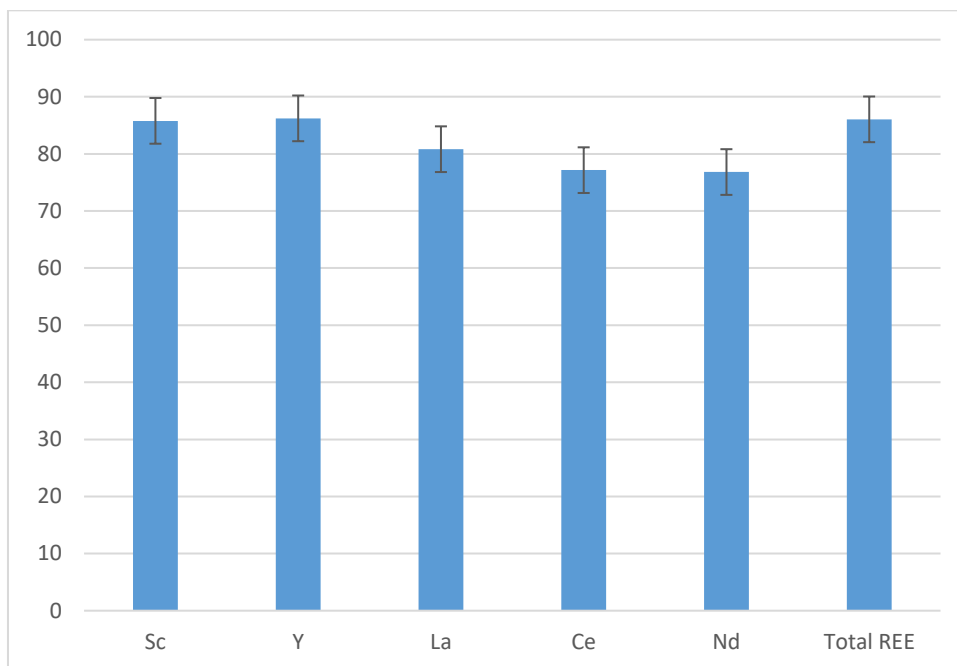The results are shown in Figure 4.34 and Table 4.11.

Figure 4.34 Total Recoveries of Sc, Y, La, Ce, Nd & Total REE of Lignite Fly Ash after Sequential Leaching Experiments

In the light of all these data, it is seen that the metal recovery efficiencies with the sequential leaching setup have increased by up to 10% compared to the leaching tests carried out before, therefore the applied process has a positive reaction on the Lignite fly ash material.

Table 4.11 Results of Sequential Leaching Experiments on Lignite Fly Ash

Total REE Recovery (%)	LREE Recovery (%)	HREE Recovery (%)
86.05	79.23	90.73

XRD analysis done in order to examine the results of the sequential leaching and resulted that the minerology is changed during leaching experiments. Based on the XRD results, fly ash contains 61% Anhydrate ($CaSO_4$), 18% Quartz (SiO_2) and 21% Anorthoclase. Results showed that feed material's minerology changed and albite content which was an aluminosilicate phase was broken and rare earth minerals can

be leached by acid. Also the formation of anorthoclase occurred. The XRD graph is given in Figure 4.35. Furthermore, Cr, Ni and Ti contents were dissolved in pregnant leach solution as impurities. So that, selective precipitation needed to reduce the impurities.
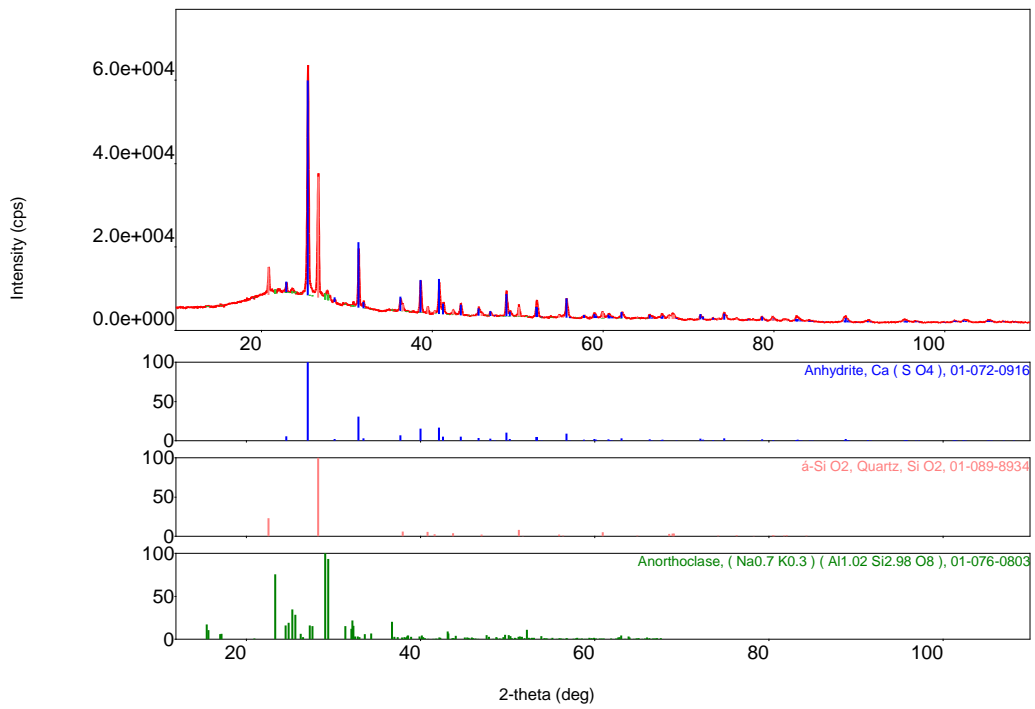
Flowsheet and the results is shown in Figure 4.36

Figure 4.35 XRD Result of Lignite Fly Ash after Sequential Leaching Experiments
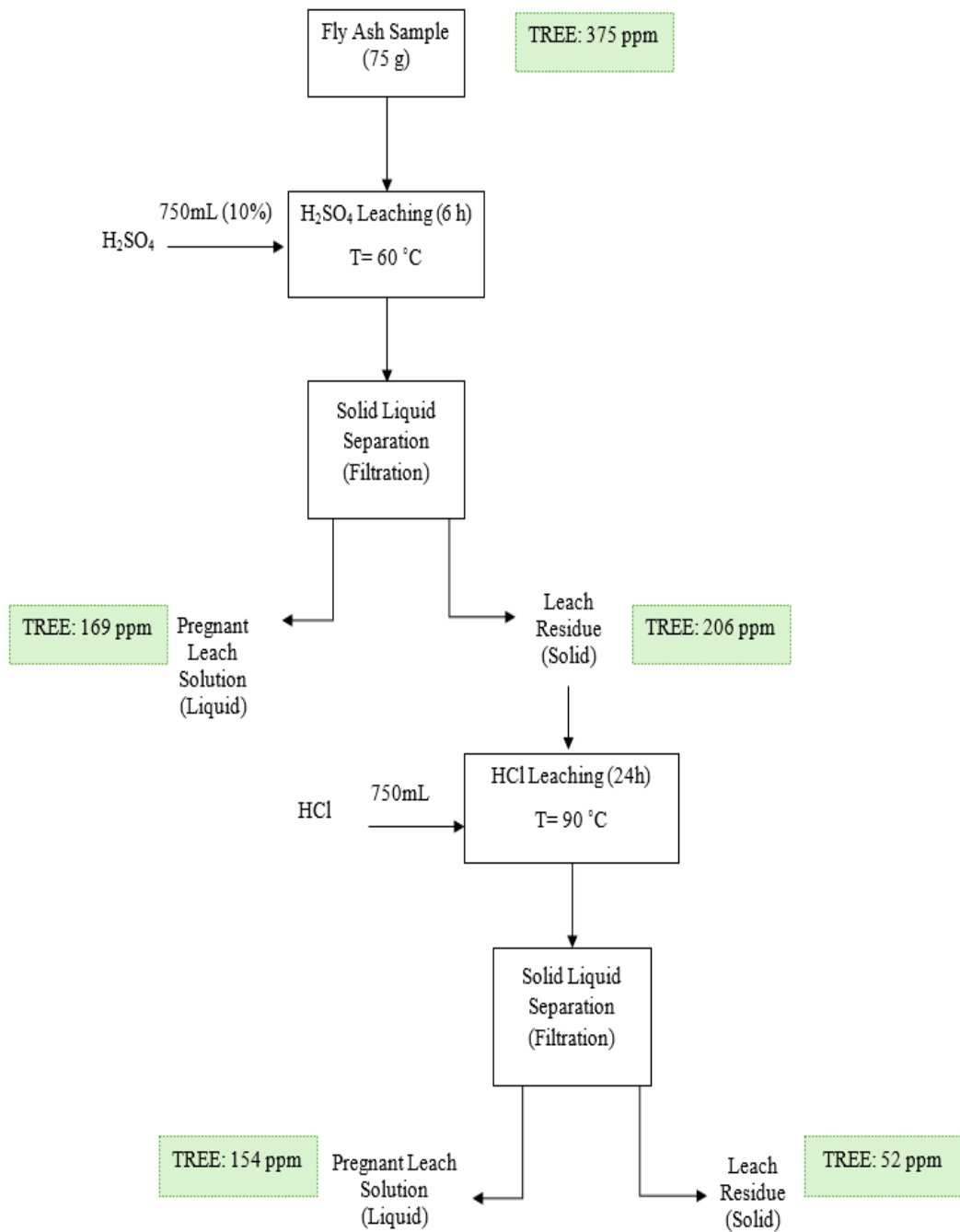
Figure 4.36 Lignite Fly Ash Sequential Leaching Experiments Flowsheet

4.1.3.2   Asphaltite Fly Ash

As a result of the asphaltite leaching tests carried out, same with Lignite fly ash, for 6 hours at 60°C and 1/10 solid-liquid ratio using 10% Sulfuric acid solution within the scope of the first stage leaching tests, 68.04% of the total rare earth element content, 64.46% of the Scandium content and 68.28% of yttrium content of the fly ash material was recovered in the leach solution.

As a result of the leaching tests carried out on the leach residue produced from sulfuric acid leaching, using 30% Hydrochloric acid solution, at 90 °C and 1/10 solid-liquid ratio for 24 hours, the Lanthanum content of the material is 86.93%, the Cerium content is 83.60%, Praseodymium 86.05% of the content, 86.35% of the Neodymium and 82.98% total rare earth element content was recovered in the leach solution.

In this context, the overall leaching efficiencies obtained as a result of the sequential leaching process are as follows;

- Scandium Leach Yield: 96.34%
- Yttrium Leach Yield: 98.84%
- Lanthanum Leach Yield: 95.78 %
- Cerium Leach Yield: 94.69%
- Praseodymium Leach Yield: 95.59%
- Neodymium Leach Yield: 95.56%
- Total Rare Earth Leach Yield: 96.93%

The results are shown in Figure 4.37 and Table 4.12.

In the light of all these data, it is seen that the metal recovery efficiencies with the sequential leaching setup have increased by up to 11% compared to the leaching tests carried out before, therefore the applied process has a positive reaction on the asphaltite fly ash material.
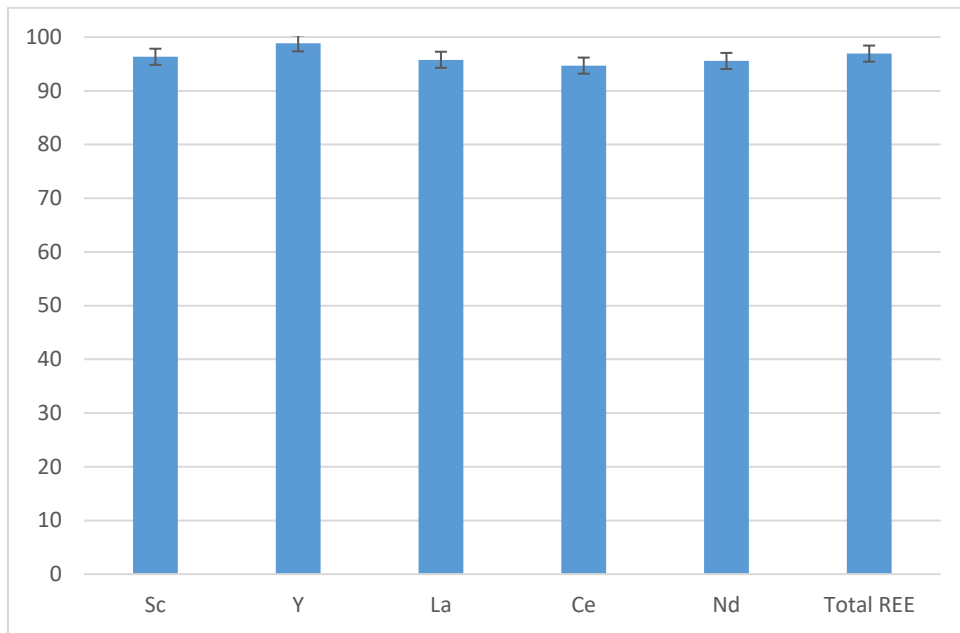
Figure 4.37 Total Recoveries of Sc, Y, La, Ce, Nd & Total REE of Asphaltite Fly Ash after Sequential Leaching Experiments

Table 4.12 Results of Sequential Leaching Experiments on Asphaltite Fly Ash

Total REE Recovery (%)	LREE Recovery (%)	HREE Recovery (%)
96.93	95.93	98.96

Flowsheet and the results is shown in Figure 4.38.

XRD analysis done in order to examine the results of the sequential leaching and resulted that the minerology is changed during leaching experiments. Based on the XRD results, fly ash contains 86.4% Gypsum ($CaSO_4.2H_2O$) and 13.6% Orthoclase ($KalSi_3O_8$). Result showed that feed material's minerology changed and Al and Si contained minerals were reduced. So that aluminosilicate phase was broken and rare earth minerals were leached by acids. Also the formation of gypsum occurred. The XRD graph is given in Figure 4.39. Furthermore, Mg and Fe contents were dissolved in pregnant leach solution as impurities. So that, selective precipitation needed to reduce the impurities.
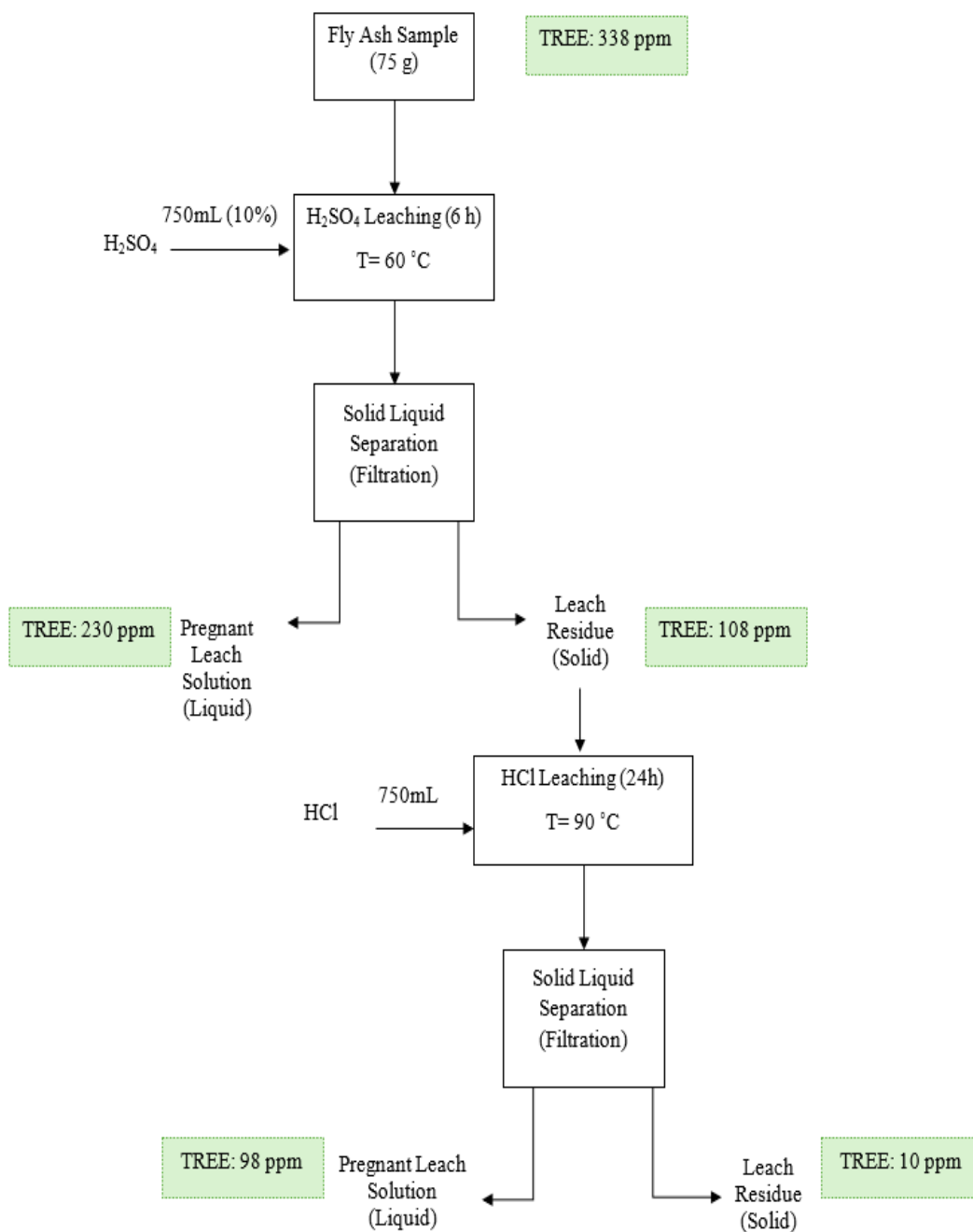
95

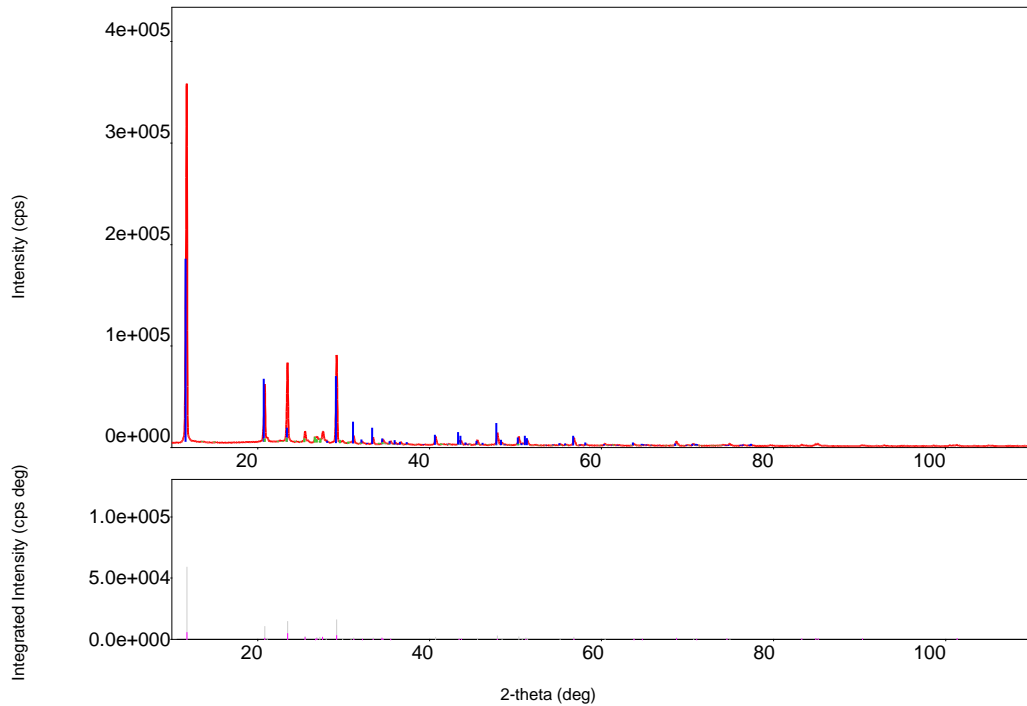Figure 4.38 Asphaltite Fly Ash Sequential Leaching Experiments Flowsheet

Figure 4.39 XRD Result of Asphaltite Fly Ash after Sequential Leaching
Experiments

4.1.3.3   Hard Coal Fly Ash

As a result of the leaching tests carried out for 6 hours at 60 °C and 1/10 solid-liquid ratio using 10% Sulfuric acid solution within the scope of the first stage leaching tests, 23.43% of the total rare earth element content, 10.49% of the Scandium content and 63.17% of yttrium content of the fly ash material was recovered in the leach solution.

As a result of the leaching tests carried out on the leach residue produced from sulfuric acid leaching, using 30% Hydrochloric acid solution, at 90 °C and 1/10 solid-liquid ratio for 24 hours, the Lanthanum content of the material is 71.15%, the Cerium content is 69.86%, Praseodymium 49.25% of the content, 70.09% of the Neodymium and 67.73% total rare earth element content was recovered in the leach solution.

In this context, the total leaching efficiency obtained as a result of the sequential leaching process is as follows;

- Scandium Leach Yield: 62.44%
- Yttrium Leach Yield: 95.08%
- Lanthanum Leach Yield: 72.15 %
- Cerium Leach Yield: 72.70%
- Praseodymium Leach Yield: 54.31%
- Neodymium Leach Yield: 73.77%
- Total Rare Earth Leach Yield: 73.45%

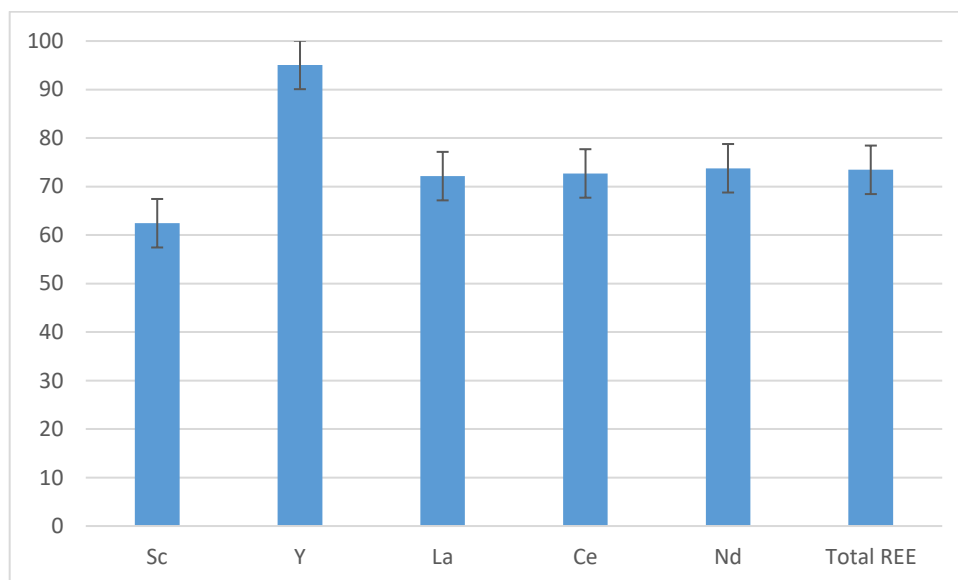The results are shown in Figure 4.40 and Table 4.13.

Figure 4.40 Total Recoveries of Sc, Y, La, Ce, Nd & Total REE of Hard Coal Fly Ash after Sequential Leaching Experiments

In the light of all these data, it is seen that the metal recovery efficiencies with the sequential leaching setup have increased by up to 9% compared to the leaching tests carried out before, therefore the applied process has a positive reaction on the hard coal fly ash material. But the recovery was not enough.

Table 4.13 Results of Sequential Leaching Experiments on Hard Coal Fly Ash

Total REE Recovery (%)	LREE Recovery (%)	HREE Recovery (%)
73.45	77.26	69.85

XRD analysis done in order to examine the results of the sequential leaching and resulted that the minerology is changed during leaching experiments. Based on the XRD results, fly ash contains 49% Quartz (SiO_2) and 51% Mullite ($Al_{4.52}Si_{1.48}O_{9.74}$). Result showed that feed material's minerology was not changed, only slightly change of the contents changed, so the recovery of the rare earth minerals are lower than the other types of fly ashes used in this thesis. The XRD graph is given in Figure 4.41.
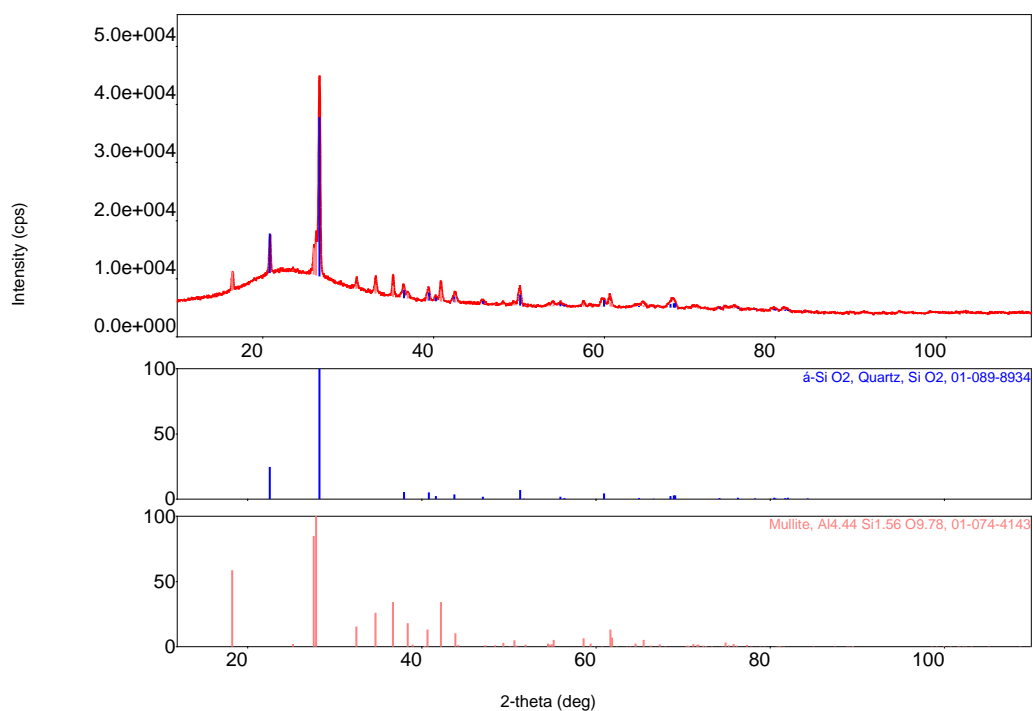

Figure 4.41 XRD Result of Hard Coal Fly Ash after Sequential Leaching Experiments

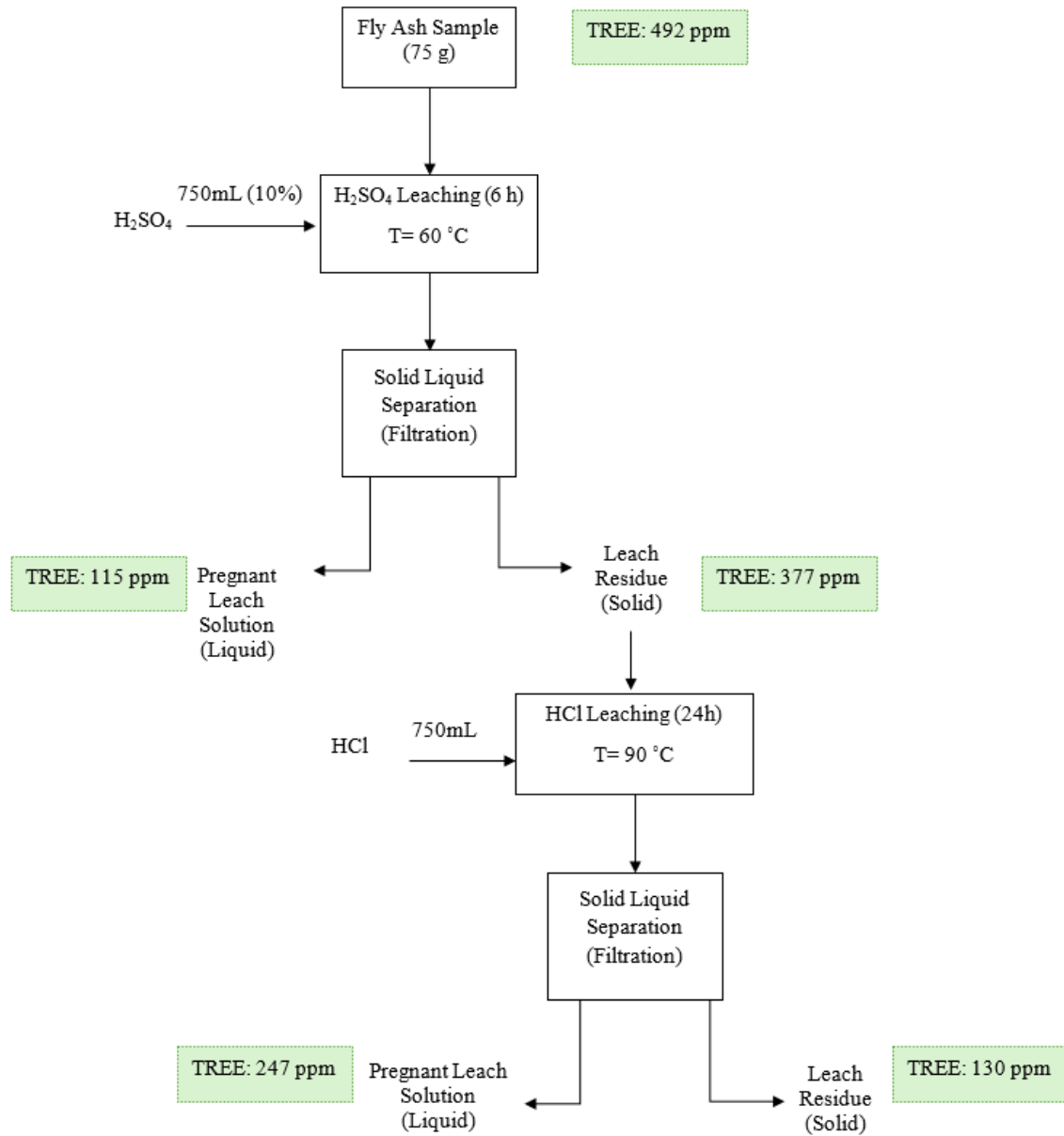Flowsheet and the final results is shown in Figure 4.42.

Figure 4.42 Hard Coal Fly Ash Sequential Leaching Experiments Flowsheet

4.2 Assessment of the Fly Ash Leach Residues by Scanning Electron Microscopy

Sequential leaching and citric acid leaching residues were subjected to SEM analysis in order to see the effects of leaching. The images are given in following sections.

4.2.1 Lignite Fly Ash

Figure 4.43 demonstrates the scanning electron microscopy (SEM) image of the leach residue of the first step of the sequential leaching experiments done 6 hours at 60 °C and 1/10 solid-liquid ratio using 10% sulfuric acid solution. Figure 4.44 shows energy-dispersive X-ray spectroscopy (EDS) analysis of the SEM image. Identified elements by EDS are labeled above the relevant peaks. EDS analysis shows abundance of silicon and oxygen in the ore represented by high-intensity peaks. Presence of calcium, aluminum and sulfur are also apparent with peaks of moderate intensities. It has been seen that sample consists of spherical and angular particles of dimensions ranging from 1-50 microns as a result of morphological examination.
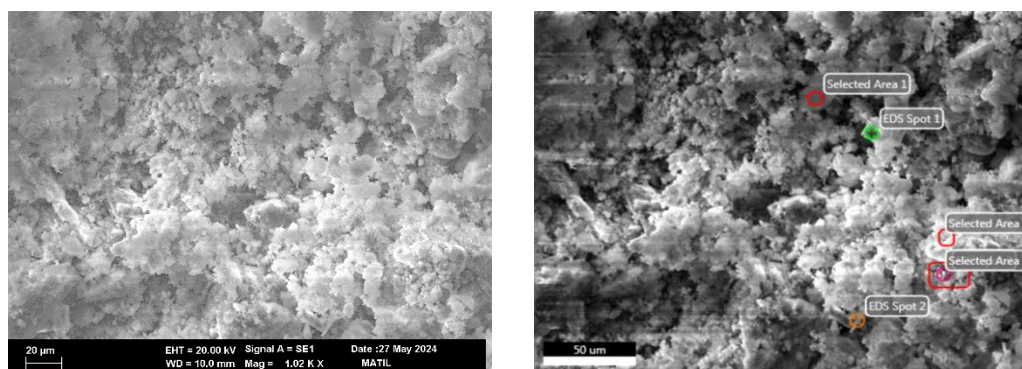

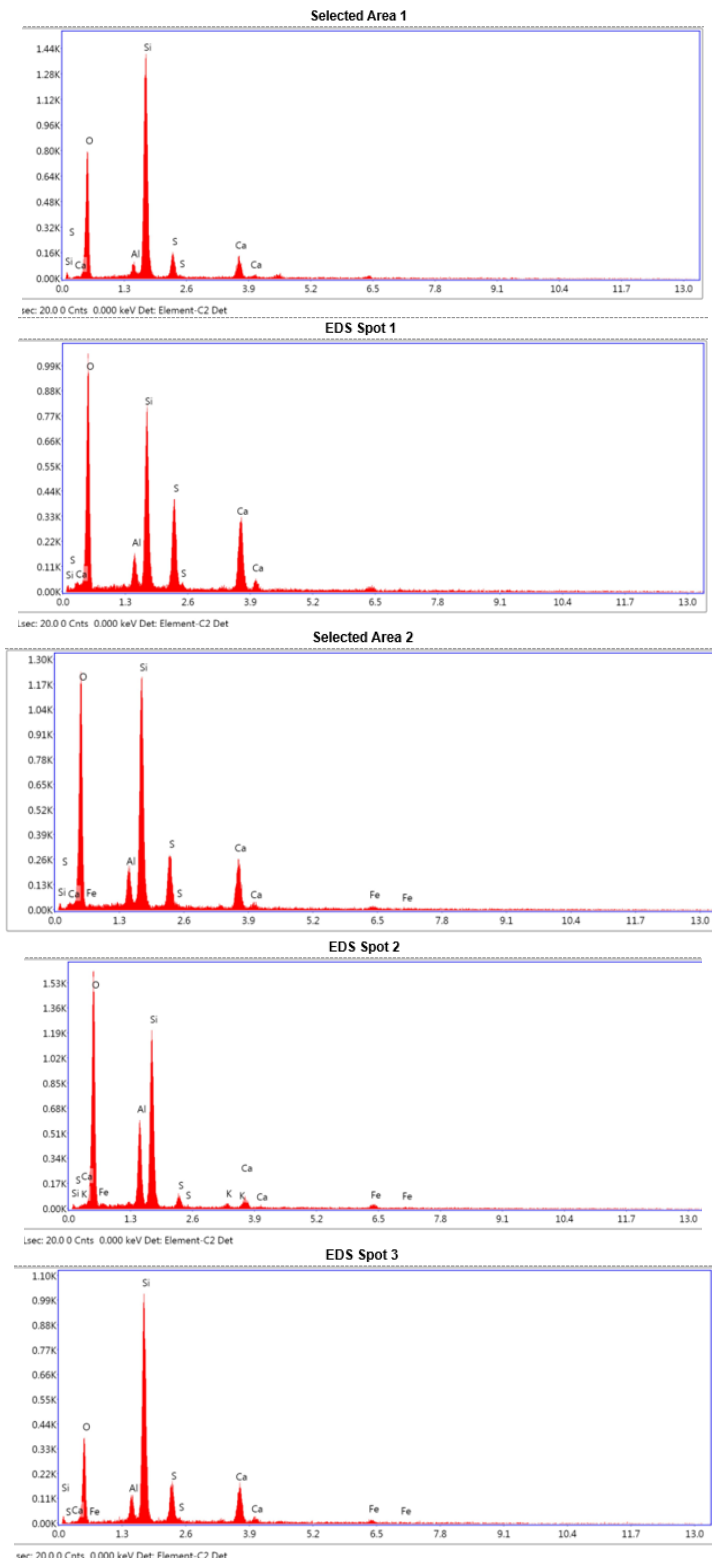Figure 4.43 SEM Images of Lignite Fly Ash Leach residue after the first step of Sequential Leaching

Figure 4.44 EDS analysis of the different spots and areas of Lignite Fly Ash Leach
residue after the first step of Sequential Leaching

Figure 4.45 shows the SEM image of the leach residue of the second step of the sequential leaching experiments done 24 hours at 90 °C and 1/10 solid-liquid ratio using 30% hydrochloric acid solution. Energy-dispersive X-ray spectroscopy (EDS) analysis of the SEM image can be seen in Figure 4.46. Identified elements by EDS are labeled above the relevant peaks. EDS analysis shows abundance of silicon and oxygen in the ore represented by high-intensity peaks. Presence of aluminum apparent with peaks of moderate intensities. Calcium and sulfur peaks were decreased and small Fe peak was seen. The morphology of the particles has changed spheres to irregular shapes.

Spherical shapes which are mostly alumina-silicate phases are reduced and recovery of rare earth minerals can be obtained.
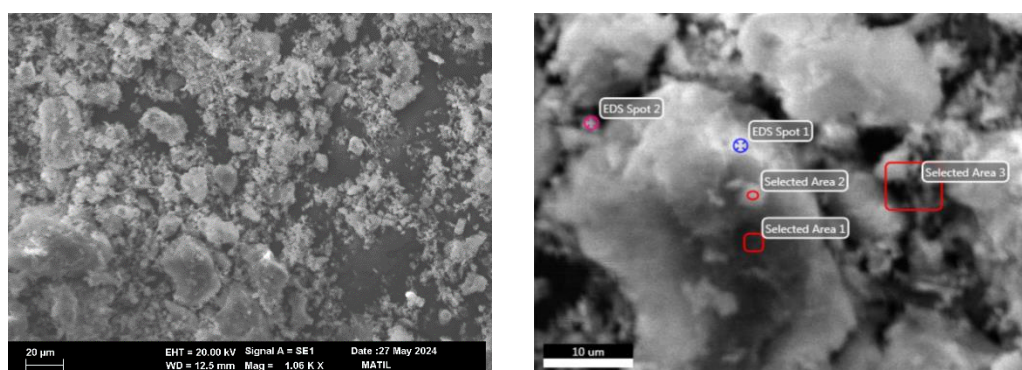

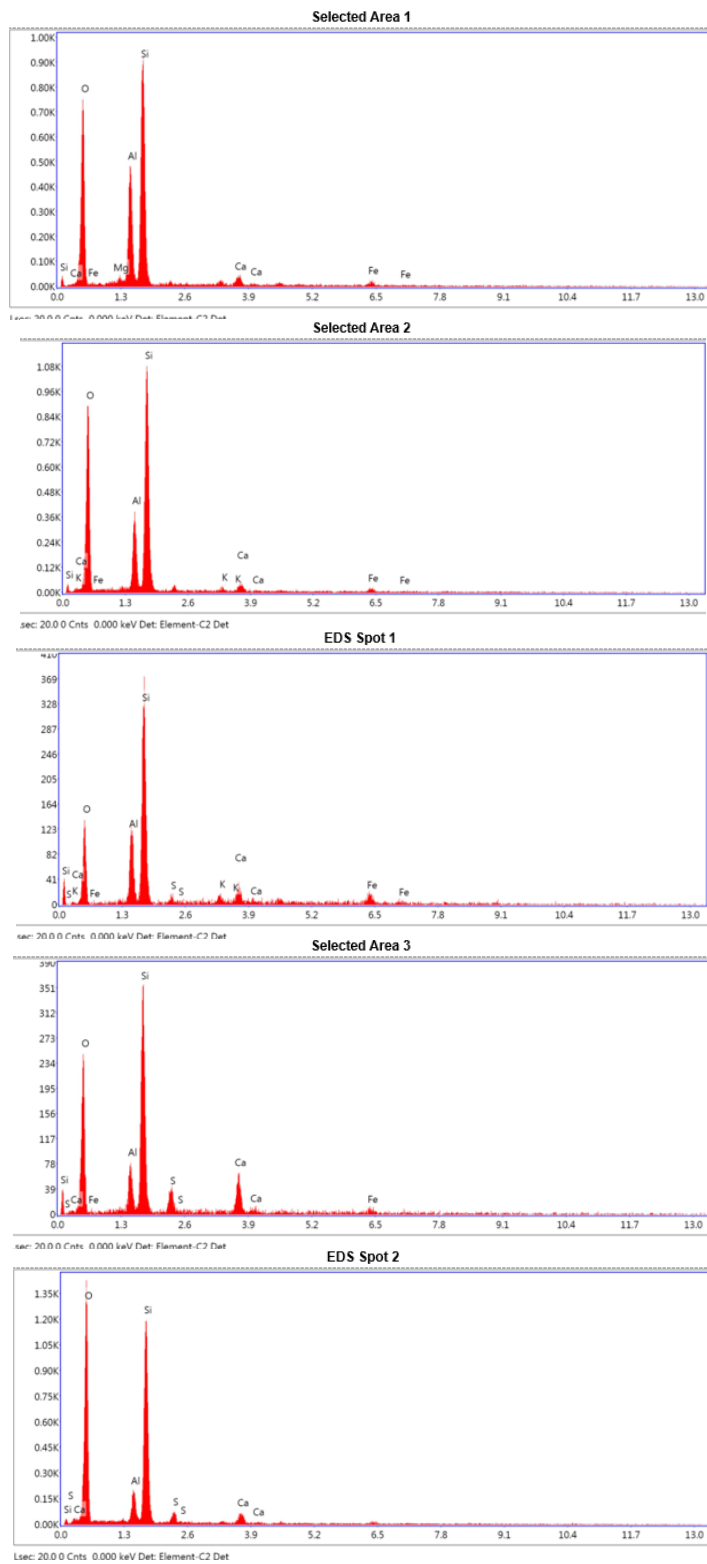Figure 4.45 SEM Images of Lignite Fly Ash Leach residue after the second step of Sequential Leaching

Figure 4.46 EDS analysis of the different spots and areas of Lignite Fly Ash Leach residue after the second step of Sequential Leaching

Characteristics of the SEM images and EDS analysis of the leach residue of citric acid leaching in 24 hours at 90 °C and 1/10 solid-liquid ratio using 30% acid solution is shown in Figure 4.47 and Figure . The morphology of the particles are very similar with the sample before experiments. High-intensity silicon and oxygen peaks are seen in the EDS analysis. Presence of aluminum and calcium apparent with peaks of moderate intensities. Small Fe and S peaks were seen.
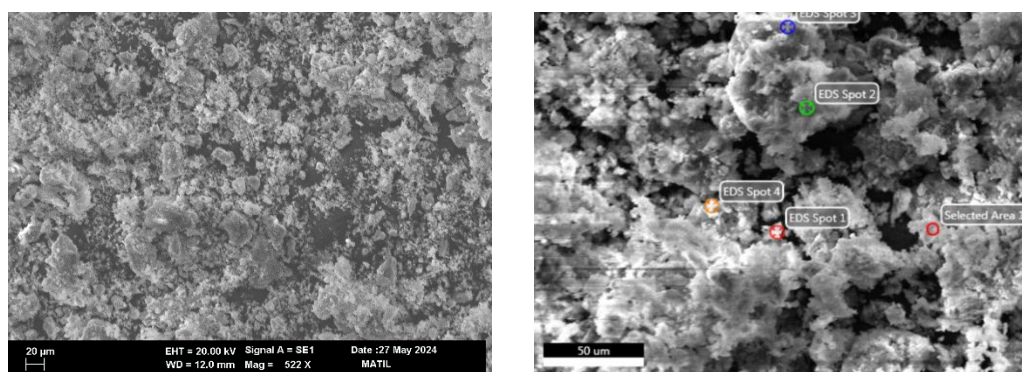

Figure 4.47 SEM Images of Lignite Fly Ash Leach residue after Citric Acid Leaching
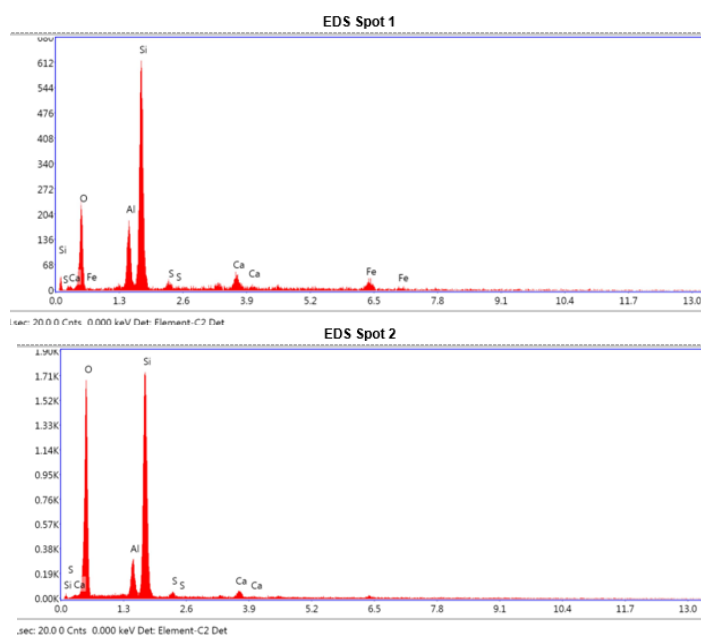
Figure 4.48 EDS analysis of the different spots and areas of Lignite Fly Ash Leach residue after Citric Acid Leaching
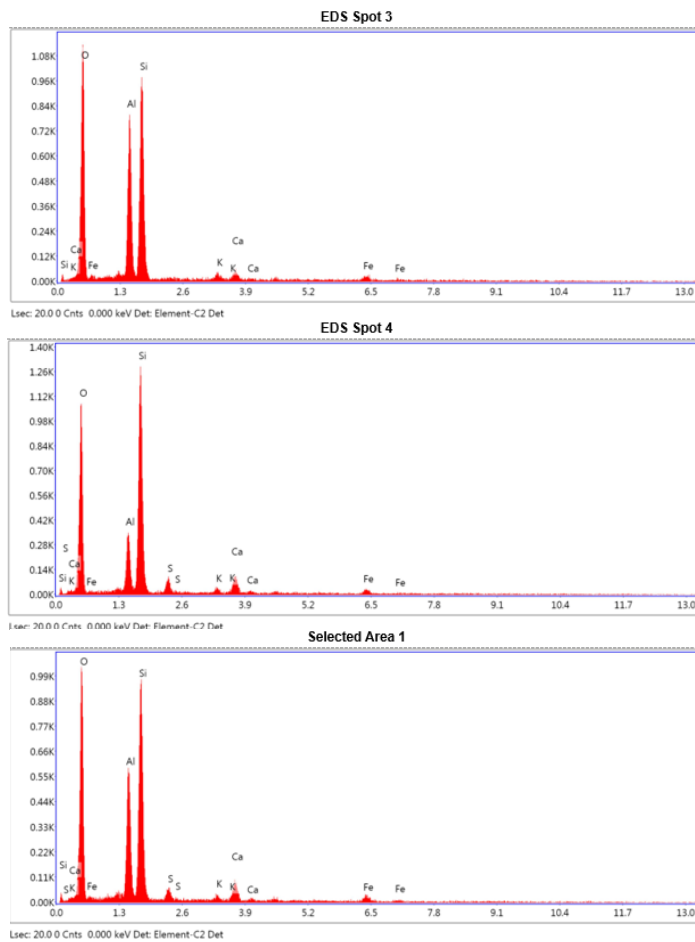
Figure 4.48 (Cont'd)

4.2.2   Asphaltite Fly Ash

Figure 4.49 shows the scanning electron microscopy (SEM) image of the leach residue of the first step of the sequential leaching experiments for 6 hours at 60 °C and 1/10 solid-liquid ratio using 10% sulfuric acid solution. Figure 4.50 shows energy-dispersive X-ray spectroscopy (EDS) analysis of the SEM image. The morphology has shown that cubical shaped particles occurred. EDS analysis shows abundance of silicon and sulfur in the ore represented by high-intensity peaks. Presence of calcium, aluminum and potassium are also apparent with peaks of moderate intensities.
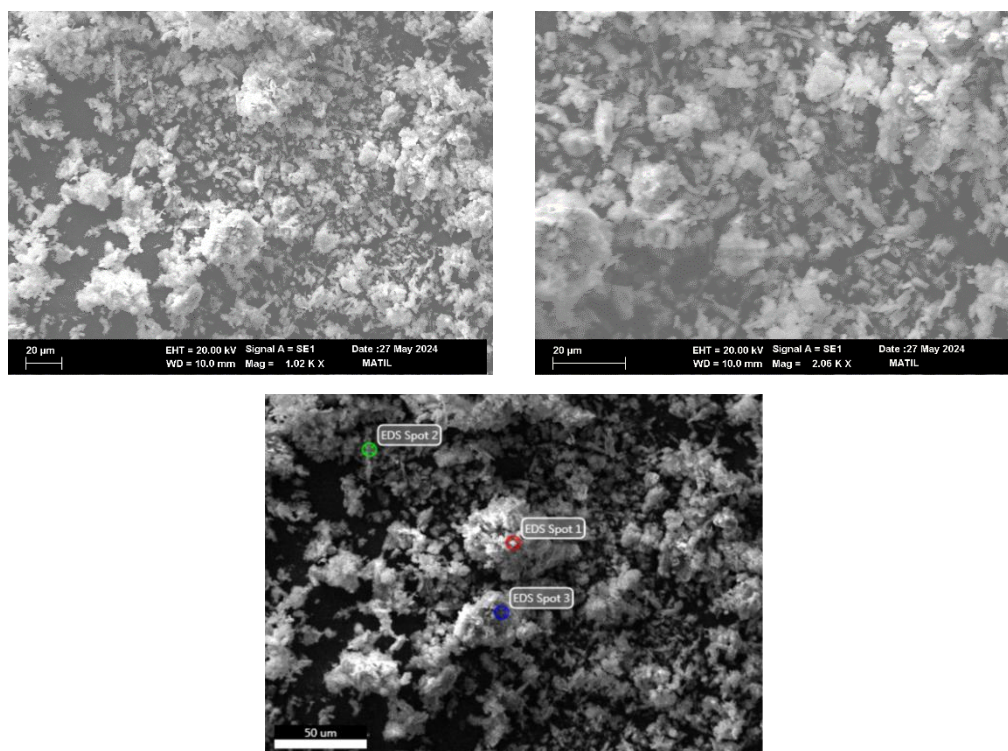
Figure 4.49 SEM Images of Asphaltite Fly Ash Leach residue after the first step of Sequential Leaching

The SEM image of the leach residue of the second step of the sequential leaching experiments done 24 hours at 90 °C and 1/10 solid-liquid ratio using 30% hydrochloric acid solution is shown in Figure 4.51. Energy-dispersive X-ray spectroscopy (EDS) analysis of the SEM image can be seen in Figure 4.52. In SEM images gypsum crystals can be seen very clearly. The morphology of the particles are very distinct crystal shape. Alumina-silicate phase has been broken. So that the recovery is 97%.

EDS analysis shows abundance of silicon, oxygen and calcium in the ore represented by high-intensity peaks. Presence of aluminum apparent with very few peaks of moderate intensities. Small potassium and sulfur peaks were seen.

Figure 4.50 EDS analysis of the different spots and areas of Asphaltite Fly Ash Leach residue after the first step of Sequential Leaching

Figure 4.51 SEM Images of Asphaltite Fly Ash Leach residue after the second step of Sequential Leaching

Figure 4.52 EDS analysis of the different spots and areas of Asphaltite Fly Ash
Leach residue after the second step of Sequential Leaching
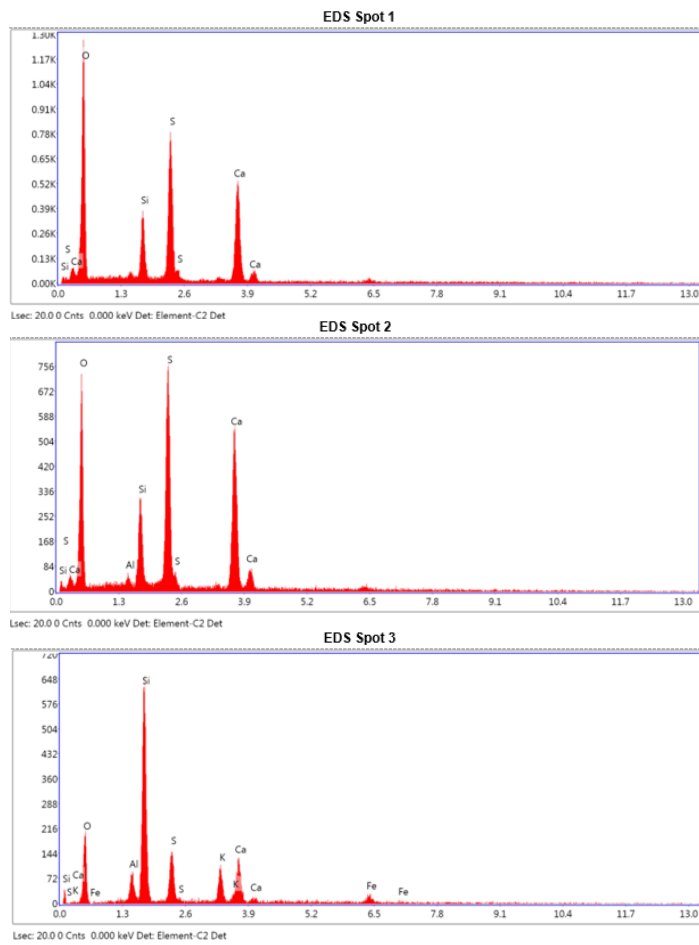
SEM images and EDS analysis of the leach residue of citric acid leaching in 24 hours at 90 °C and 1/10 solid-liquid ratio using 30% acid solution is shown in Figure 4.53 and Figure . The morphology of the particles are very similar with the sample before experiments spherical and needle shaped particles can be seen. High-intensity silicon, calcium and oxygen peaks seen in the EDS analysis. Presence of iron and potassium apparent with peaks of moderate intensities. Small S peaks were seen.
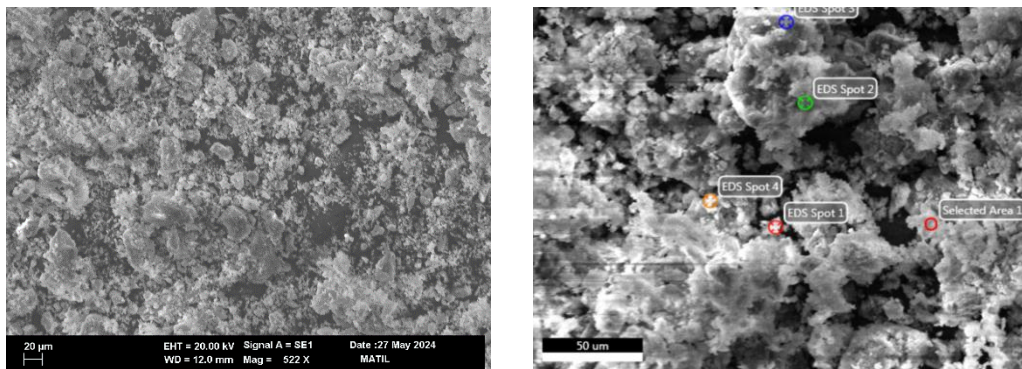
Figure 4.53 SEM Images of Asphaltite Fly Ash Leach residue after Citric Acid Leaching
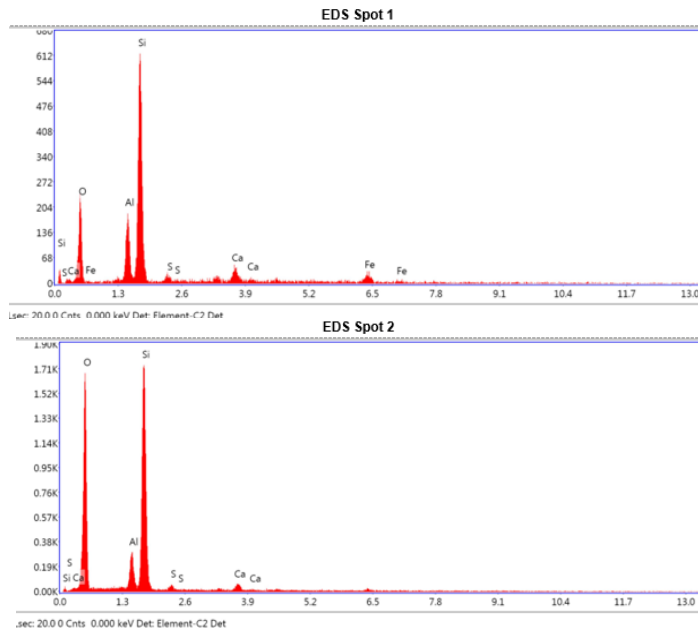
Figure 4.54 EDS analysis of the different spots and areas of Asphaltite Fly Ash Leach residue after Citric Acid Leaching
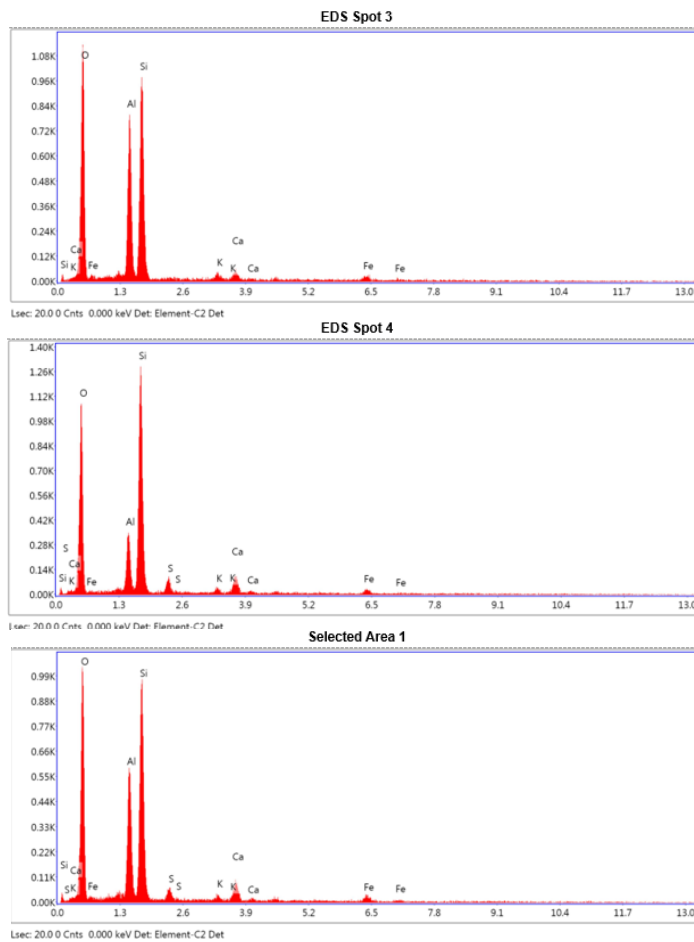
Figure 4.54 (Cont'd)

4.2.3   Hard Coal Fly Ash

Figure 4.55 demonstrates the scanning electron microscopy (SEM) image of the leach residue of the first step of the sequential leaching experiments which was done for 6 hours at 60 °C and 1/10 solid-liquid ratio using 10% sulfuric acid solution. Figure shows energy-dispersive X-ray spectroscopy (EDS) analysis of the SEM image. Identified elements by EDS are labeled above the relevant peaks. EDS analysis shows abundance of silicon and oxygen in the ore represented by high-intensity peaks like lignite and asphaltite fly ash samples. Presence of aluminum is also apparent with peaks of moderate intensities. It has been seen that sample consists

of spherical of dimensions ranging from 1-50 microns as a result of morphological examination.

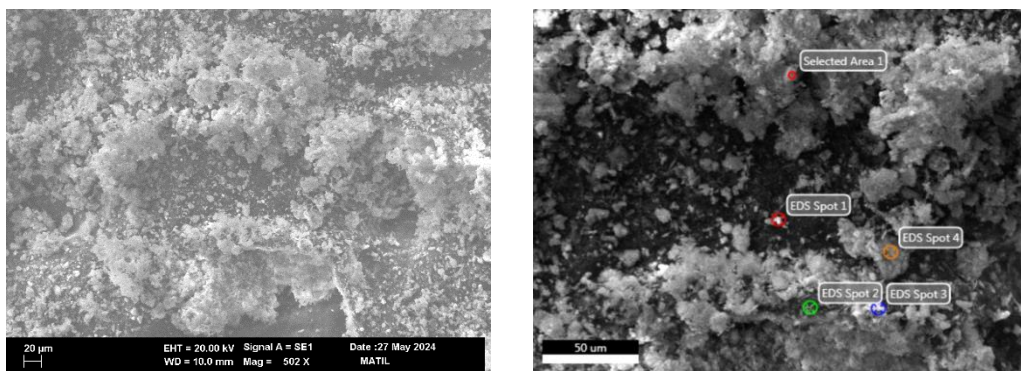
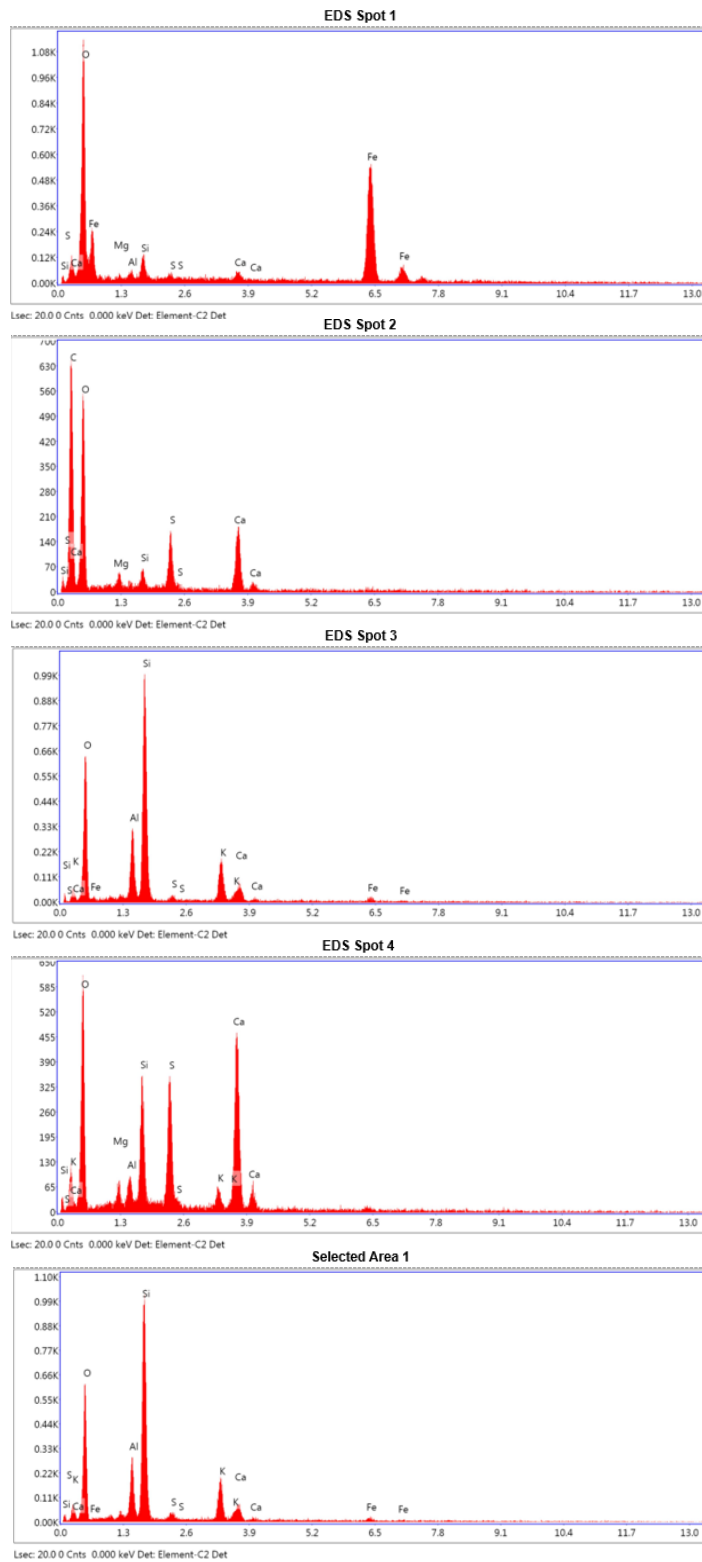Figure 4.55 SEM Images of Hard Coal Fly Ash Leach residue after the first step of Sequential Leaching

Figure 4.56 EDS analysis of the different spots and areas of Hard Coal Fly Ash Leach residue after the first step of Sequential Leaching
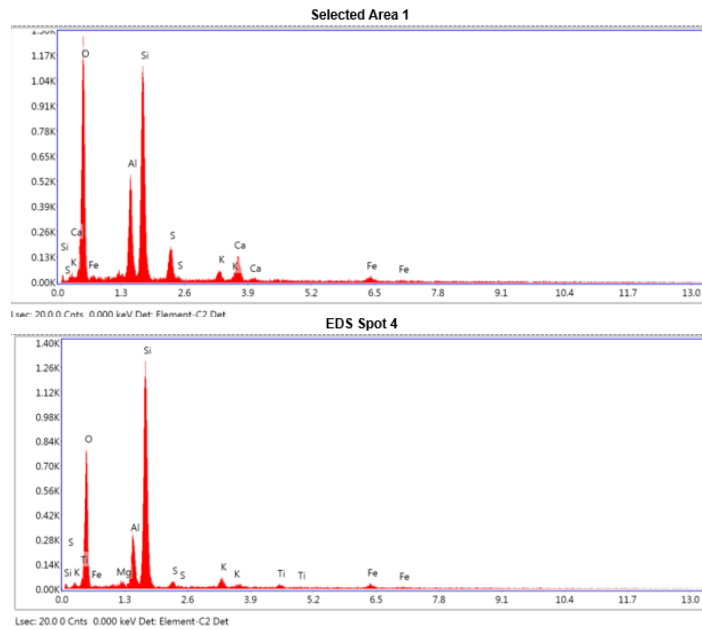
Figure 4.56 (Cont'd)
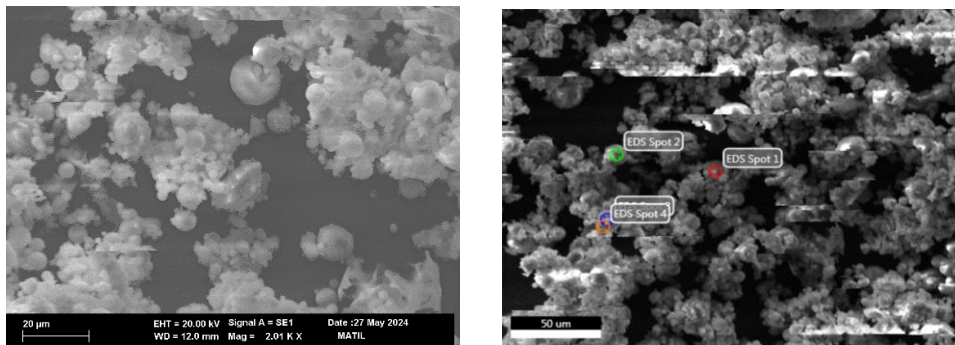
Figure 4.57 SEM Images of Hard Coal Fly Ash Leach residue after the second step
of Sequential Leaching

Figure 4.57 shows the SEM image of the leach residue of the second step of the
sequential leaching experiments done 24 hours at 90 °C and 1/10 solid-liquid ratio
using 30% hydrochloric acid solution. Energy-dispersive X-ray spectroscopy (EDS)
analysis of the SEM image can be seen in Figure 4.58. Identified elements by EDS
are labeled above the relevant peaks. EDS analysis shows abundance of silicon and
oxygen in the ore represented by high-intensity peaks. Presence of aluminum
apparent with peaks of moderate intensities. Calcium and iron peaks were decreased

and small Fe peak was seen. The morphology of the particles spheres in different sizes.
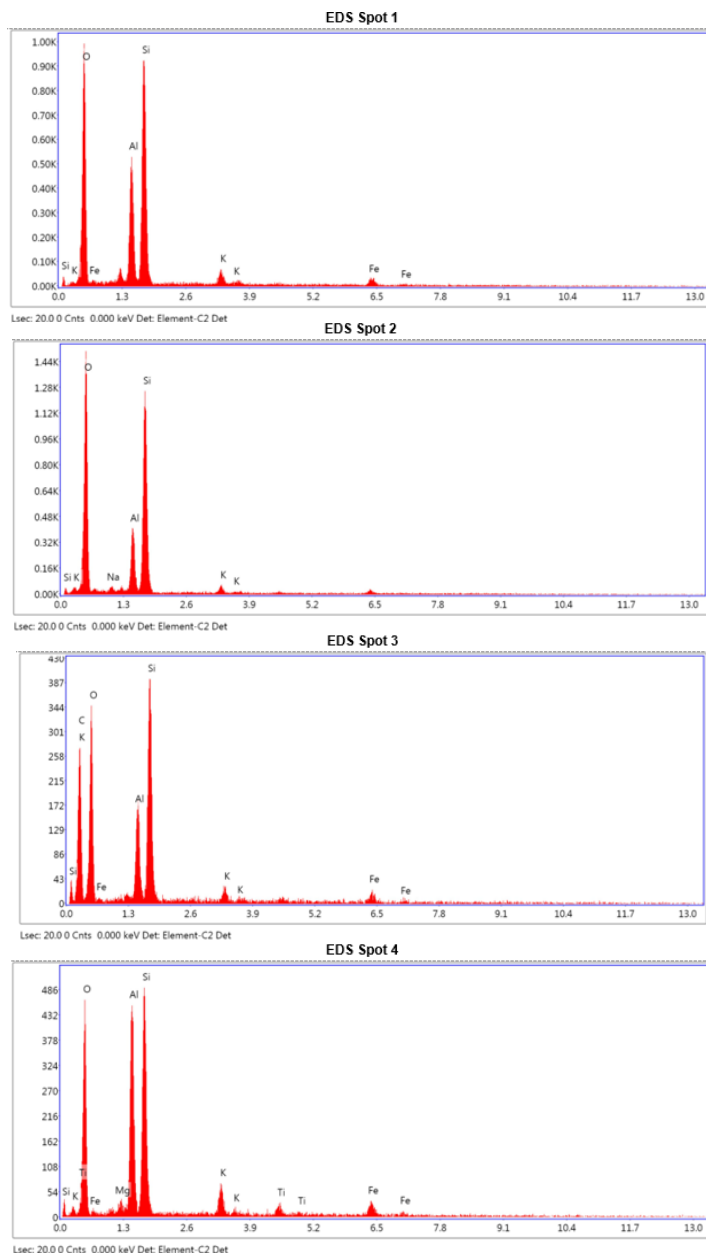
Figure 4.58 EDS analysis of the different spots and areas of Hard Coal Fly Ash Leach residue after the second step of Sequential Leaching

114

The SEM images and EDS analysis of the leach residue of citric acid leaching in 24 hours at 90 °C and 1/10 solid-liquid ratio using 30% acid solution is shown in Figure 4.59 and Figure 4.60. The morphology of the particles are very similar with the sample before experiments which are spheres. High-intensity silicon, aluminum and oxygen peaks seen in the EDS analysis. Presence of iron and potassium apparent with peaks of small intensities.
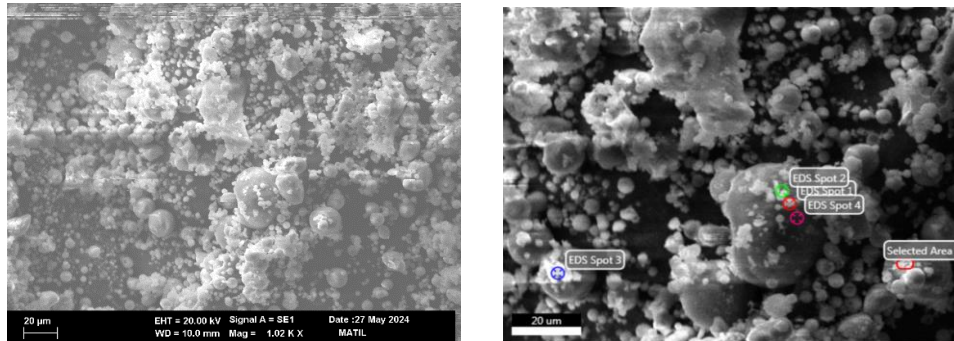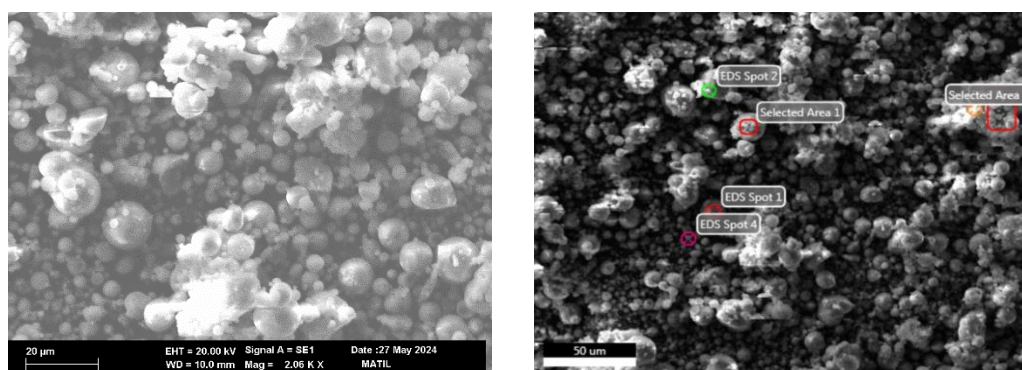

Figure 4.59 SEM Images of Hard Coal Fly Ash Leach residue after Citric Acid Leaching
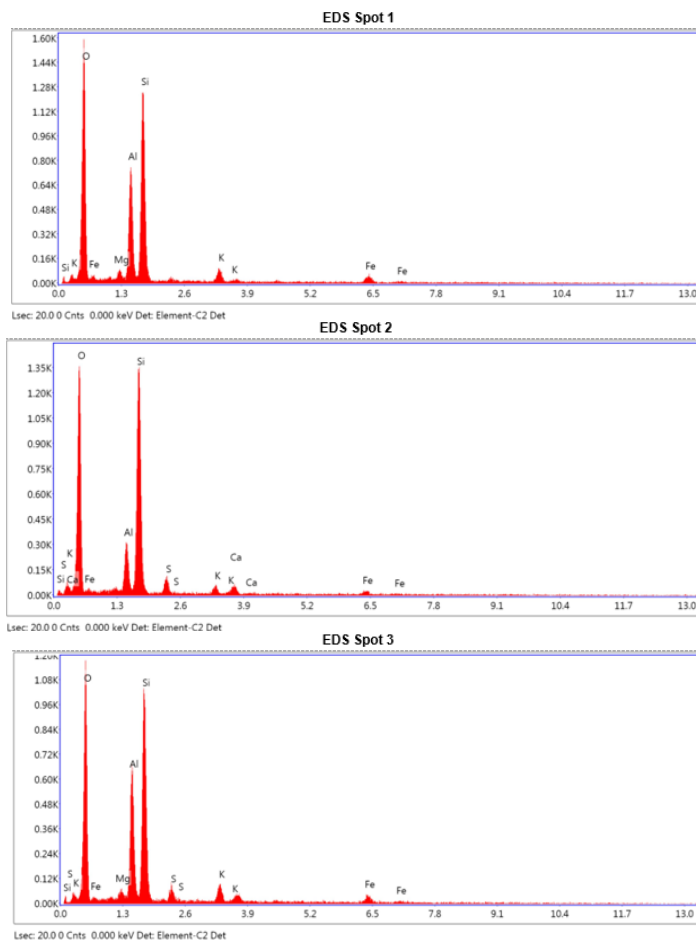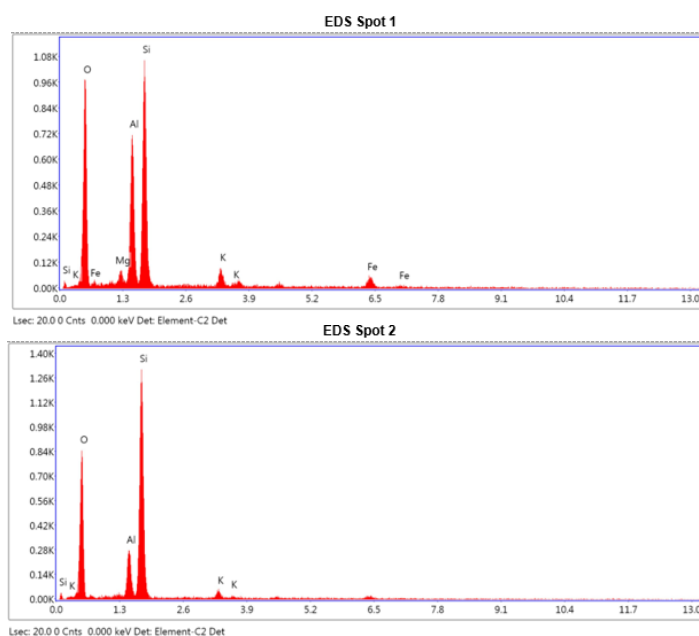

Figure 4.60 EDS analysis of the different spots and areas of Hard Coal Fly Ash Leach residue after Citric Acid Leaching
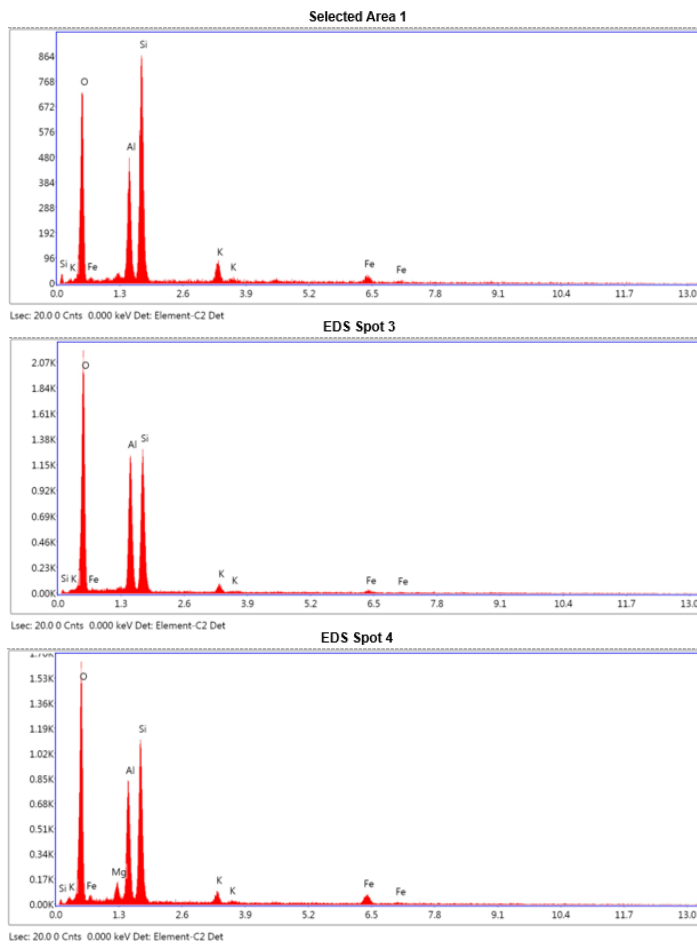
Figure 4.60 (Cont'd)

4.3   Neutralization - Selective Precipitation Experiments

Within the scope of neutralization - selective precipitation tests, by precipitating the Rare Earth Element contents of the pregnant leach solution (PLS) obtained from hydrometallurgical leaching tests, a precipitate (cake) with REE content at a reasonable grade is obtained. In the tests carried out, different concentrations of NaOH solutions were used as pH regulator and precipitates were obtained at different pHs. Flow diagram of neutralization – selective precipitation tests is given in Figure 4.61.

As a result of systematic neutralization - precipitation tests, the precipitation behavior of REE contained in the pregnant leach solution at different pH values was examined, while the precipitation behavior of the impurity content of the solution was also examined. In this context, when the pH values were first increased to 3 in a controlled manner during the tests, it was observed that elements such as Al, Fe, V and Mo, which are considered the basic impurities of the solution, as well as scandium and low amounts of other rare earth elements, also precipitated, thus reducing the grade of the resulting precipitate. In order to relatively decrease the grade of the obtained neutralization fluid after this precipitation process in terms of impurities like Al, the pH values were increased to 4.5 in a controlled manner and the REE, Mg and Ca contents of the solution were ensured not to precipitate (Figure 4.62). At the same time, it has been observed that +3-valent iron elements tend to precipitate less at these pH values. As a result of the evaluations made at this stage, it was observed that the REE contents of the solution mainly precipitated in the pH range of 5-9. In order to relatively increase the grade of the obtained precipitate in terms of rare earth elements the neutralization fluid's pH is increased to 8.5 after filtration of the first precipitate. Also it is seen that Mg and Ca contents remain in the solution after second precipitation phase.

Precipitation test are done for the sequential leaching with inorganic leaching PLS of each fly ash sample because of the highest recovery of rare earth element obtained by that experimental procedure.

It was thought that total rare earth element recovery were high enough in controlled precipitation at pH 4.5 values, it was found that Al and Fe recoveries were high enough in controlled precipitation at pH 4.5 values, so gradual precipitation at lower pH values might be beneficial in order to increase the grade values of the resulting precipitate (second, pH=8.5). In this context, the pH values were increased to 4.5 in a controlled manner, and after the filtration of the resulting precipitate, a second precipitation was carried out by increasing the pH values to 8.5 in a controlled manner. It was observed that the precipitate obtained from precipitation at pH 4.5 values was relatively enriched in Fe^{2+} and Al and the Sc content of the solution was

relatively less precipitated. Additionally, it was determined that the REE content (rather than Sc) of the leaching solution did not tend to precipitate at pH 4.5, therefore the REE content of the resulting precipitate was low.
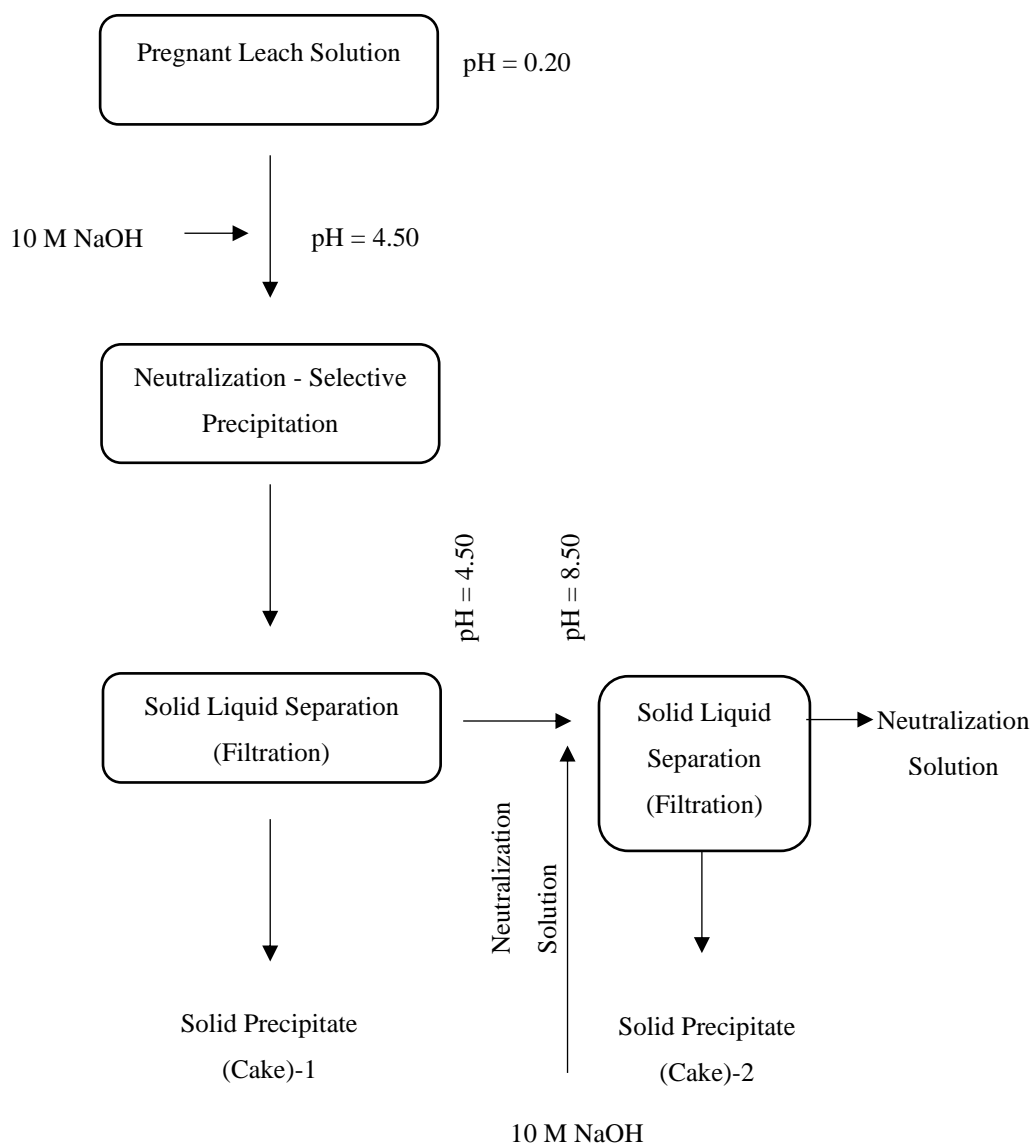
Figure 4.61 Neutralization - Selective Precipitation Flowsheet

118
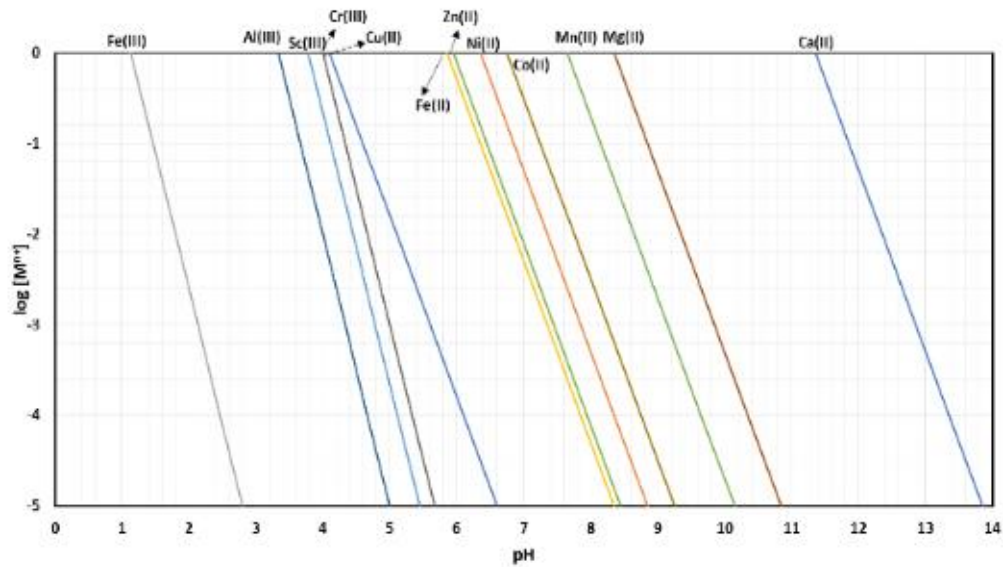
Figure 4.62. Metal Hydroxide Precipitation Diagram (Solubility of hydroxide ions at 25 °C) (Ferizoğlu, Kaya, & Topkaya, 2017)

It has been observed that increasing the concentrations of NaOH solutions used as pH regulators during neutralization - selective precipitation tests accelerates the reaction kinetics, thus relatively increasing the total REE yield value.

The reaction occurred during precipitation of REE in the second stage is ((Silva, De Morais, & Teixeria, 2018):

$$REE^{3+}_{(aq)}+3OH^{-}_{(aq)} \rightarrow REE(OH)_3 \tag{1}$$

Eh-PH diagrams and literature were used for the precipitation of rare soil elements. After sequential leaching, all rare earth elements were precipitated as hydroxide as the equation seen above. When Eh-PH diagram of the La, Ce and Nd examined (Figure 4.63, Figure 4.64 & Figure 4.65), REE is observed to form hydroxide after pH 8. Differently, Sc starts dissolving at pH 4.5 (Figure 4.66).
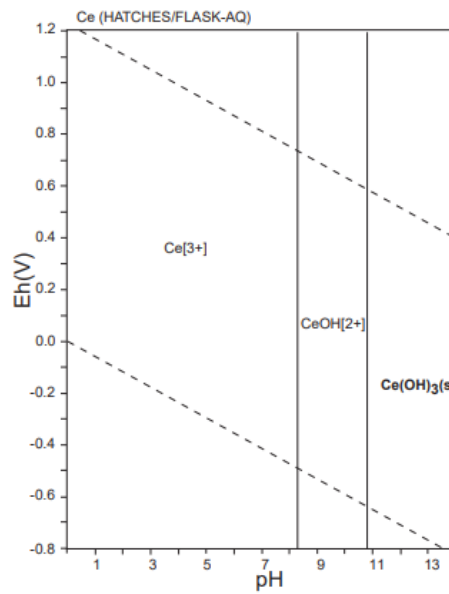
Figure 4.63. Eh-pH diagram of the system Ce-O-H. Ce = 10^{-10}, 298.15K, 10^5 Pa.
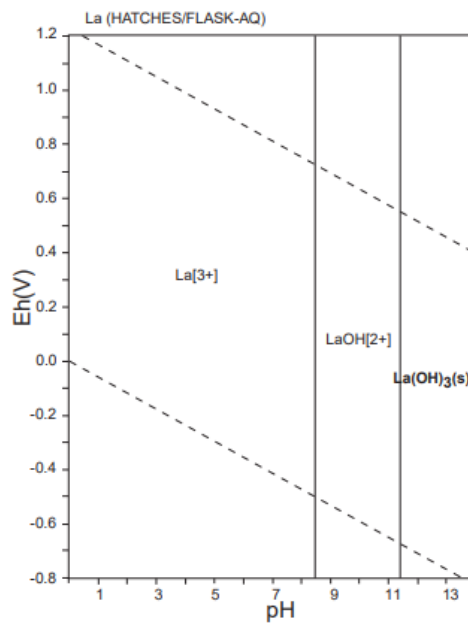
(Takeno, 2005)

Figure 4.64. Eh-pH diagram of the system La-O-H. La = 10^{-10}, 298.15K, 10^5 Pa.

(Takeno, 2005)

120
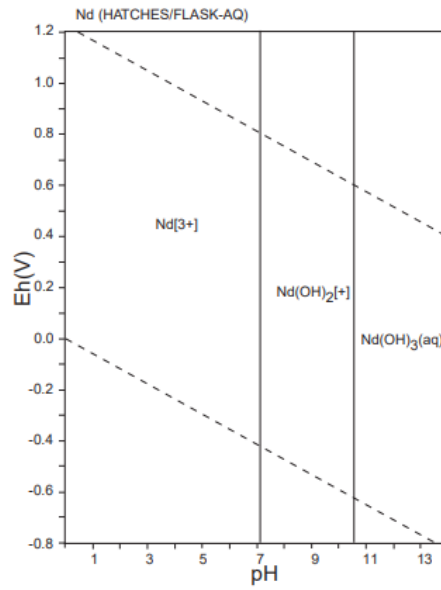
Figure 4.65. Eh-pH diagram of the system Nd-O-H. Nd = 10^{-10}, 298.15K, 10^5 Pa.
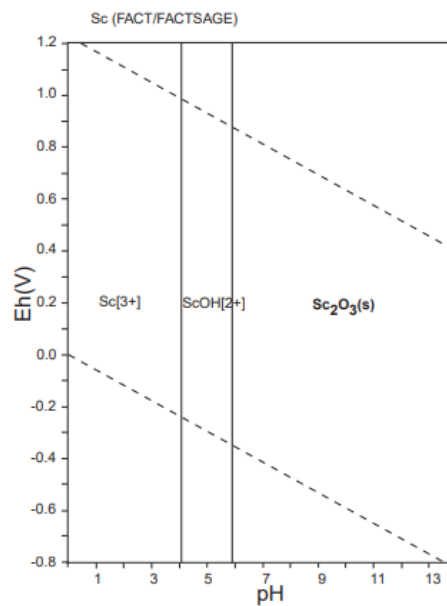
(Takeno, 2005)

Figure 4.66. Eh-pH diagram of the system Sc-O-H. Sc = 10^{-10}, 298.15K, 10^5 Pa.

(Takeno, 2005)

For the precipitation process to complete the reaction 2 hours waited in pH 8.5. The products obtained after the filtration process were dried for 2 hours in 105 ℃.

The results of each type of Fly Ash sample is shown in the following sections.

4.3.1   Lignite Fly Ash

When the analysis results of systematically performed neutralization - selective precipitation tests are considered, the feed material grade was approximately 323 ppm total REE from the pregnant leach solution. By using 10 M NaOH solution and increasing the pH value to 4.5 in a controlled manner, 130 ppm total REE, 7.13% Al and 1.2% Fe in the precipitate (cake) with was obtained with 30.98% total REE, 94.39% Al and 77.71% Fe recovery, respectively. This stage is done in order to remove the impurities mainly Al and Fe. Therefore, Sc is precipitated as well with Al and Fe in this stage with 80% recovery. But the Sc content of the fly ash is very low (27ppm in the feed of leaching experiments), so it is negligible for this study.

Following the precipitation of the pregnant leach solution at pH 5 values, the pH values were increased to 8.5 in a controlled manner and the second stage precipitation was performed in order to increase the yields of REE. As a result of the second stage precipitation, the precipitate with 2830 ppm total REEEs grades was obtained with 97.15% total REE recovery. The main impurity precipitated was Fe^{+2} valence which was having 13.90% recovery and 0.9% grade. This cake was the final product of the Lignite fly ash precipitation experiments. The results are shown in Figure 4.67.

The precipitation is not done in higher pH because Ca and Mg would precipitate in that pH values (9-12). In this way, the Al, Ca and Mg contents of the PLS obtained in sequential leaching experiments were removed, and only the part of the Fe content depending on the +2 valence was obtained in the precipitate.

Figure 4.67 Neutralization - Selective Precipitation Total REE Results of Lignite
Fly Ash

4.3.2   Asphaltite Fly Ash

For the Asphaltite Fly Ash, the feed PLS grade was approximately 328 ppm total
REE from the pregnant leach solution. Same with the Lignite fly ash, by using 10 M
NaOH solution and increasing the pH value to 4.5 in a controlled manner, 136 ppm
total REE, 7.21% Al and 0.86% Fe in the precipitate (cake) with was obtained with
31.78% total REE, 93.65% Al and 72.94% Fe recovery, respectively. This stage is
done in order to remove the impurities mainly Al and Fe. Therefore Sc is precipitated
as well with Al and Fe in this stage with 72% recovery. But the Sc content of the fly
ash is very low (29ppm in the feed of leaching experiments), so it is also negligible
for this study.

Following the precipitation of the pregnant leach solution at pH 4.5 values, the pH
values were increased to 8.5 in a controlled manner and the second stage
precipitation was performed in order to increase the yields of REE. As a result of the
second stage precipitation, the precipitate with 2765 ppm total REEEs grades was
obtained with 94.39% total REE yields. The main impurity precipitated was Fe^{+2}

valence which was having 51.68% recovery and 0.65% grade. This cake was the final product of the asphaltite fly ash precipitation experiments. The results are shown in Figure 4.68.

Moreover, the precipitation was not continued in higher pH because Ca and Mg would precipitate in that pH values (9-12). In this way, the Al, Ca and Mg contents of the PLS obtained in sequential leaching experiments were removed, and only the part of the Fe content depending on the +2 valence was obtained in the precipitate.

Figure 4.68 Neutralization - Selective Precipitation Total REE Results of Asphaltite Fly Ash

4.3.3 Hard Coal Fly Ash

The feed material grade was approximately 362 ppm total REE from the pregnant leach solution. By using 10 M NaOH solution and increasing the pH value to 4.5 in a controlled manner, 73 ppm total REE, 1.2% Al and 1.3% Fe in the precipitate (cake) with was obtained with 22.86% total REE, 98.74% Al and 83.92% Fe recovery, respectively. This stage is done in order to remove the impurities mainly Al and Fe but the contents in the feed is less than previous two fly ash samples.

Similarly, Sc is precipitated as well with Al and Fe in this stage with 63% recovery. But the Sc content of the fly ash is very low (30ppm in the feed of leaching experiments), so it is negligible for this study.

Following the precipitation of the pregnant leach solution at pH 5 values, the pH values were increased to 8.5 in a controlled manner and the second stage precipitation was performed in order to increase the yields of REE. As a result of the second stage precipitation, the precipitate with 2232 ppm total REEEs grades was obtained with 89.98% total REE yields. The main impurity precipitated was Fe^{+2} valence which was having 15% recovery and 0.3% grade. This cake was the final product of the hard coal fly ash precipitation experiments. The results are shown in Figure 4.69.

The precipitation is not done in higher pH because Ca and Mg would precipitate in that pH values (9-12). In this way, the Al, Ca and Mg contents of the PLS obtained in sequential leaching experiments were removed, and only the part of the Fe content depending on the +2 valence was obtained in the precipitate.
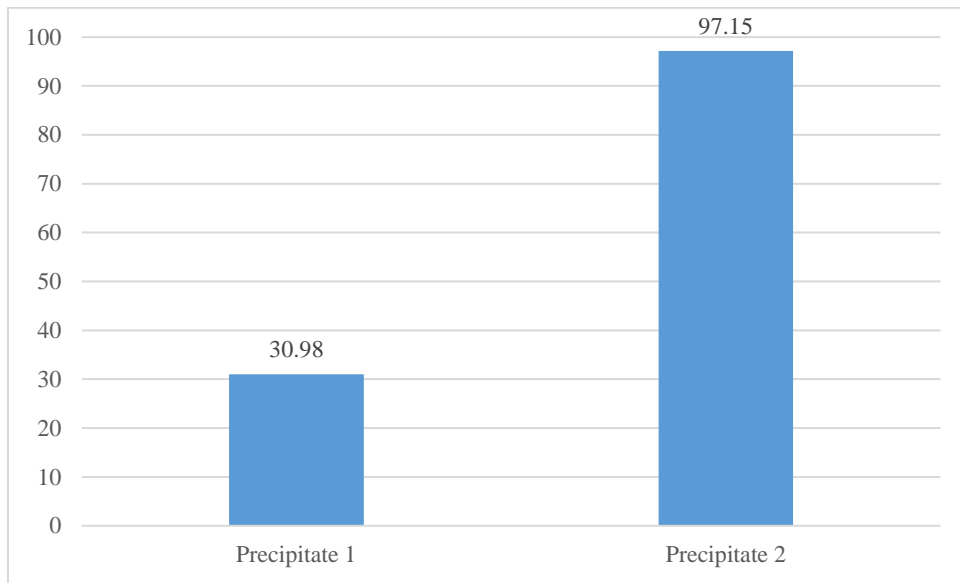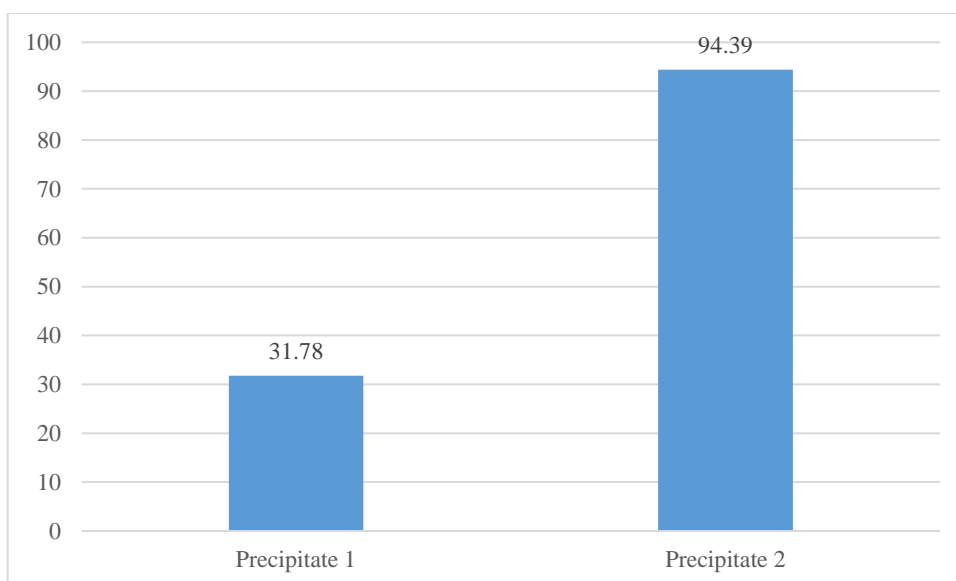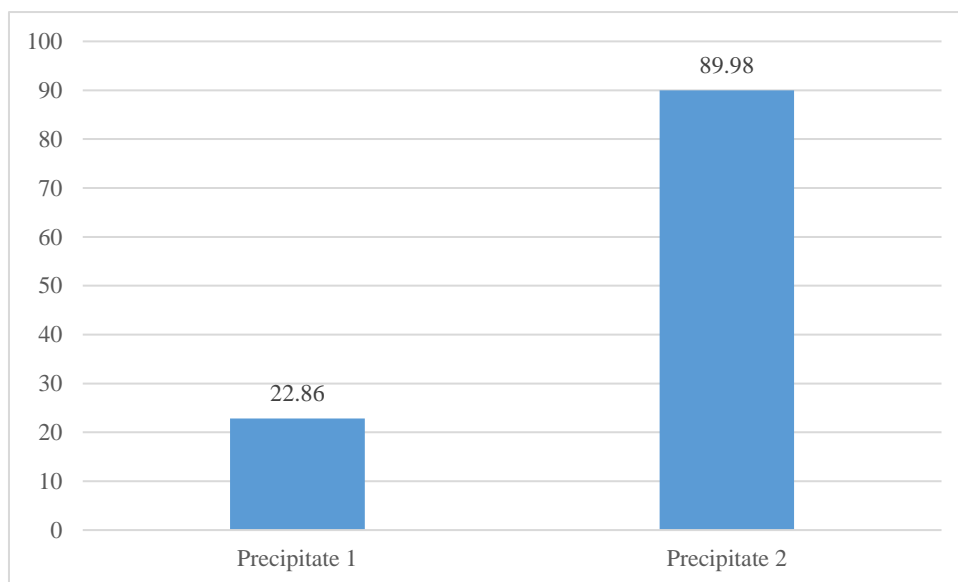

Figure 4.69 Neutralization - Selective Precipitation Total REE Results of Hard Coal Fly Ash

CHAPTER 5

CONCLUSION

In this study, hydrometallurgical leaching and neutralization - selective precipitation studies and results performed with "Fly Ash" materials delivered to the laboratory are included. The aim of the study was to determine the rare earth metal extraction from coal by products. In the study 3 different fly ash types were used: lignite, hard coal and asphaltite.

In this thesis, chemical characterization, hydrometallurgical leaching and neutralization – selective precipitation results of fly ash materials are presented. In addition, it also includes detailed procedures and metallurgical data of the systematic hydrometallurgical leaching and neutralization – selective precipitation tests.

Within the scope of hydrometallurgical studies, all fly ash samples were first subjected to chemical characterization. Based on the chemical characterization results done in ICP-MS, it was determined that the total rare earth element grades of the feed material were 365 ppm, 428 ppm and 439 ppm, of lignite, asphaltite and hard coal respectively. It was also observed by XRD and SEM analysis that all samples contained Ca, Al, Si and Fe content in terms of major impurities.

As a result of the characterization, all the fly ash samples subjected to direct leaching with two inorganic and one organic acid leaching. The acids used were sulfuric acid, hydrochloric acid and citric acid. Best conditions obtained for all the acid types were hydrometallurgical leaching at 90° C for 24 hours using 30% acid concentration by volume. After the leaching tests statistical analysis done and by that the optimum conditions for leaching were chosen.

The study continued with the sequential leaching with inorganic acids. The reason to choose inorganic acids for sequential leaching was the recoveries of the inorganic acid leaching is higher than the citric acid leaching. Also the chemical decomposition od the aluminosilicate phase was seen in the SEM images of the inorganic acid leaching, mostly in hydrochloric acid case.

First hydrometallurgical leaching at 60°C for 6 hours using 10% sulfuric acid concentration by volume were done. After filtration process, leach residue subjected to hydrometallurgical leaching at 90°C for 24 hours using 30% hydrochloric acid concentration by volume. The total REE efficiencies of sequential leaching of lignite, asphaltite and hard coal fly ashes were 86.05%, 96.93% and 73.45%, respectively.

In neutralization - selective precipitation experiments using the pregnant leach solution obtained following hydrometallurgical leaching processes, as a result of increasing the pH values to 4.5 and then 8.5 using 10 M NaOH solution. This proses is done to the sequential leaching pregnant leach solutions of lignite, asphaltite and hard coal fly ashes. The reason for 2 staged precipitation is the purifying the REE from impurities like Al, Ca, Mg and Fe. First stage of the precipitation was done in order to reduce the Al and Fe^{+3} content of the PLS. The second stage of the precipitation was done in pH 8.5 and its aim was precipitating the total REE. At the end samples contained 2830 ppm (lignite fly ash), 2765 ppm (asphaltite fly ash) and 2232 ppm (hard coal fly ash) of total REE with the yields of 97.15%, 94.39% and 89.98%, respectively.

As a result, it has been understood that all the fly ash materials responded positively to the applied hydrometallurgical leaching and neutralization - selective precipitation processes, and that the material was suitable for the applied processes in terms of obtaining precipitate (cake) with relatively high grades in REEs.

For further studies, suitability of the fly ash samples leach residues for the cement production could be determined. If they are compromise with the standards and the minerology is appropriate, this study is important for sustainability. We must live in a way that supports sustainable development, which entails meeting present needs

128

without compromising the ability of future generations to meet their own, if we hope for a better tomorrow. For our civilizations and our planet to survive, we need a more sustainable world. Two of the United Nations' seventeen Sustainable Development Goals are relevant to this thesis (United Nations, 2024). These goals are 9 (Industry, innovation and infrastructure) and 12 (Responsible consumption and production) (The Sustainable Development Goals Report 2023: Special Edition, 2023). Goal 9B is to ensure that policies that support industrial diversification and the addition of value to commodities are in place, among other things, in order to promote domestic technical development, research, and innovation in developing countries (United Nations, 2024). Coal is an important energy resource for Turkey and by-products can be reuse with the extraction of valuable elements in them. 12.2: Achieve the efficient and sustainable use of natural resources by 2030; and 12.5: considerably decrease waste generation by 2030 through prevention, reduction, recycling, and reuse are the targets of goal 12 (United Nations, 2024).

Also, solvent extraction tests can be done in order to increase the grade of REEs and decrease the impurities.

REFERENCES

Altaş, Y., Tel, H., İnan, S., Sert, Ş., Çetinkaya, B., Sengül, S., & Özkan, B. (2018). An experimental design approach for the separation of thorium from rare earth elements. *Hydrometallurgy, 178*, 97-105.

Baştürkcü , E., Şavran, C., Yüce, A., & Timur, S. (2022). Revealing the effects of mechanical attrition applied on Eskisehir-Beylikova REE ore utilizing MLA. *Minerals Engineering, 186*, 1-12.

Beaudry, B. J., & Gschneidner, Jr. , K. A. (1978). Preparation and basic properties of rare earth metals. In J. K. Gschneidner, *Handbook on the Physics and Chemistry of Rare Earths,* (pp. 173-232). North Holland, Amsterdam.

Blissett, R. S., & Smalley, N. R. (2014). An investigation into six coal fly ashes from United Kingdom and Poland to evaluate rare earth element content. *Fuel*, 119-236.

Blissett, R., Smalley, N., & Rowson, N. (2013). An investigation into six coal fly ashes from the United Kingdom and Poland to evalute rare earth element content. *Fuel*, 236-239.

Chi, R., & Tian, J. (2008). *Weathered crust elution-deposited rare earth ores.* Newyork: Nove Science Publishers.

Chi, R., Zhu, G., Zhou, Z., & Xu, Z. (2000). A novel process for recovering rare earth from weathered black earth. *Metall. Mater. Trans. B 31B*, 191-196.

Dai, S., Cherkryzhov, I. Y., Seredin, V. V., Nechaev, V. P., Graham, I. T., Hower, J. C., . . . Wang, X. (2016). Metalliferous coal deposits in East Asia (Primorye of Russia and South China): A review of geodynamic controls and styles of mineralization. *Gondwana Research*, 60-82.

Dai, S., Graham, I. T., & Ward, C. R. (2016). A review of anomalous rare earth elements and yttrium in coal. *International Journal of Coal Geology*, 82-95.

Dai, S., Liu, J., Ward, C. R., Hower, J. J., French, D., Jia, S., . . . Garrison, T. M. (2016). Mineralogical and geochemical compositions of Late Permian coals and host rocks from the Guxu Coalfield, Sichuan Province, China, with emphasis on enrichment of rare metals. *International Journal of Coal Geology*, 71-95.

Dai, S., Xie, P., Ward, C. R., Yan, X., Gou, W., French, D., & Graham, I. T. (2017). Anomalies of rare metals in Lopingian uper-high-organic-sulfur coals from the Yishan Coalfield, Guangxi, China. *Ore Geology Reviews*, 235-250.

Ferizoğlu, E., Kaya, Ş., & Topkaya, Y. A. (2017). Solvent extraction behaviour of scandium from lateritic nickel-cobalt ores using different organic reagents. *Physicochemical Problems of Mineral Processing*.

Ferron, C. J., Bulatovic, S. M., & Salter, R. S. (1991). Beneficiation of rare earth oxide mineral. *Matter. Sci. Forum*, (pp. 251-270).

Folgueras, M. B., Alonso, M., & Fernandez, F. J. (2017). Coal and sewage sludge ashes as sources of rare earth elements. *Fuel*, 128-139.

Franus , W., Wiatros-Motyka, M. M., & Wdowin, M. (2015). Coal fly ash as a resource for rare earth elements. *Environ Sci Pollut Res*, 22-74.

Gambogi, J. (2013). Rare Earths. In *U.S.G.S. 2011 Minerals Yearbook* (pp. 60.1-60.12). United States Geological Survey.

Güneş, H., Obuz, H. E., Akçay, H., Kara, Ç., & Erdem, A. (2023). Production of rare-earth oxides from Eskişehir-Beylikova complex ores. *Bulletin of the Mineral Research and Exploration, 170*, 87-97.

Gupta, B., Malik, P., & Deep, A. (2002). Extraction of uranium, thorium, and lanthanides using Cyanex-923: their separations and recovery from monazite. *J. Radioanal. Nucl. Chem.*, 451-456.

Haxel, G. B., Hendrick, J. B., & Orris, G. J. (2002). *Rare Earth Elements—Critical Resources for High Technology*. USGS.

Hower, J. C., Dai, S., Seredin, V. V., Zhao, L., Kostova, I. J., Silva, L. F., . . . Gürdal, G. (2013). A note on Occurrence of Yttrium and Rare Earth Elements in Coal Combustion Products. *Coal Combustion and Gasification Products*, 39-47.

Hower, J. C., Eble, C. F., Dai, S., & Belkin, H. E. (2016). Distribution of rare earth elements in eastern Kentucky coals: Indicators of multiple modes of enrichment? *International Journal of Coal Geology*, 73-81.

Hower, J. C., Groppo, J. G., Henke, K. R., Hood, M. M., Eble, C. F., Honaker, R. Q., . . . Qian, D. (2015). Notes on the Potential for the Concentration of Rare Earth Elements and Yttrium in Coal Combustion Fly Ash. *Minerals*, 356-366.

Hower, J. C., Groppo, J. G., Joshi, P., Dai, S., Moecher, D. P., & Johnston, M. N. (2013). Location of Cerium in Coal-Combustion Fly Ashes: Implications for Recovery of Lanhanides. *Coal Combustion and Gasification Products*, 73-78.

İnan, S., Tel, H., Sert, Ş., Çetinkaya, B., Sengül, S., Özkan, B., & Altaş, Y. (2018). Extraction and separation studies of rare earth elements using Cyanex 272 impregnated Amberlite XAD-7 resin. *Hydrometallurgy, 181*, 156-163.

Jiang, Y., Yang, Y., Liu, L., Wang, W., & Liu, Y. (2019). Extraction of rare earth elements from fly ash by alkali fusion followed by acid leaching. *Minerals Engineering*(132), 160-167.

Ju, T., Jiang, J., Meng, Y., Yan, F., Xu, Y., Gao, Y., & Aihemaiti, A. (2020). An investigation of the effect of ultrasonic waves on the efficiency of silicon extraction from coal fly ash. *Ultrasonics - Sonochemistry, 60*.

Kang, S., Zhang, J., & Wang, S. (2020). Enhancing rare earth element extraction from coal fly ash through ultrasonic-assisted leaching. *Ultrasonics Sonochemistry*(64), 105024.

Kaya, Ş., Dittrich, C., Stopic, S., & Friedrich, B. (2017). Concentration and Separation of Scandium from Ni. *Metals, 557*.

Kim, J. S., Lee, C. H., Han, S. H., & Suh, M. Y. (2014). Studies on complexation and solvent extraction of lanthanides in the presence of diaza-18-crown-6-di-isopropionic acid. *Talanta*, 437–444.

King, H. M. (2017, 04 20). *REE - Rare Earth Elements and their Uses.* Retrieved from Geology.com: https://geology.com/articles/rare-earth-elements/

Kolker, A., Scott, C., Hower, J. C., Vazquez, J. A., Lopano, C. L., & Dai, S. (2017). Distribution of rare earth elements in coal combustion fly ash, determined by SHRIP-RG ion microprobe. *International Journal of Coal Geology*, 1-10.

Krishnamurthy, N., & Gupta, C. K. (2016). *Extractive Metallurgy of Rare Earths* (2nd ed.). Boca Raton, FL: CRC Press.

Kul, M., Topkaya, Y., & Karakaya, İ. (2008). Rare earth double sulfates from pre-concentrated bastnasite. *Hydrometallurgy, 93*(3-4), 129-135.

Kumari, A., Panda, R., Jha, M. K., Kumar, J. R., & Lee, J. Y. (2015). Process development to recover rare earth metals from monazite. *Minerals Engineering*, 102-115.

Kuppusamy, V. K., & Holuszko, M. (2022). Sulfuric acid baking and water leaching of rare earth elements from coal tailings. *Fuel, 319*.

Kurşun, İ., Özdemir, O., Tombal, T. D., Terzi, M., & Hacıhafızoğlu, H. (2017). Bastnazit Kompleks Cevherinden (EskiĢehir, Türkiye) Bazı Nadir Toprak Elementlerinin (Ce, Nd, La) Asit Liçi ile Çözünürlüklerinin Araştırılması. *Çukurova Üniversitesi Mühendislik Mimarlık Fakültesi Dergisi, 32*(1), 207-214.

Kurşunoğlu, S., Hussaini, S., Top, S., Ichlas, Z. T., Gökçen, H. S., Özsaraç, Ş., & Kaya, M. (2021). Production of mixed rare earth oxide powder from a

thorium containing complex Bastnasite ore. *Powder Technology, 379*, 641-654.

Kurşunoğlu, S., Top, S., Hussaini, S., Gökçen, H. S., Altıner, M., Özsaraç, Ş., & Kaya, M. (2020). EXTRACTION OF LANTHANUM AND CERIUM FROM A BASTNASITE ORE BY DIRECT ACIDIC LEACHING. *Bilimsel Madencilik Dergisi, 59*(2), 85-92.

Li, L., Ge, J., & Wu, F. (2010). Recovery of cobalt and lithium from spent lithium ion batteries using organic citric acid as leachant. *Journal of Hazard Mater, 176*, 288-293.

Li, W., Wang, D., & Yu, J. (2017). Recovery of rare earth elements from fly ash by magnetic separation and acid leaching. *Minerals Engineering*(105), 28-35.

Lin, R., Howard, B. H., Rot, E. A., Bank, T. L., Granite, E. J., & Soong, Y. (2017). Enrichment of rare earth elements from coal and coal by-products by physical separations. *Fuel*, 506-520.

Mcdonald, R. G., & Whittinghton, B. I. (2008). Atmospheric acid leaching of nickel laterites review. Part II. Chloride and bio-technologies. *Hydrometallurgy, 91*, 56-69.

Mokoena, K., Mokhahlane, L. S., & Clarke, S. (2022). Effects of acid concentration on the recovery of rare earth elements from coal fly ash. *International Journal of Coal Geology*.

Munir, M. M., Liu, G., Yousaf, B., Ali, M. U., & Abbas, Q. (2018). Enrichment and distribution of trace elements in Padhrar, Thar and Kotli coals from Pakistan: Comparison to coals from China with an emphasis on the elements distribution. *Journal of Geochemical Exploration*, 153-169.

Özbayoğlu, G., & Atalay, M. Ü. (2000). Beneficiation of bastnaesite by a multi-gravity separator. *Journal of Alloys and Compounds, 303-304*, 520-523.

Phuoc, T. X., Wang, P., & Mclntyre, D. (2015). Detection of rare earth elements in Powder River Basin sub-bituminous coal ash using laser-induced breakdown spectroscopy (LIBS). *Fuel*, 129-132.

Ponou, J., Dodbiba, G., Anh, J.-W., & Fujita, T. (2016). Selective recovery of rare earth elements from aqueous solution obtained from coal power plant ash. *Journal of Environmental Chemical Engineering*, 3761-3766.

Powell, J. E., & Spedding, F. H. (1959). The separation of rare earths by ion exchange. *Trans*.

Querol, X., Fernández-Turiel , J., & López-Soler, A. (1995). Trace elements in coal and their behaviour during combustion in a large power station. *Fuel*, 331-374.

Rabie, K. A., Sayed, S. A., Lasheen, T. A., & Salama, I. (2007). Europium separation from a middle rare earths concentrate derived from Egyptian black sand monazite. *Hydrometallurgy*, 121–130.

Ribeiro, J. P., Silva, C. M., & Ferreira, A. F. (2019). Recovery of rare earth elements from coal fly ash using amino acids as leaching agents. *Chemical Engineering Journal*(366), 587-595.

Robert L. Thompson, T. B. (2017). Analysis of rare earth elements in coal fly ash using laser ablation inductively coupled plasma mass spectrometry and scanning electron microscopy. *Spectrochimica Acta Part B*, 1-11.

Ronghong Lin, T. L. (2017). Organic and inorganic associations of rare earth elements in central Appalachian coal. *International Journal of Coal Geology*, 295-301.

Sadri, F., Rashchi, F., & Amini, A. (2017). Hydrometallurgical digestion and leaching of Iranian monazite concentrate containing rare earth elements Th, Ce, La and Nd. *International Journal of Mineral Processing*, 7-15.

Şahiner, M., Akgök, Y. Z., Arslan, M., & Ergin, M. H. (2017). *Dünyaa ve Türkiyede Nadir Toprak Elementleri (NTE).* Ankara: MTA.

Scott, C., Deonarine, A., Kolker, A., Adams, M., & Holland, J. (2015). Size Distribution of Rare Earth Elements in Coal Ash. *World of Coal Ash (WOCA) Conference.* Nasvhille.

Seredin, V. V., Dai, S., Sun, Y., & Chekryzhov, I. Y. (2013). Coal deposits as promising sources of rare metals for alternative power and energy-efficient technologies. *Applied Geochemistry*, 1-11.

Seredin, V. V., Dai, S., Sun, Y., & Cherkryzhov, I. Y. (2013). Recovery of rare earth elements from coal fly ash by hydrometallurgical processes. *Journal of Hazardous Materials*(254-255), 276-284.

Shaw, S., Nash, J., & Miller, C. (2022). Pilot-scale testing of an integrated process for the extraction of rare earth elements from coal fly ash. *Minerals Engineering*(175), 107330.

Silva, R. G., De Morais, C. A., & Teixeria, L. V. (2018). Selective removal of Impurities from Rare Earth Sulphuric Liquor Using Different Reagents. *Minerals Enineering*, 238-246.

Smolka-Danielowska, D. (2010). Rare earth elements in fly ashes created during the coal burning process in certain coal-fired power plants operating in Poland – Upper Silesian Industrial Region. *J Environ Radioact*, 965-973.

Szabadvary, F. (1988). The history of the discovery and separation of the rare earths. In J. K. Gschneidner, *Handbook on the Physics and Chemistry of Rare Earths* (pp. 33-80). North Holland, Amsterdam.

Taggart, R. K., Hower, J. C., Dwyer, G. S., & Hsu-Kim, H. (2016). Trends in the Rare Earth Element Content of U.S.-Based Coal Combustion Fly Ashes. *Environmental Science & Technology*, 5919-5926.

Takeno, N. (2005). *Atlas of Eh-pH diagrams Intercomparison of thermodynamic databases.* National Institute of Advanced Industrial Science and Technology. Japan: Research Center for Deep Geological Environments.

Tang, M., Yang, S., Wu, A., & Liu, C. (2020). Selective recovery of rare earth elements from coal fly ash using environmentally benign processes. *Journal of Cleaner Production*(272), 122637.

(2023). *The Sustainable Development Goals Report 2023: Special Edition.* United Nations.

Thompson, R., Bank, T., Montross, S., Roth, E., Howard, B., Verba, C., & Granite, E. (2018). Analysis of rare earth elements in coal fly ash using laser ablation inductively coupled plasma mass spectrometry and scanning electron microscopy. *Spectrochimica Acta Part B*, 1-11.

United Nations. (2024, 7 5). Retrieved from Sustainable Development Goals: https://www.un.org/sustainabledevelopment/sustainable-development-goals/

Vassilev, S. V., & Menendez, R. (2005). Phase-mineral and chemical composition of coal fly ashes as a basis for their multicomponent utilization. 4. Characterization of heavy concentrates and improved fly ash residues. *Fuel*, 84-91.

Vassilev, S. V., Vassileva, C. G., Song, Y. C., Li, W. Y., & Feng, J. (2016). Rare earth elements in coal and coal fly ash. *Fuel*(180), 1-7.

Weeks, M. (1956). *Discovery of the Elements.* American Chemical Society: American Chemical Society.

Welt, M. A., Brooklyn, N. Y., & Smutz, M. (1958). *Patent No. 2,849,286.*

Wu, H., Liu, X., Xu, G., & Li, Q. (2018). Thermal treatment and acid leaching for enhanced recovery of rare earth elements from coal fly ash. *Journal of Environmental Management*(218), 127-133.

Zhang, W., Dou, Z., Lv, Z., & Wnag, L. (2015). Extraction of rare earth elements from coal fly ash using supercritical carbon dioxide and chelating agents. *Journal of Cleaner Production*(103), 530-536.

Zhang, W., Rezaee, M., Bhagavatula, A., Li, Y., Groppo, J., & Honaker, R. (2015). A review of the occurrence and promising recovery methods of rare earth elements from coal and coal by-products. *Coal Prep Util*, 295–330.

Zhang, W., Xu, Y., Wang, D., Huang, Y., & Zhang, L. (2021). Hydrometallurgical processing of rare earth elements from coal fly ash: An overview. *Minerals Engineering*(169), 106969.

CURRICULUM VITAE

Surname, Name: Büyüktanır Aktar, Karden

email: karden@metu.edu.tr

EDUCATION

Degree	Institution	Year of Graduation
MS	METU Mining Engineering	2017
BS	METU Mining Engineering	2015
High School	Ankara (Anadolu) High School, Ankara	2009

WORK EXPERIENCE

Year	Place	Enrollment
2015- Present	METU Department of Mining Engineering	Research Assistant

FOREIGN LANGUAGES

Advanced English,

Beginner French and German

PUBLICATIONS

1. Büyüktanır, K. (2017). Cyanide leaching behavior of an arsenic rich refractory gold ore. Ankara: METU.

2. Cetin, Mahir C., Altun, N. E., Atalay, M. Ü., & Büyüktanır, K. (2017). Bottle Roll Testing for Cyanidation of Gold Ores: Problems related to Standardized Procedures on Difficult-to-Process Ores. Proceedings of the 3rd World Congress on Mechanical, Chemical, and Material Engineering (MCM'17) (p. 9). Italy: MMME.

3. Büyüktanır, K., Tokoğlu, M., Vardar, O., Sarıçam, T., Taştekin, Y. A., & Düzgün, H. Ş. (2014). Mine Closure And Reclamation Planning For Abandoned Ovacik Coal Mine Using Remote Sensing and Geographical Information Systems. 19th Coal Congress of Turkey (p. 12). Zonguldak: Uctea The Zonguldak Branch Of Chamber Of Mining Engineers.

HOBBIES

Ceramics, Art, Motor Sports